Description of correlation and relativistic effects in calculations of molecular properties.

Ph.D. thesis by
Jesper Kielberg Pedersen

Department of Chemistry
University of Southern Denmark
September 1, 2004

Preface

What you are about to read is the result of 4 years of Ph.D studies at the University of Southern Denmark, Odense. Starting my Ph.D study in theoretical chemistry with limited computer knowledge and no programming nor Unix experience, a lot of time has gone into learning the "tools" needed to bring the exiting and ground-breaking theory of quantum chemistry into practice. Nevertheless it has been an extremely educational 4 years that leave me with a much deeper knowledge of quantum chemistry, programming and computers in general.

The majority of my work has been on method development, trying to improve the currently available methods and implementing new ideas. Reviewing the past 4 years I think my Ph.D studies have been somewhat different than the studies of the previous members of the group. Rather than specializing in a specific area of quantum chemistry I have had many different projects covering a broad spectrum of some of the major topics of this field of research like electron correlation and relativity. The title of my thesis reflects that, and so will this thesis itself.

Throughout my Ph.D studies I have benefited greatly from the help and support of the DIRAC developer team, especially my supervisor Hans Jørgen Aa. Jensen, who has been a tremendous help in guiding me in the right direction. Also the wave function DFT hybrid project would not have reached such a mature state if it had not been for the "French connection". Thanks to Trond Saue for giving me a solid introduction to Density Functional Theory and showing me Strasbourg. Also thanks to Andreas Savin and all the members of the quantum chemistry group of Jussieu. You made my stay in Paris a pleasure and left me with a much deeper understanding of Density Functional theory and its coupling to wave function theory.

Finally I wish to thank my friends and especially my family for supporting and encouraging my endless studies and for accepting that I have not yet been able to fully make them understand what I have been doing the past 4 years.

Odense August 30, 2004

Jesper Kielberg Pedersen

Contents

List of Tables

List of Figures

Chapter 1

Abstract

With the rapidly increasing computer power and the almost equally rapid decrease in hardware costs, it can seem strange to some that such big efforts are put into making efficient models for describing atoms and molecules by means of computers. Moore's law has surprisingly well predicted that since 1970 the computer power has been doubled every 18 months. It could seem that the fast increase in computer power would satisfy our needs for doing calculations on larger and larger systems with higher and higher accuracy, but this is unfortunately not the case. One needs to know that even though the techniques are known to treat atoms and molecules with as high quality as needed these models scale tremendously bad with system size ($\approx \mathcal{O}(N^7)$), N being a measure of the system size. So even if we just double the system size we would have to wait some years for the computer power to increase enough to compensate ($10\frac{1}{2}$ years). Therefore our wish to accurately treat larger and larger systems makes the search for efficient and computationally inexpensive methods very relevant.

The main goals of my Ph.D studies have been to investigate less computationally expensive alternatives to the standard ways of performing quantum chemical calculations accounting for both electron correlation and relativistic effects. Under normal circumstances both these effects have relatively little influence on the total energy, both can nevertheless not be neglected when high accuracy is needed. At the end of this thesis it should be clear that the nature both correlation and relativity allows us to treat them is a much more efficient way than described by the *standard* computational methods without loosing control of how our approximations affect the energy or property in question.

The first chapter will briefly review the history of applied quantum chemistry and thereby define electron correlation and introduce the *standard* meth-

ods for accounting for correlation.

The second chapter will describe the investigations done on an approximate way of introducing efficient treatment of electron correlation in otherwise dynamically uncorrelated wave functions.

Chapter four will present the wave function DFT hybrid method that succesfully present and effecient way of dealing with both static and dynamic correlation.

In chapter five a complete different topic will be discussed. Namely relativistic effects and how to reduce the computational cost of 4-component methods without loosing accuracy.

Finally some concluding remarks and an outlook on future research will be given.

Part I

The standard Methods.

Chapter 2

Introduction

The task of Quantum Chemistry can be summarized to striking simplicity. Finding a solution to the eigenvalue problem (the Schrödinger equation [1])

$$\hat{H}\Psi = E\Psi \tag{2.0.1}$$

To a very good approximation the Born-Oppenheimer approximation [2] can be applied to reduce this to a purely electronic problem leaving us with the following non-relativistic n-electron Hamiltonian ($\hat{H}_e$) for N nuclei

$$\hat{H}_e = -\tfrac{1}{2}\sum_{i}^{n}\nabla_i^2 + \sum_{A<B}^{N}\frac{Z_A Z_B}{R_{AB}} - \sum_{i}^{n}\sum_{A}^{N}\frac{Z_A}{r_{iA}} + \sum_{i<j}^{n}\frac{1}{r_{ij}} \tag{2.0.2}$$

The great disappointment is that even after having reduced this to an electronic problem the simple looking eigenvalue equation (2.0.1) can only be solved analytically for one-electron systems, greatly limiting the usefulness. This is where the *standard* Quantum Chemical methods come into play. If we cannot find an analytical solution, providing us with the true wave function of the system (Ψ), we can try to find a good approximation to it. This has become the goal of most Quantum Chemical research and since the birth of Quantum Chemistry this has spawned a hierarchy of methods.

Any introduction to the methods of quantum chemistry would have to take its starting point in the Hartree-Fock (HF) method. The HF can be considered a branching point in quantum chemistry. Further approximations lead to the semi-empirical methods while improvements to the HF method of the description of the correlated motion of electrons, lead to the correlated ab initio methods, like the Møller Plesset (MP), the Coupled Cluster (CC) perturbation approaches, the variational Configuration Interaction (CI) method and the Multi-configurational Self Consistent Field (MCSCF) method. An

understanding of what the HF method does and does not include in its description of atoms and molecules lets us understand the concepts of static and dynamic correlation. The following sections deal with these topics.

Chapter 3

The Single Determinant Ansatz.

One of the earliest attempt to achieve an approximation for the wave function was to form the Ψ from a simple product of orthonormal molecular orbitals (MOs) or spin orbitals (χ_i)[1]

$$\Psi = \chi_1(\mathbf{x}_1)\chi_2(\mathbf{x}_2)\cdots\chi_N(\mathbf{x}_N) \tag{3.0.1}$$

In this, the Hartree approximation [3–5], the electrons move independently of each other, or said in a different way the movement of the electrons is completely uncorrelated. It was quickly realized that the Hartree approach was invalid in the sense that it does not satisfy the Pauli Exclusion Principle which states that since electrons are indistinguishable from each other : *the wave function must be antisymmetric with respect to electron interchange.* In 1930 Fock [6] showed that the Hartree product could be made antisymmetric by appropriately adding and subtracting all possible permutation of the Hartree product, and later Slater [7, 8] showed that the resulting antisymmetric wave function could be described by a Slater determinant.

$$\Psi = \left(\frac{1}{N!}\right)^{\frac{1}{2}} \begin{vmatrix} \chi_1(\mathbf{x}_1) & \chi_2(\mathbf{x}_1) & \cdots & \chi_N(\mathbf{x}_1) \\ \chi_1(\mathbf{x}_2) & \chi_2(\mathbf{x}_2) & \cdots & \chi_N(\mathbf{x}_2) \\ \chi_1(\mathbf{x}_3) & \chi_2(\mathbf{x}_3) & \cdots & \chi_N(\mathbf{x}_3) \\ \vdots & \vdots & & \vdots \\ \chi_1(\mathbf{x}_N) & \chi_2(\mathbf{x}_N) & \cdots & \chi_N(\mathbf{x}_N) \end{vmatrix} \tag{3.0.2}$$

[1] A spin-orbital is a function $\chi(\mathbf{x})$, constructed as the product of a function of space and a function of spin : $\chi(\mathbf{x}) = \phi(\mathbf{r})\binom{\alpha}{\beta}$. In this notation the coordinate $\mathbf{x}$ contains the coordinates of both space and spin.

From the properties of determinants we know that interchanging two columns (changing the electron label) changes the sign of the determinant. Furthermore if two columns are identical the determinant vanishes and therefore with the Slater determinantal ansatz for the wave function no two electrons with equal spin can occupy the same spatial orbital.

Variationally determining the optimal set of MO coefficient that minimize the electronic energy ($E_e = \frac{\langle\Psi|\mathbf{H}_e|\tilde{\Psi}\rangle}{\langle\Psi|\Psi\rangle}$) under the constraint that the orbitals are kept orthonormal, yields the Hartree-Fock approach.

3.1 The Correlation Energy.

To be able to analyze this single determinant approach further the density is introduced. For this purpose it is convenient to introduced the generalized 1 and 2 electron density matrices

$$\rho_1(\mathbf{x}_1;\mathbf{x}_1^{'}) = N\int \Psi(\mathbf{x}_1,\mathbf{x}_2,\ldots,\mathbf{x}_N)\Psi^*(\mathbf{x}_1^{'},\mathbf{x}_2,\ldots,\mathbf{x}_N)d\mathbf{x}_2\ldots d\mathbf{x}_N \quad (3.1.3)$$

$$\rho_2(\mathbf{x}_1,\mathbf{x}_2;\mathbf{x}_1^{'},\mathbf{x}_2^{'}) = N(N-1)\int \Psi(\mathbf{x}_1,\mathbf{x}_2,\ldots,\mathbf{x}_N)\Psi^*(\mathbf{x}_1^{'},\mathbf{x}_2^{'},\ldots,\mathbf{x}_N)d\mathbf{x}_3\ldots d\mathbf{x}_N \quad (3.1.4)$$

In the special case where Ψ is a single determinant wave function (3.0.2) the density matrices are particularly simple.

$$\rho_1(\mathbf{x}_1;\mathbf{x}_1^{'}) = \sum_{i\ (occ)}\chi_i(\mathbf{x}_1)\chi_i(\mathbf{x}_1^{'}) \quad (3.1.5)$$

$$\begin{aligned}\rho_2(\mathbf{x}_1,\mathbf{x}_2;\mathbf{x}_1^{'},\mathbf{x}_2^{'}) &= \sum_{i,j}\Big[\chi_i(\mathbf{x}_1)\chi_j(\mathbf{x}_2)\chi_i^*(\mathbf{x}_1^{'})\chi_j^*(\mathbf{x}_2^{'}) \\ &\qquad -\chi_i(\mathbf{x}_2)\chi_j(\mathbf{x}_1)\chi_i^*(\mathbf{x}_1^{'})\chi_j^*(\mathbf{x}_2^{'})\Big] \\ &= \rho(\mathbf{x}_1;\mathbf{x}_1^{'})\rho(\mathbf{x}_2;\mathbf{x}_2^{'}) - \rho(\mathbf{x}_2;\mathbf{x}_1^{'})\rho(\mathbf{x}_1;\mathbf{x}_2^{'}) \quad (3.1.6)\end{aligned}$$

To be able to analyze the Hartree-Fock density the spin components are written explicitly

$$\rho_1(\mathbf{x}_1;\mathbf{x}_1^{'}) = \rho_1^{\alpha}(\mathbf{r}_1;\mathbf{r}_1^{'})\alpha(s_1)\alpha^*(s_1^{'}) + \rho_1^{\beta}(\mathbf{r}_1;\mathbf{r}_1^{'})\beta(s_1)\beta^*(s_1^{'}) \quad (3.1.7)$$

$$\begin{aligned}\rho_2(\mathbf{x}_1,\mathbf{x}_2;\mathbf{x}_1^{'},\mathbf{x}_2^{'}) &= \rho_2^{\alpha\alpha}(\mathbf{r}_1,\mathbf{r}_2;\mathbf{r}_1^{'},\mathbf{r}_2^{'})\alpha(s_1)\alpha(s_2)\alpha^*(s_1^{'})\alpha^*(s_2^{'}) + \\ &\quad \rho_2^{\alpha\beta}(\mathbf{r}_1,\mathbf{r}_2;\mathbf{r}_1^{'},\mathbf{r}_2^{'})\alpha(s_1)\beta(s_2)\alpha^*(s_1^{'})\beta^*(s_2^{'}) + \\ &\quad \rho_2^{\beta\alpha}(\mathbf{r}_1,\mathbf{r}_2;\mathbf{r}_1^{'},\mathbf{r}_2^{'})\beta(s_1)\alpha(s_2)\beta^*(s_1^{'})\alpha^*(s_2^{'}) + \\ &\quad \rho_2^{\beta\beta}(\mathbf{r}_1,\mathbf{r}_2;\mathbf{r}_1^{'},\mathbf{r}_2^{'})\beta(s_1)\beta(s_2)\beta^*(s_1^{'})\beta^*(s_2^{'}) \quad (3.1.8)\end{aligned}$$

Inserting (3.1.7) in (3.1.6) we can pick out the $\alpha\alpha$ and $\alpha\beta$ parts from (3.1.8).

$$\rho_2^{\alpha\alpha}(\mathbf{r}_1,\mathbf{r}_2;\mathbf{r}_1^{'},\mathbf{r}_2^{'}) = \rho_1^{\alpha}(\mathbf{r}_1;\mathbf{r}_1^{'})\rho_1^{\alpha}(\mathbf{r}_2;\mathbf{r}_2^{'}) - \rho_1^{\alpha}(\mathbf{r}_2;\mathbf{r}_1)\rho_1^{\alpha}(\mathbf{r}_1;\mathbf{r}_2) \quad (3.1.9)$$

$$\rho_2^{\alpha\beta}(\mathbf{r}_1,\mathbf{r}_2;\mathbf{r}_1^{'},\mathbf{r}_2^{'}) = \rho_1^{\alpha}(\mathbf{r}_1;\mathbf{r}_1^{'})\rho_1^{\beta}(\mathbf{r}_2;\mathbf{r}_2^{'}) \quad (3.1.10)$$

From $\rho_2^{\alpha\alpha}$ and $\rho_2^{\alpha\beta}$ we can identify how electrons of equal and opposite spin are treated in one-determinant wave functions. The $\rho_2^{\alpha\alpha}$ term consists of the product of the α one-electron densities at $\mathbf{r}_1$ and $\mathbf{r}_2$ respectively, but this product is reduced by the *'off-diagonal'* elements of the α-part of the two-electron density matrix. In the limit $\mathbf{r}_2 \rightarrow \mathbf{r}_1$ the terms cancel meaning the two electron have zero probability of coinciding. The one-determinant wave function, and antisymmetric wave functions in general, hence account for Fermi correlation. The $\rho_2^{\alpha\beta}$ term however is a simple product of the one electron densities and so the event that a volume element is taken up by two electrons of opposite spin is everywhere just the product of the probabilities that the volume element is taken up by each of the electrons without reference to each other. Therefore electrons of different spin are not correlated in the HF-model, and this is clearly a defect of the one-determinant wave function since particles with equal-signed charges repel each other. In other words the HF model does not predict a Coulomb hole around the electrons. The situation is schematically shown in fig 3.1.1 where the drop in density is

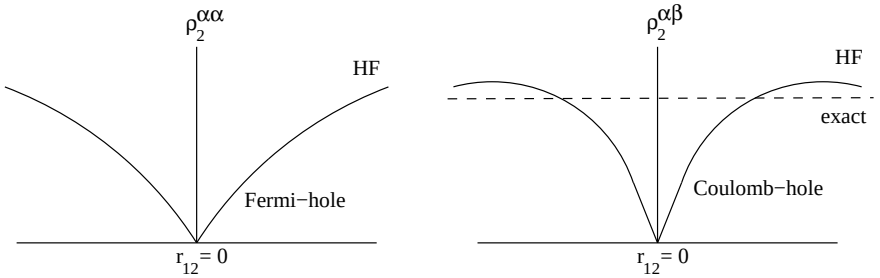

Figure 3.1.1: $\alpha\alpha$- and $\alpha\beta$-part of ρ_2 shown schematically in the neighborhood of a fixed electron, for an exact wave function and a one-determinant wave function

shown in the neighborhood of a fixed electron. The first figure shows how the Fermi-correlation introduces a hole around the fixed electron, the *Fermi-hole*. With the electrons having opposite spin the density is unaffected by the inter electronic distance becoming small in the HF-model, whether as the exact wave function has a *Coulomb-hole* around the fixed electron.

By its deficiencies the single determinant ansatz defines correlation. Usually the correlation energy is defined as

$$E_c = E_{exact,non.rel.} - E_{HF} \quad (3.1.11)$$

This definition can however be a bit misleading since the antisymmetric single determinant wave function already includes some correlation of electrons with opposite spin - the*Fermi correlation*. This correlation is therefore sometimes also referred to as the *pre-correlation energy*. This energy is brought on purely by the Pauli-exclusion principle and is also called the exchange energy. It cancels the classical Coulomb, or Hartree, energy for isolated electrons meaning that the HF model is *self-interaction* free. A property that is lost if the HF exchange is replaced by approximate exchange terms as in Density Functional Theory (DFT, see Sec.4.5).
The Fermi hole of the single determinant wave function is however only an approximation for the true Fermi hole and E_c can therefore not entirely be related to the missing Coulomb hole of the HF approach. Without reference to spin we therefore define *dynamical correlation* as the correlated motion of closely interaction electrons. For a simple system like He the HF model therefore only lacks dynamical correlation.

A completely different type of correlation arises from the fact that in many applications a single determinant is not sufficient for giving a qualitatively correct description of the system in question. Effects like degeneracy or near degeneracy, curve crossing and qualitatively wrong dissociation are collectively denoted *non-dynamical correlation* or *static correlation*. Classical examples for which the one-determinant wave function is a bad choice are Be, and H_2. In the former, the near degeneracy of the 2s and 2p orbitals makes it wrong to designate the ground state as a single determinant, in the latter, the neglect of the contribution to the wave function of the σ_u-orbital in the HF-model, makes the H_2-molecule dissociate in equal amounts of ionic and covalent terms : H^+H^- and H•H•. Unfortunately it is impossible to separate the two types of correlation from each other. Methods that address static correlation will inevitably include some dynamic correlation. An important difference between the two types of correlation is that while dynamical correlation is extremely difficult to describe with high precision, static correlation effects can fairly easy be recovered.

The same way dynamic correlation can be associated with short range electronic interaction we can associate static correlation with long range interactions. This classification is very useful and will form the basis for the approximate approaches to correlation of parts II and III of this thesis.

3.2 Correlation Holes. The Coulomb Cusp.

The Fermi and Coulomb holes can conveniently be defined from the two electron density ($\rho_2(\mathbf{x}_1, \mathbf{x}_2)$) of Eq. 3.1.4. As seen for a single determinant wave function (3.1.9), ρ_2 can be written as the product of the one electron densities minus the product of the off diagonal elements of the reduced density matrix. More general it can be written

$$\rho_2^{\alpha\alpha}(\mathbf{r}_1, \mathbf{r}_2) = \rho_1^{\alpha}(\mathbf{r}_1)\rho_1^{\alpha}(\mathbf{r}_2)[1 + h^{\alpha\alpha}(\mathbf{r}_1, \mathbf{r}_2)] \tag{3.2.1}$$

$$\rho_2^{\alpha\beta}(\mathbf{r}_1, \mathbf{r}_2) = \rho_1^{\alpha}(\mathbf{r}_1)\rho_1^{\beta}(\mathbf{r}_2)[1 + h^{\alpha\beta}(\mathbf{r}_1, \mathbf{r}_2)] \tag{3.2.2}$$

whereby the Fermi ($h^{\alpha\alpha}$) and Coulomb ($h^{\alpha\beta}$) hole functions have been defined. In the HF case $\rho_1^{\alpha}(\mathbf{r}_1)\rho_1^{\alpha}(\mathbf{r}_2)h^{\alpha\alpha}(\mathbf{r}_1, \mathbf{r}_2)$ is approximated by $-\rho_1^{\alpha}(\mathbf{r}_2; \mathbf{r}_1)\rho_1^{\alpha}(\mathbf{r}_1; \mathbf{r}_2)$ while $h^{\alpha\beta}(\mathbf{r}_1, \mathbf{r}_2)$ is zero.
The Fermi, or exchange hole is now defined as

$$\rho_x^{\alpha\alpha}(\mathbf{r}_1, \mathbf{r}_2) = \rho_1^{\alpha}(\mathbf{r}_1)h^{\alpha\alpha}(\mathbf{r}_1, \mathbf{r}_2) = \frac{\rho_2^{\alpha\alpha}(\mathbf{r}_1, \mathbf{r}_2)}{\rho_1^{\alpha}(\mathbf{r}_2)} - \rho_1^{\alpha}(\mathbf{r}_1) \tag{3.2.3}$$

and integrates to

$$\int \rho_x^{\alpha\alpha}(\mathbf{r}_1, \mathbf{r}_2)d\mathbf{r}_2 = -1 \tag{3.2.4}$$

The Coulomb hole is defined as

$$\rho_c^{\alpha\beta}(\mathbf{r}_1, \mathbf{r}_2) = \rho_1^{\alpha}(\mathbf{r}_1)h^{\alpha\beta}(\mathbf{r}_1, \mathbf{r}_2) = \frac{\rho_2^{\alpha\beta}(\mathbf{r}_1, \mathbf{r}_2)}{\rho_1^{\beta}(\mathbf{r}_2)} - \rho_1^{\alpha}(\mathbf{r}_1) \tag{3.2.5}$$

and integrates to

$$\int \rho_c^{\alpha\beta}(\mathbf{r}_1, \mathbf{r}_2)d\mathbf{r}_2 = 0 \tag{3.2.6}$$

We could have defined the total exchange correlation hole likewise

$$\rho_{xc}(\mathbf{r}_1, \mathbf{r}_2) = \rho_1(\mathbf{r}_1)h_{xc}(\mathbf{r}_1, \mathbf{r}_2) = \frac{\rho_2(\mathbf{r}_1, \mathbf{r}_2)}{\rho_1(\mathbf{r}_2)} - \rho_1(\mathbf{r}_1) \tag{3.2.7}$$

which will then integrate up to -1 like the exchange hole. The repulsion between the density and the exchange-correlation hole (E_{xc})

$$E_{xc} = \frac{1}{2}\iint \frac{\rho_1(\mathbf{r}_1)\rho_{xc}(\mathbf{r}_1, \mathbf{r}_2)}{r_{12}}d\mathbf{r}_1 d\mathbf{r}_2 \tag{3.2.8}$$

will together with the classical Coulomb (Hartree) energy

$$J = \frac{1}{2}\iint \frac{\rho_1(\mathbf{r}_1)\rho_1(\mathbf{r}_2)}{r_{12}}d\mathbf{r}_1 d\mathbf{r}_2 \tag{3.2.9}$$

add up to the exact two electron repulsion energy ($V_{ee} = J + E_{xc}$).
Had we known the exact exchange-correlation hole function we could therefore solve the Schrödinger equation exact. The task of Quantum Chemists is therefore to approximate the exchange-correlation hole function. This viewpoint is directly transferable to DFT but of course also holds for wave function based methods.

The difficulty in approximating the the exchange-correlation hole lies in its shape for small interelectronic distances (as sketched on fig.3.1.1). From the non-relativistic Hamiltonian (2.0.2) its clear that this operator has singularities both in the nuclear attraction operator (for r_iA) and in the Coulomb operator (for $r_i = r_j$). For the exact solution to the Schrödinger equation these singularities have to be balanced by Ψ. This requirement on Ψ can be formulated at the nuclear and Coulomb cusp condition [9].

$$\lim_{r_{iA}\to 0}\left(\frac{\partial\Psi}{\partial r_{iA}}\right)_{\text{sp.ave}} = -Z_A\Psi(r_{iA}=0) \tag{3.2.10}$$

$$\lim_{r_{ij}\to 0}\left(\frac{\partial\Psi}{\partial r_{ij}}\right)_{\text{sp.ave}} = \frac{1}{2}\Psi(r_{ij}=0) \tag{3.2.11}$$

where a spherical averaging is performed. The typical procedure in ab initio methods is to expand the wave function in simple analytical functions, centered at the nucleus (atomic orbitals). It is therefore up to these atomic orbital to make the total wave function obey the nuclear cusp condition, and the Slater Type Orbitals (STOs) achieve that. This is not the case for the more common choice, the Gaussian Type Orbitals (GTOs), that have a squared r_{iA}-dependence. Suitable linear combinations do however succeed to a satisfactory level, and the ease with which integrals over Gaussian type functions can be evaluated analytically (see appendix A.1), gives a computational advantage, greater than the disadvantage of having to use a larger number of functions.
The Coulomb cusp condition has more serious consequences. It states that the Coulomb hole should have a cusp at the points of coalescence and should increase linearly in whatever direction one moves from the point $r_{ij} = 0$ (again as illustrated on fig.3.1.1). The following sections introduces ways of modeling this complex situation.

Chapter 4

Post HF Methods

The previous sections dealt with the deficiencies of the single determinant ansatz for the approximate wave function. It is in order to comment on the accuracy of the HF method before claiming that post-HF methods are needed. While the energy gained from going from the simple product (Hartree) wave function to the HF wave function (the exchange energy) is relatively large the HF energy typically account for something like 99% of the total energy. The remaining energy being the correlation energy (3.1.11). How small an energy contribution the correlation energy is the total ground state energy and be decomposed in energy contributions corresponding to the operators that make up the non-relativistic Hamiltonian (2.0.2). E. Clementi and G. Corongiu [10] have made this decomposition for atoms with nuclear charges Z=1,54 and fitted the energy contributions to simple expressions of the form $E = aZ^b$ with a, b given below. Here I mention the fits for E_{coul}, E_x and E_c energies.

E_{coul}	a = 0.33781	b = 2.27092	%err = 2.89
E_x	a = -0.27874	b = 1.62198	%err = 1.19
E_c	a = -0.01696	b = 1.31023	%err = 7.78

These fits are seen plotted in fig.4.0.1 It is clear that even though significantly smaller than the Coulomb energy, the exchange makes a considerable contribution to the total energy. On the other hand the correlation energy is not even visible on the main graph and only barely visible on the inlay graph. The correlation energy could seem a negligible contribution to the total energy. In some applications this is the case and for example HF often gives good estimates of equilibrium geometries, though slightly over binding molecules. If however high, or even medium accuracy is required the correlation energy cannot be ignored and one has to resort to more advanced methods. As a final comment to fig.4.0.1 it should be noted that the ex-

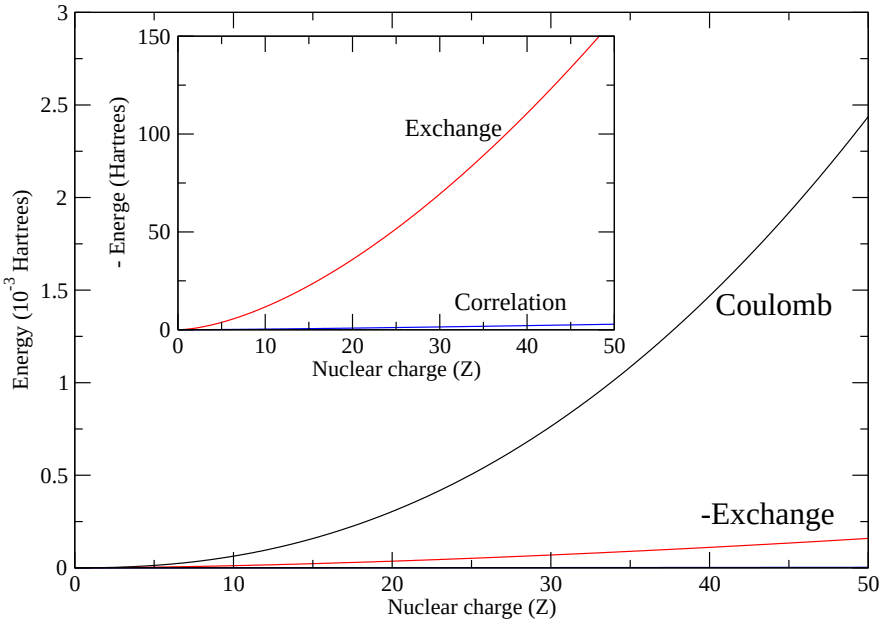

Figure 4.0.1: Coulomb, Exchange and Correlation energies of the ground state of atoms with nuclear charge Z=1,50

change and correlation energy is not only different in magnitude but also in nature clearly having different Z dependence.

That correlation presents such a small perturbation to the HF wave function suggest that correlation can be introduced by simple corrections. This forms the basis for Coulomb Hole models (see later) and DFT while standard post HF methods mentioned in the following sections present a more involved path to dynamic correlation.

4.1 Configuration Interaction

The conceptually most simple approach to correlation is the Configuration Interaction (CI) method. While being computationally expensive it does in principal offer a systematic way of recovering as much of the correlation energy as needed.
The lack of correlation in the HF method can be characterized as the inflexibility of the wave function to keep the electrons apart. For example the electrons of H_2 are less likely found in the center of the H-H bond than on each Hydrogen atom. The HF wave function does not account for this since both electrons a forced to be in the totally symmetric bonding σ_g orbital. If

the electrons are allowed to occupy the non-bonding σ_u orbital the dominant left-right correlation of the two electrons are described. If the electrons could occupy π-type orbitals, angular correlation could be described etc. This is the idea behind the CI method where the wave function is built up as a linear combination of the HF determinant and determinants generated as single, double etc. excitations of electrons from this HF determinant.

$$\Psi = \mathrm{c}_1\Phi_{\mathrm{HF}} + \sum_{\mathrm{S}} \mathrm{c}_{\mathrm{S}}\Phi_{\mathrm{S}} + \sum_{\mathrm{D}} \mathrm{c}_{\mathrm{D}}\Phi_{\mathrm{D}} + \cdots \tag{4.1.1}$$

By optimization of the coefficients of each excited determinant the CI method arises. Including all possible excited determinants in a given basis set the expansion is complete (Full CI) and gives the best possible energy within this basis set. Unfortunately this approach is only applicable to small systems. The number of determinants in a system with n electrons and M basis functions is

$$\binom{2M}{n} \tag{4.1.2}$$

A number that grows dramatically with system size. In practice the CI expansion is therefore truncated at a suitable level. In CISD only singly and doubly exited determinants are considered. Still this is not a computationally cheap method scaling as $\mathcal{O}(N^6)$.

As the size of the CI expansion is increased more and more of the correlation energy is recovered. In the Coulomb hole picture this means that our approximate wave function presents a better and better approximation to the wave function and the critical regions of electron coalescence, as illustrated on fig.4.1.2. The convergence towards the true wave function is extremely slow. For the ground state of Helium one can perform a CI type expansion of the wave function in orders of the principal quantum number N (each level including the next set of N orbitals, 1s, 2s2p, 3s3p3d etc.) [11]. It is found that in the asymptotic limit the energy error as a function of N is approximately

$$\Delta E(N) = CN^{-3} \tag{4.1.3}$$

Actually, in a finite basis set the CI wave function will never satisfy the Coulomb cusp condition and coincide with the true wave function since the expansion of the CI wave function in terms of the interelectronic distance is always in terms of r_{12}, hence having vanishing derivatives at $r_{12} = 0$. A wave function that explicitly obeys the Coulomb cusp condition can easily be designed from a CI type wave function (Ψ^{CI}) by letting r_{12} enter the wave function

$$\Psi^{CI}_{r_{12}} = (1 + \tfrac{1}{2}r_{12})\Psi^{CI} \tag{4.1.4}$$

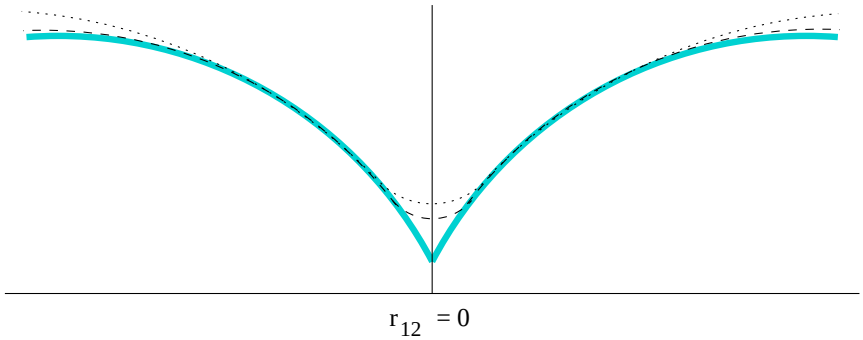

Figure 4.1.2: Schematic illustration of the true wave function (thick gray line), compared to two CI-type wave functions where the dashed one is of higher accuracy than the dotted one.

Such methods employing r_{12} to impose a better description of the cusp are called explicitly correlated or r12 methods. While being able to provide a faster convergence of the correlation energy their computational cost makes them less appealing. Implementations that efficiently evaluate the "new" types of two electron integrals have been devised and r12 second order Møller Plesset Perturbation (MP2) [12,13] and r12 Couples Cluster methods [14,15] have been performed, though these methods are still not applicable to large systems.
The most complete explicitly correlated CI type wave function is the Hylleraas wave function [16,17]. By letting the CI expansion include all power of the interelectronic distance the wave function is written as (in the simplified totally symmetric, singlet two electron case)

$$\Psi^H = \exp[-\xi(r_1 + r_2)] \sum_{ijk} C_{ijk}(r_1^i r_2^j + r_2^i r_1^j) r_{12}^k \tag{4.1.5}$$

This wave function is capable of recovering the correlation energy with micro Hartree (μE_h) accuracy.

It is without doubt that the existence of the Coulomb hole is the reason for the need of long CI expansions if high accuracy is needed. An important conclusion to draw however is that an accurate description of the cusp itself is not needed in the regime of accuracy we are normally interested in (mE_h). In this regime the description of the entire Coulomb hole is the goal. Only if μE_h errors are the goal is the description of the cusp important. This viewpoint has been brought forward by P. Gilbert [18] and more recently

by Prendergast *et al.* [19], where an investigation of the CI convergence was carried out using a cuspless two electron operator. The conclusion is not surprising however. The level of detail you should put into the description of the Coulomb hole and the cusp depends on what level of accuracy you are aiming at. Finally it should be clear that a CI type wave function that has been released from dealing with the Coulomb hole should experience a fast converge. This is the main motivation for the hybrid models presented in chapter III.

4.2 Multi Configurational Self Consistent Field

The CI wave functions built from the HF ground state determinant and determinants generated by exciting electrons from the HF determinant has some drawbacks. The HF determinant might not be a good approximation to the state of the system in question. As a result it might be necessary to include a large number of determinants to describe this state. In other words the CI expansion was not done in a suitable basis of Slater determinants.
The Multi Configuration Self Consistent Field (MCSCF) method avoids these problems. It too is a CI type wave function expansion (4.1.1) but instead of just optimizing the CI coefficient the MOs used for constructing the Slater determinants are also optimized in a self consistent manner. The procedure is therefore iterative like the HF method, and can in fact be though of as reducing to regular CI if the MOs are fixed, or reducing to HF if only a single Slater determinant is considered.
Since the CI expansion of MCSCF theory is performed in the optimal set of determinants (within the given basis set and active set of orbitals chosen) the CI expansion can be expected to shorter than in regular CI. The simultaneous optimization of MOs and Slater determinants however makes it more computationally expensive than a CI with a determinant expansion of equal length. A compromise would be to get the few optimal configurations needed in a given application from a MCSCF optimization and subsequently perform a Multi Reference Configuration Interaction (MRCI) calculation in this basis of configurations.
The MO optimization in MCSCF rarely recovers a significant amount of dynamic correlation but generating the optimal set of configurations it is an efficient way of recovering static correlation. The MCSCF method is however general and in principle capable of recovering both static and dynamic correlation.

4.3 Perturbation Theory.

Perturbation theory presents another way of improving upon the HF method. Møller Plesset Perturbation theory [20] assumes that the HF Hamiltonian[1] H_0 present a good approximation to the Hamiltonian, meaning that the difference between the HF and the true H can be written as a small perturbation

$$\hat{H} = \hat{H}_0 + \lambda \hat{V} \tag{4.3.6}$$

Since the sum of Fock operators count the electron repulsion twice the perturbation becomes the exact electron repulsions minus twice the electron repulsion from H_0. Taylor expanding the exact energy and wave function in powers of the perturbation

$$\Psi = \Psi^{(0)} + \lambda\Psi^{(1)} + \lambda^2\Psi^{(2)} + \cdots \tag{4.3.7}$$
$$E = E^{(0)} + \lambda E^{(1)} + \lambda^2 E^{(2)} + \cdots \tag{4.3.8}$$

the perturbed Schrödinger equation writes

$$\begin{aligned}&(\hat{H}_0 + \lambda\hat{V})(\Psi^{(0)} + \lambda\Psi^{(1)} + \lambda^2\Psi^{(2)} + \cdots) = \\ &(E^{(0)} + \lambda E^{(1)} + \lambda^2 E^{(2)} + \cdots)(\Psi^{(0)} + \lambda\Psi^{(1)} + \lambda^2\Psi^{(2)} + \cdots)\end{aligned} \tag{4.3.9}$$

We can collect terms of equal power in λ

$$\hat{H}_0\Psi^{(0)} = E^{(0)} \tag{4.3.10}$$
$$\hat{H}_0\Psi^{(1)} + \hat{V}\Psi^{(0)} = E^{(0)}\Psi^{(1)} + E^1\Psi^{(0)} \tag{4.3.11}$$
$$\hat{H}_0\Psi^{(2)} + \hat{V}\Psi^{(1)} = E^{(0)}\Psi^{(2)} + E^1\Psi^{(1)} + E^2\Psi^{(0)} \tag{4.3.12}$$

and so forth. Multiplication from the left with $\Psi^{(0)}$ and integration yields the n'th order energy corrections

$$E^{(0)} = \langle\Psi^{(0)} \mid \hat{H}_0 \mid \Psi^{(0)}\rangle \tag{4.3.13}$$
$$E^{(1)} = \langle\Psi^{(0)} \mid \hat{V} \mid \Psi^{(0)}\rangle \tag{4.3.14}$$
$$E^{(2)} = \langle\Psi^{(0)} \mid \hat{V} \mid \Psi^{(1)}\rangle \tag{4.3.15}$$

and so on. The 1st order correction therefore adds up to the usual HF energy and the second order correction is needed to include any correlation. For this the first order correction to the wave function is needed. To proceed it is utilized that the solutions to the unperturbed Schrödinger equation form

[1] H_0 is the sum of Fock operators : $H_0 = \sum_i^N \left(\mathbf{h}_i + \sum_j^N [\mathbf{J}_{ij} - \mathbf{K}_{ij}]\right)$

a complete set of functions ($\Phi_i^{(0)}$) in which we can expand the first order correction to the wave function

$$\Psi^{(1)} = \sum_n c_n^{(1)} \Phi_n^{(0)} \tag{4.3.16}$$

Inserting this into Eq.4.3.11, multiplying from the left with $\Psi^{(0)}$ and integrating these expansion coefficients can be found

$$c_n^{(1)} = -\frac{\langle \Phi_n^{(0)} \mid \hat{V} \mid \Phi_0^{(0)} \rangle}{E_n^{(0)} - E_0^{(0)}} \tag{4.3.17}$$

With this the second order correction to the energy can be derived

$$E^{(2)} = \frac{1}{4} \sum_{i,j} \sum_{a,b} \frac{[(ia \mid jb) - (ib \mid ja)]^2}{\varepsilon_a + \varepsilon_b - \varepsilon_i - \varepsilon_j} \tag{4.3.18}$$

where i, j denotes occupied orbitals and a, b denotes virtual orbitals.

Including up to the second order correction in the energy yields the second order Møller Plesset method (MP2). Computation of the second order energy correction requires the transformation of the two electron integrals from the AO basis to MO basis. A procedure that scales as N^5. Still MP2 is a fairly cheap way of including a major part of the dynamic correlation giving reliable geometries [11, 21]. Higher order energy and wave function corrections can be included to give the MP3, MP4 etc. methods. These methods have become less popular, both because an unfavorable cost accuracy ratio compared to methods like Coupled Cluster (CC, see below) and because the convergence of the MPn series is known to oscillate for some systems [11].

An attempt to provide a more general perturbative approach to correlation that is also capable of dealing with static correlation is provided by CASPT2 [22]. This is essentially an extension of MCSCF theory to let dynamical correlation be described by second order perturbation theory, but while high accuracy can be achieved this way the computational cost still prohibits large scale calculations.

4.4 Coupled Cluster Theory.

The main idea of the perturbative Coupled Cluster Theory (CC) [23, 24] is to include all corrections of a given type to infinite order. The CC wave

function is written

$$\begin{aligned} \Psi &= \exp(\hat{T})\Psi_{HF} \\ &= \exp(\hat{T}_1 + \hat{T}_2 + \hat{T}_3 + \cdots)\Psi_{HF} \end{aligned} \tag{4.4.19}$$

where $\hat{T}_i$ generates all the i'th excited determinants from the reference (HF) wave function

$$\hat{T}_1\Psi_{HF} = \sum_i \sum_a c_i^a \Psi_i^a \tag{4.4.20}$$

$$\hat{T}_2\Psi_{HF} = \sum_{i<j} \sum_{a<b} c_{ij}^{ab} \Psi_{ij}^{ab} \tag{4.4.21}$$

and so on, where the expansion coefficients c (or amplitudes) are the unknowns.
Expansion of the exponential operator yields

$$\begin{aligned} \exp(\hat{T}) &= 1 + \hat{T} + \tfrac{1}{2}\hat{T}^2 + \tfrac{1}{6}\hat{T}^3 + \cdots \\ &= 1 + \hat{T}_1 + (\hat{T}_2 + \tfrac{1}{2}\hat{T}_1^2) + (\hat{T}_3 + \hat{T}_2\hat{T}_1 + \tfrac{1}{6}\hat{T}_1^3) + \cdots \end{aligned} \tag{4.4.22}$$

where the terms have been grouped so that the first term generates all singly excited determinants, the terms in the first parenthesis generate all double exited determinants, etc.
To make CC theory computationally feasible the Cluster operator $\hat{T}$ is truncated at some level. Including only single and double excitations in $\hat{T}$ yields the CCSD method where the wave function can be written

$$\begin{aligned} \Psi_{CCSD} &= \Psi_{HF} + \hat{T}_1\Psi_{HF} + \left(\hat{T}_2 + \tfrac{1}{2}\hat{T}_1^2\right)\Psi_{HF} + \left(\hat{T}_2\hat{T}_1 + \tfrac{1}{6}\hat{T}_1^3\right)\Psi_{HF} \\ &+ \left(\tfrac{1}{2}\hat{T}_2^2 + \tfrac{1}{2}\hat{T}_2\hat{T}_1^2 + \tfrac{1}{24}\hat{T}_1^4\right)\Psi_{HF} + \cdots \end{aligned} \tag{4.4.23}$$

From this the advantage of CC theory is clear. Even though the cluster operator is truncated at n=2 the CCSD wave function includes contributions to triple, quadruple and higher order excitations as products of first and second order excitations. In the "CI picture" this means that in the CCSD model all determinants have nonzero coefficients in the FCI expansion of the wave function whereas CISD only includes up to doubly excited determinants. In particular the CCSD method includes the dominant contribution to the quadruple excitations ($\hat{T}_2^2$).
This non-linear parameterization of the CC wave function means that CC converges much faster towards the FCI limit than CI. The inclusion of all

excitations from a truncated cluster operator to infinite order furthermore means that the CC method is size consistent in contrast to the truncated CI methods.

Deriving the expression for the amplitudes and the energy is beyond the scope of this CC review. Here I will restrict myself to just mention that the amplitudes can be derived by multiplying the Schrödinger equation

$$\exp(-\hat{T})\hat{H}\exp(\hat{T})\Psi_{HF} = E_{CC}\Psi_{HF} \tag{4.4.24}$$

from the left by all singles and doubles configurations and solving the non-linear equations for the amplitudes (see for example [11]). The CC energy is obtained from Eq.4.4.24 upon multiplication form the left by the reference wave function Ψ_{HF}.

As a final note on CC theory it should be mentioned that while the CCSD method is applicable to fairly large system (N^6 scaling) the higher order corrections become unpractical for anything but the smallest systems (N^8 scaling). A economical compromise is to include the effects of the triples from perturbation theory which defines the CCSD(T) method [25]. With a N^7 scaling this method is readily applied to small and medium sized systems and typically reduces the error in the correlation energy with a factor of 5 to 10 compared to the CCSD model which typically already recovers 95% of the correlation energy [26].

4.5 Density Functional Theory

4.5.1 Introduction

While the standard methods presented in the previous sections are in principle capable of providing as high accuracy as needed their computational cost prohibits this in practice. This was seen to be due to the difficulty in describing closely interaction electrons, i.e the exchange and correlation holes. To put it differently, the wave function based methods need to deal with a complex wave function of 4N variables, the spatial and spin variables for each electron. The force of Density Functional Theory (DFT) is that it avoids dealing directly with the wave function but instead derive the energy of a system in terms of the electronic density, thereby reducing the dimensionality of the problem significantly.
As such, DFT is as old as quantum mechanics itself and actually predates the HF model. In 1927 Thomas [27] and Fermi [28] proposed a simple expression for the kinetic energy of a uniform electron gas and combined with the nuclear attraction and classical Coulomb repulsion their gave an expression for the energy of an atom purely in terms of the density. Shortly thereafter Dirac [29] expressed the exchange energy of a uniform electron gas in terms of the density, a functional form of the exchange energy that was reused, yet with a different prefactor, when Slater [30] sought an approximation for the Hartree-Fock Exchange (the X_α or Hartree-Fock-Slater exchange).

4.5.2 The Hohenberg-Kohn Theorems

Though DFT and wave function theory (WFT) are of equal age, DFT was not given a formal footing until 1964 when Hohenberg and Kohn [31] showed that the electron density in fact does uniquely determine the system and its properties. To quote the famous article : "*the external potential* $V_{ext}(\mathbf{r})$ *is (to within a constant) a unique functional of* $\rho(\mathbf{r})$*; since, in turn* $V_{ext}(\mathbf{r})$ *fixes* $\hat{H}$ *we see that the full many particle ground state is a unique functional of* $\rho(\mathbf{r})$". The proof of this first theorem is strikingly elementary and runs by contradiction. A just as elegant way of looking at the DFT WFT correspondence is the following. As mentioned in the previous section the exact wave function obeys the Nuclear cusp condition. The equivalent condition for the density writes

$$\frac{\partial}{\partial \mathbf{r}_A}\rho(\mathbf{r}_A)\bigg|_{\mathbf{r}_A=0} = -2Z_A\rho(0) \tag{4.5.1}$$

Given the exact density we are in principle therefore capable of locating the position of the nuclei of the system where the density has its cusps. Moreover

the charge of the nuclei can be determined from the slope of the density in these points. Given this information the full Hamiltonian of the Schrödinger equation is known and the wave function can in principle be found. In fact since the Hamiltonian can be built from the ground state density the properties of all states, ground state and excited states, can in principle be found from the ground state density. The fact that DFT is termed a ground state theory is due to the *second Hohenberg-Kohn theorem* which brings the variational principle into DFT. In short, it states that for any trial density $\tilde{\rho}(\mathbf{r})$, with $\tilde{\rho}(\mathbf{r}) \geq 0$ and $\int \tilde{\rho}(\mathbf{r})d\mathbf{r} = N$, the energy associated with the trial density is an upper bound for the ground state energy.

$$E_0 = E[\rho] \leq E[\tilde{\rho}] \tag{4.5.2}$$

Again the proof is simple since the first theorem relates the trial density $\tilde{\rho}(\mathbf{r})$ to a trial Hamiltonian $\tilde{H}$ and trial wave function $\tilde{\Psi}$ for which the variation principle relates the expectation value of the Hamiltonian to the expectation value of the ground state wave function.

$$\langle \tilde{\Psi} \mid \tilde{H} \mid \tilde{\Psi} \rangle = \int \tilde{\rho}(\mathbf{r}) v_{\text{ext}}(\mathbf{r}) d\mathbf{r} + T[\tilde{\rho}] + V_{ee}[\tilde{\rho}] = E[\tilde{\rho}] \geq E_0[\rho_0] = \langle \Psi_0 \mid \hat{H} \mid \Psi_0 \rangle \tag{4.5.3}$$

where $v(r_i) = V_{\text{ext}}(r_i) = \sum_A^N -\frac{Z_A}{r_{iA}}$. Two assumptions have been made. That the ground state is not degenerate and that the density arises from an antisymmetric wave function with a Hamiltonian determined by some external potential. Such a density is called v-representable.

4.5.3 The Constrained Search Formulation

The Levy Constrained Search [32] formulates a practical way of searching for the optimal density and at the same time lifts the constraints present in the second Hohenberg-Kohn theorem.
The sought density only needs to be N-representable, i.e. it can be obtained from an antisymmetric wave function. The starting point is again the variational principle which allows a comparison of the energy of the ground state energy E_0 and that of a trial wave function Ψ_{ρ_0} that integrates to the ground state density $\rho_0(\mathbf{r})$.

$$\langle \Psi_{\rho_0} \mid \hat{H} \mid \Psi_{\rho_0} \rangle \geq \langle \Psi_0 \mid \hat{H} \mid \Psi_0 \rangle = E_0 \tag{4.5.4}$$

The external potential is determined purely be the density which is equal for the wave functions considered here. Hence it can be eliminated from the inequality

$$\langle \Psi_{\rho_0} \mid \hat{T} + \hat{V}_{ee} \mid \Psi_{\rho_0} \rangle \geq \langle \Psi_0 \mid \hat{T} + \hat{V}_{ee} \mid \Psi_0 \rangle \tag{4.5.5}$$

The optimal wave function Ψ_0 is therefore the wave function that minimizes the expectation value of $\hat{T}$ and $\hat{V}_{ee}$. Levy defined the universal functional $F[\rho]$ as

$$F[\rho] = \min_{\Psi \to \rho} \langle \Psi \mid \hat{T} + \hat{V}_{ee} \mid \Psi \rangle \tag{4.5.6}$$

which searches all Ψ that yield a given density ρ. The ground state energy is now found by searching for N-representable ρ which yield the minimum energy

$$E_0 = \min_{\rho \to N} \left[F[\rho] + \int v(\mathbf{r}) \rho(\mathbf{r}) d\mathbf{r} \right] \tag{4.5.7}$$

In the case of a degenerate ground state only one wave function would be picked out by $F[\rho]$ out of the set of degenerate Ψ. Namely the Ψ associated with ρ_0.

4.5.4 The Kohn Sham Approach

With the Hohenberg-Kohn theorems the existence of the universal functional $F[\rho]$ (4.5.6) was proven. Had it been known the solution to the Schrödinger equation would have been known. Indeed the earliest attempts at DFT can be viewed as attempts to find approximate forms to the contributions to $F[\rho]$. It quickly became clear that finding sufficiently good approximations to each term separately was impossible and this could very well be why DFT was largely ignored until 1965 when Kohn and Sham [33] presented their approach. This approach introduces the non-interacting system: a fictitious system of N electrons not interacting by Coulombic interactions but subjected to an effective potential to ensure this reference system has the same density as the physical system. The introduction of this reference system was motivated by the observation that since the kinetic energy constitutes such a large fraction of the total energy this term should be accurately presented. For the non-interacting system the exact solution is known to be a single determinant with the kinetic energy given by

$$T_s[\rho] = -\tfrac{1}{2} \sum_{i}^{N} \langle \phi_i \mid \nabla^2 \mid \phi_i \rangle \tag{4.5.8}$$

where ϕ_i is a spin-orbital of the Slater determinant as in 3.0.2, although not the same ones as in HF theory and ρ given as $\rho(\mathbf{r}) = \sum_i^N \mid \phi_i(\mathbf{r}) \mid^2$. With ρ being the same as the true density $T_s[\rho]$ is a very good approximation, but not equal to, the exact kinetic energy $T[\rho]$. Kohn and Sham decomposed the energy as

$$E[\rho] = T_s[\rho] + J[\rho] + \int v(\mathbf{r}) \rho(\mathbf{r}) + E_{xc}[\rho] \tag{4.5.9}$$

where the only unknown $E_{xc}[\rho]$ now contains all the problematic terms : the remaining part of the kinetic energy and the non-classical two electron interaction

$$E_{xc}[\rho] = (T[\rho] - T_s[\rho]) + (V_{ee}[\rho] - J[\rho]) \tag{4.5.10}$$

Though the energy is purely a functional of the ground state density, orbitals need to be introduced to equate the non-interacting kinetic energy T_s. Minimization of the energy under the constraint that the Kohn-Sham orbitals stay orthonormal yields the Kohn-Sham equations

$$\left[-\tfrac{1}{2}\nabla^2 + v_{\text{eff}}(\mathbf{r})\right]\phi_i = \varepsilon_i\phi_i \tag{4.5.11}$$

$$v_{\text{eff}}(\mathbf{r}) = v(\mathbf{r}) + \int \frac{\rho(\mathbf{r}')}{\mid \mathbf{r} - \mathbf{r}' \mid} d\mathbf{r}' + v_{xc}(\mathbf{r}) \tag{4.5.12}$$

$$v_{xc}(\mathbf{r}) = \frac{\partial E_{xc}[\rho]}{\partial \rho(\mathbf{r})} \tag{4.5.13}$$

Just like the Hartree-Fock equation, the Kohn-Sham equations Eq.4.5.11 needs to be solved iteratively since the effective potential depends on the density. Had E_{xc} been known the solution to the Kohn-Sham pseudo eigenvalue equations would have been the exact solution, covering all correlation effects. In practice we have to resort to approximate functionals.

4.5.5 The Adiabatic Connection

The adiabatic connection [34] offers a convenient way of connecting the non-interacting system with the interacting (physical) system. At the same time it provides information on how to construct good approximate exchange correlation functionals by making a connection between the unknown functional and the exchange and Coulomb holes mentioned in sec.3.2.
In the adiabatic connection an effective Hamiltonian is built from the real Hamiltonian by introducing a coupling strength parameter μ

$$\hat{H}_{\text{eff}}(\mu) = \hat{T} + \hat{V}^{\mu}_{\text{eff}} + \hat{W}^{\mu}_{ee} \tag{4.5.14}$$

$\hat{W}^{\mu}_{ee}$ is the μ-dependent two-electron interaction and $\hat{V}^{\mu}_{\text{eff}}$ is an effective external potential that keeps the density of the system equal to that of the real physical system. Many forms of the μ-dependence of $\hat{W}^{\mu}_{ee}$ could be chosen. For this purpose we choose a simple form

$$\hat{W}^{\mu}_{ee} = \mu \sum_{i<j} \frac{1}{r_{ij}} \tag{4.5.15}$$

The Kohn-Sham non-interacting system (recovered at $\mu = 0$) is now connected to the fully interaction system ($\mu = 1$) by partially interacting systems ($\mu =]0, 1[$). The energy of the physical (fully interacting) system is now given from the non-interacting system by

$$\begin{aligned} E_{\mu=1} &= E_{\mu=0} + \int_0^1 \frac{dE(\mu)}{d\mu} d\mu \qquad (4.5.16) \\ &= \langle \Psi^\mu \mid \hat{T}_s + \hat{V}_{\text{eff}}^{\mu=0} \mid \Psi^\mu \rangle + \int_0^1 \frac{dE(\mu)}{d\mu} d\mu \qquad (4.5.17) \end{aligned}$$

To be able to benefit from this connection an expression for the μ-dependence of E is found

$$\frac{dE(\mu)}{d\mu} = \left\langle \Psi^\mu \left| \frac{d\hat{H}_{\text{eff}}(\mu)}{d\mu} \right| \Psi^\mu \right\rangle = \left\langle \Psi^\mu \left| \frac{d\hat{V}_{\text{eff}}^\mu}{d\mu} \right| \Psi^\mu \right\rangle + \left\langle \Psi^\mu \left| \frac{d\hat{W}_{ee}^\mu}{d\mu} \right| \Psi^\mu \right\rangle \qquad (4.5.18)$$

which upon integration of μ**?**yields

$$\int_0^1 d\mu \left\langle \Psi^\mu \left| \frac{d\hat{V}_{\text{eff}}^\mu}{d\mu} \right| \Psi^\mu \right\rangle = \int d\mathbf{r} [\hat{V}_{\text{ext}}(\mathbf{r}) - \hat{V}_{\text{eff}}^{\mu=0}(\mathbf{r})] \rho(\mathbf{r}) \qquad (4.5.19)$$

and

$$\begin{aligned} \int_0^1 d\mu \left\langle \Psi^\mu \left| \frac{d\hat{W}_{ee}^\mu}{d\mu} \right| \Psi^\mu \right\rangle &= \int_0^1 d\mu \frac{1}{2} \iint d\mathbf{r}_1 d\mathbf{r}_2 \frac{d\hat{W}_{ee}^\mu}{d\mu} \rho_2^\mu(\mathbf{r}_1, \mathbf{r}_2) \\ &= \int_0^1 d\mu \frac{1}{2} \iint d\mathbf{r}_1 d\mathbf{r}_2 \frac{d\hat{W}_{ee}^\mu}{d\mu} [\rho(\mathbf{r}_1)\rho(\mathbf{r}_2) + \rho(\mathbf{r}_1) h^\mu(\mathbf{r}_2; \mathbf{r}_1)] \\ &= \frac{1}{2} \iint \frac{\rho(\mathbf{r}_1)\rho(\mathbf{r}_2)}{r_{12}} d\mathbf{r}_1 d\mathbf{r}_2 + \\ &\quad \frac{1}{2} \iint \int_0^1 \frac{dh^\mu(\mathbf{r}_2; \mathbf{r}_1)}{d\mu} d\mu \frac{\rho(\mathbf{r}_1)}{r_{12}} d\mathbf{r}_1 d\mathbf{r}_2 \qquad (4.5.20) \end{aligned}$$

Collecting all terms the energy writes

$$E[\rho] = E_{\mu=1}[\rho] = \langle \Psi^\mu \mid \hat{T}_s + \hat{V}_{\text{ext}} \mid \Psi^\mu \rangle + \frac{1}{2} \iint \frac{\rho(\mathbf{r}_1)\rho(\mathbf{r}_2)}{r_{12}} d\mathbf{r}_1 d\mathbf{r}_2 + E_{xc}[\rho] \qquad (4.5.21)$$

as in (4.5.9). The new thing is that the exchange correlation functional has now been expressed by the coupling strength dependent exchange correlation hole

$$E_{xc}[\rho] = \frac{1}{2} \iint \int_0^1 \frac{dh^\mu(\mathbf{r}_2; \mathbf{r}_1)}{d\mu} d\mu \frac{\rho(\mathbf{r}_1)}{r_{12}} d\mathbf{r}_1 d\mathbf{r}_2 \qquad (4.5.22)$$

The difference in this expression and the one found earlier for the exchange correlation hole (3.2.7) is that (4.5.22) also includes the correction for the error introduced by replacing the kinetic energy for the physical system with the much easier computed kinetic energy for the non-interaction system. This correction is handled by the integration of the hole over the coupling strength parameter (μ).

4.5.6 Approximate Functionals

The big accomplishment of the Kohn-Sham formulation is that as much of the energy as possible is computed exactly so that the exchange correlation functional *only* had to cover minor corrections.
The adiabatic connection made a correspondence between the exchange correlation hole and the functionals that we seek. Thus the functionals must describe the spherical average of the exact hole. A simple model system is the *uniform electron gas* which works surprisingly well considering its simple nature. Model functionals derived from the uniform electron gas have already been presented in sec.4.5.1, the Dirac and Dirac-Slater exchange. The correlation part cannot likewise be derived analytically but instead several analytical expressions have been suggested on the basis of accurate Monte Carlo calculations on the uniform electron gas. The most widely used representation is due to Vosko, Wilk and Nusair [35], denoted the VWN correlation functional. When combined with Slater Exchange this exchange correlation functional is referred to as the Local Density Functional (LDA) and widely used. Although LDA is by no means the most accurate approximate functional available it has been, and still is, successfully applied in many application and remains a very reliable model. The errors of LDA are very systematic with the total exchange typically being underestimated by 10% while correlation is typically overestimated by a factor of 2 or 3. Since the exchange energy is an order of magnitude larger than the correlation energy the LDA model benefits from an error cancellation which brings the typical LDA exchange correlation error to about 7%. HOMO LUMO gaps are consistently underestimated by LDA and just as consistently LDA over binds molecules. However at small inter electronic distances the exchange correlation hole provided by LDA agrees reasonable well with the exact hole, a property that is also reflected in its name. In LDA the neighborhood of a reference electron is treated as if it was part of a homogenous electron gas of constant density. This is a good approximation in solid state physics but might not always apply to atoms and molecules where the density can be expected to vary considerably. The logical step to take from LDA is letting the functional not only depend on the density but also of the gradient

of the density. Such *Gradient Expansion approximations* (GEA) try to take the non-homogeneity into account. A straightforward implementation of this idea would however not improve on LDA due to the fact that the holes of GEA functionals, unlike LDA holes, does not fulfill the sum rules of the exact holes. Enforcing these properties and thereby "fixing" the holes greatly improves upon GEA and produces the *generalized gradient approximation* (GGA). Popular implementations of these ideas is the exchange functional by Becke [36], called B^{88} or just B, which presents a correction to Dirac exchange, and the correlation functional by Lee, Yang and Parr [37] which is basically a functional fitting of an expression for the correlation energy by Colle and Salvetti [38] that will be mentioned in chapter 6. The combination of the exchange and correlation functionals (BLYP) present a very successful approximation.

Another class of functionals arise from the same motivation that led Kohn and Sham to let the kinetic energy be evaluated from a Slater determinant. If this was a success the why not apply the same reasoning to the exchange energy since this by far is the largest contribution to E_{xc}. Letting the exchange energy be calculated from the Slater determinant (exact exchange) and combining with a functional for the correlation hole proves to be an unsuccessful combination. In short one can say that the approximate functionals rely to some degree on the fact that the total exchange correlation hole is localized around the reference electron while each component can be delocalized. By construction both the exchange and correlation holes are fairly localized meaning that the total functional can be a good approximation to the total exact hole, but each component separately can not. Therefore the combination of a localized approximate correlation hole with a delocalized "exact" exchange hole is not a good idea. Becke viewed this problem in the light of the adiabatic connection and proposed that the exchange energy can be written as a mixture of exact exchange (the $\mu = 0$ limit) and the exchange energy from a functional (an approximation to the $\mu = 1$ limit). As a first approximation a half and half mixture of exact and functional exchange was proposed [39] but this this was significantly improved by the three parameter combination of Becke exchange with exact exchange and LYP correlation [40] (B3LYP). This is perhaps the most popular functional of modern density functional theory.

Despite the fact that modern approximate functionals do normally provide sufficiently accurate descriptions of the exchange correlation hole there are some problems associated with taking this "short-cut" to correlation. As mentioned a property of the exchange term in HF theory is that it completely

cancels with the classical Coulomb term for $r_2 \rightarrow r_1$. Replacing the HF exchange with an approximate functional exchange this is not fulfilled in DFT giving rise to the *self interaction error* - the fact that in DFT the isolated electron has a non-vanishing contribution from $J[\rho] + E_{xc}[\rho]$. Though several approaches to remedy this has been proposed the increased complexity associated with these *self-interaction corrections* (SIC) means they are not widely applied. Actually it is sometimes found that SIC deteriorates the DFT results. The work of Cremer *et al.* [41] even suggests that the effect self interaction has on the density mimics the effect of static correlation. This does not mean that DFT in general accounts for all static correlation effects, unless the exact functional is found. Being a single determinant ansatz DFT with approximate functionals is not capable of dealing with degeneracy and dissociation. Ensemble DFT is an attempt to deal with these issues [42].

A related classic problem of DFT is the asymptotic behavior of the exchange correlation potential. The exact potential should behave like $-\frac{1}{r}$ for large distances from the nuclei. The approximate potentials decay exponentially instead, i.e. much too fast. This could seem an unimportant defect but it does have unwanted consequences for virtual Kohn-Sham orbitals which will affect properties like electron affinities and properties related to the response of the system to electromagnetic fields [43, 44].

Chapter 5

Summary

It should be clear by now that though the post-HF mentioned above in principal provide us with the means to compute the wave function to as high accuracy as wanted this is not possible in practice and the post-HF methods all have their pros and cons. The multi-reference methods (especially MCSCF) can efficiently deal with static correlation and provide qualitative correct reference wave functions. They do however present a very cumbersome route to covering dynamic correlation. The single reference correlated methods : DFT, MP2, CCSD, CCSD(T) (listed with increasing computational cost) more efficiently deal with dynamic correlation but fail in efficiently describing static correlation. An ultimate goal would be a way of letting a MCSCF wave function provide a qualitatively correct reference wave function and constructing an efficient way of describing dynamic correlation from this reference wave function. If this could be achieved we would have a high quality wave function that would allow computations of energies and properties of both ground and excited states.

The next two chapters present two different proposals for such a CI/MCSCF with effective dynamic correlation scheme.

Bibliography

[1] E. Schrödinger. *Ann. Physik.*, 79:361, 1926.

[2] M. Born and J. R. Oppenheimer. *Ann. Physik.*, 84:457, 1927.

[3] D. R. Hartree. *Proc. Camb. Phil. Soc.*, 24:89, 1928.

[4] D. R. Hartree. *Proc. Camb. Phil. Soc.*, 24:111, 1928.

[5] D. R. Hartree. *Proc. Camb. Phil. Soc.*, 24:426, 1928.

[6] V. Fock. *Z. Phys*, 61:126, 1930.

[7] J. C. Slater. *Phys. Rev.*, 34:1293, 1929.

[8] J. C. Slater. *Phys. Rev.*, 35:509, 1930.

[9] T. Kato. *Commun. Pure Appl. Math.*, 10:151, 1957.

[10] E. Clementi and G. Corongiu. *Int. J. Quant. Chem.*, 62:571, 1997.

[11] T. Helgaker, P. Jørgensen, and J. Olsen. *Molecular Electronic-Structure Theory.* Wiley, Chichester, 2000.

[12] W. Klopper. *J. Chem. Phys.*, 120:10890, 2004.

[13] P. Wind, W. Klopper, and T. Helgaker. *Theor. Chem. Acc.*, 107:173, 2002.

[14] J. Noga, W. Kutzelnigg, and W. Klopper. *Chem. Phys. Lett.*, 199:497, 1992.

[15] J. Noga and W. Kutzelnigg. *J. Chem. Phys.*, 101:7738, 1994.

[16] E. A. Hylleraas. *Adv. Quant. Chem.*, 1:1, 1964.

[17] E. A. Hylleraas. *Z. Phys*, 54:347, 1929.

[18] T. L. Gilbert. *Rev. Mod. Phys.*, 35:491, 1963.

[19] D. Prendergast, M. Nolan, C. Filippi, S. Fahy, and J. C. Greer. *J. Chem. Phys.*, 115:1626, 2001.

[20] C. Møller and M. S. Plesset. *Phys. Rev. A*, 46:628, 1934.

[21] F. Pawlowski, A. Halkier, P. Jorgensen, K. L. Bak, T. Helgaker, and W. Klopper. *J. Chem. Phys.*, 118:2539, 2003.

[22] B. O. Roos, K. Andersson, M. P. Fülscher, P.-Å. Malmqvist, L. Serrano-Andrés, K. Pierloot, and M. Merchán. In I. Prigogine and S. A. Rice, editors, *Advances in Chemical Physics Vol. XCIII*, page 219. Wiley, New York, 1996.

[23] J. Cizek. *J. Chem. Phys.*, 45:4256, 1966.

[24] J. Cizek. *Adv. Chem. Phys.*, 14:35, 1969.

[25] K. Raghavachari, G. W. Trucks, J. A. Pople, and M. Head-Gordon. *Chem. Phys. Lett.*, 157:479, 1989.

[26] M. Head-Gordon. *J. Phys. Chem.*, 100:13213, 1996.

[27] L. H. Thomas. *Proc. Camb. Phil. Soc.*, 23:542, 1927.

[28] E. Fermi. *Z. Phys*, 43:73, 1928.

[29] P. A. M. Dirac. *Proc. Camb. Phil. Soc.*, 26:376, 1930.

[30] J. C. Slater. *Phys. Rev.*, 81:385, 1951.

[31] P. Hohenberg and W. Kohn. *Phys. Rev. B*, 136:864, 1964.

[32] M. Levy. *Phys. Rev. A*, 26:1200, 1982.

[33] W. Kohn and L. J. Sham. *Phys. Rev. A*, 140:1133, 1965.

[34] O. Gunnarsson and B. I. Lundqvist. *Phys. Rev. B*, 13:4274, 1976.

[35] S. J. Vosko, L. Wilk, and M. Nusair. *Can. J. Phys.*, 58:1200, 1980.

[36] A. D. Becke. *Phys. Rev. A*, 38:3098, 1988.

[37] C. Lee, W. Yang, and R. G. Parr. *Phys. Rev. B*, 37:785, 1988.

[38] R. Colle and O. Salvetti. *Theor. Chem. Acc.*, 37:329, 1975.

[39] A. D. Becke. *J. Chem. Phys.*, 98:1372, 1993.

[40] P. J. Stephens, F. J. Devlin, C. F. Chabalowski, and M. J. Frisch. *J. Chem. Phys.*, 98:11623, 1994.

[41] D. Cremer, M. Filatov, V. Polo, E. Kraka, and S. Shaik. *Int. J. Mol. Sci.*, 3:604, 2002.

[42] E. K. Gross, L. N. Oliveira, and W. Kohn. *Phys. Rev. A*, 37:2809, 1988.

[43] E. Engel, J. A. McDonald, and S. H. Vosko. *Z. Phys. D.*, 23:7, 1992.

[44] N. Rösch and S. B. Trickey. *J. Chem. Phys.*, 106:8940, 1997.

Part II

Coulomb Hole Models.

Chapter 6

Introduction

DFT is a different route to correlation than wave function theory (WFT) in that the density is the central quantity in the attempt to describe the correlation hole. Yet another category of models can be defined that directly attempts to craft the correlation hole into WFT by modifying or adding new operators to the Hamiltonian. One could say that while DFT approximates the entire expression in (4.5.22) the *Coulomb hole* models try to introduce an approximation for the hole function h^{μ} directly in the Hamiltonian.

The motivation behind the Coulomb hole models is that, as seen earlier, the Coulomb hole is a small perturbation to the electronic density when compared to the exchange hole. The latter is to a large degree taken care of when using antisymmetric wave functions and so it should be possible to reliably model the Coulomb hole which is known to only be of importance for closely interacting electrons. In the cases where static correlation is important one could, at least to a first approximation, assume that static and dynamic correlation can be treated separately and let an MCSCF type wave function deal with static correlation while an approximate scheme for recovering the final part of the dynamical correlation energy could be used. This is what the coulomb-hole models set out to provide. Care should be taken though. An obvious choice of reference wave function could be of the 'Complete Active Space Self-Consistent Field' (CASSCF) or 'Restricted Active Space Self-Consistent Field' (RASSCF) type [1], since this approach is an effective way of recovering static correlation. But being a CI-type wave function it will recover some part of the dynamic correlation as well, giving the possibility of counting part of the dynamic correlation effects twice if a coulomb-hole model is simply applied on top. If however one succeeds in making such a combination of MCSCF theory with an approximate scheme for dynamic correlation one would have a general method being capable of

describing correlation effects efficiently and allowing calculations in situations where single reference correlated methods *can* fail : near degeneracies, dissociation, exited states etc.

The Coulomb hole models try to constrain the approach of the electrons to each other, and in the earliest *hard Coulomb hole* models of E. Clementi [2, 3] this is attempted by introducing non-overlapping spheres around each electron to be seen by electrons of opposite spin. In the later *soft Coulomb hole* models of E. Clementi [4–7] and I. Panas [8–10] a smoother modeling of the Coulomb hole is attempted by performing a modification of the Coulomb operator,

$$\frac{1}{r_{12}} \rightarrow \frac{\theta(r_{12})}{r_{12}} \tag{6.0.1}$$

where $\theta(r_{12})$ is a function of the inter-electronic distance, with the properties that,

1. it approaches 1 for large inter-electronic distances, giving back the unperturbed Coulomb operator outside the Coulomb hole.

2. it decreases faster than r_{12} inside the hole, and approaches zero for small inter-electronic distances.

In this way electrons far away from each other are unaffected by the modification as our standard models have no problem describing that situation, and the only part of the interaction-space we attempt to improve is the short-range space.

Clementi's choice of such a function was $\theta(\mu r_{12}) = 1 - e^{-\mu r_{12}^2}$ where μ depended on the basis set. The Colle-Salvetti functional [11–13] is likewise a functional of the pair density (3.1.4) and can also be considered a Coulomb hole model although a connection to a modified two electron operator of the form (6.0.1) is less clear. The success of the Colle-Salvetti in modeling the Coulomb hole is evident from the fact that the LYP [14] correlation functional used in the Kohn-Sham formulation of DFT is a refitting of this functional to the density.

Chapter 7

The Coulomb Hole model of I. Panas

Panas' choice of a function that has the properties listed above, is the error-function [8–10]

$$\theta(\mu r_{12}) = \mathrm{erf}(\mu r_{12}) = \frac{2}{\sqrt{\pi}} \int_0^{\mu r_{12}} e^{-t^2} dt \tag{7.0.1}$$

where the parameter μ has been introduced to allow adjustment of the extent to which the approach of the electrons to each other should be constrained. This is illustrated on the figure of this function 7.0.1. The bigger the value of μ, the more of the unmodified Coulomb repulsion do the electrons experience. The connection between the modified two electron operator and the exchange correlation hole is clear from writing the electronic repulsion energy using the exchange correlation hole as in Eq.3.2.2

$$\begin{aligned} V_{ee}[\rho] &= \tfrac{1}{2} \iint \frac{\rho_2(\mathbf{r}_1, \mathbf{r}_2)}{r_{12}} d\mathbf{r}_1 d\mathbf{r}_2 \\ &= \tfrac{1}{2} \iint \frac{\rho(\mathbf{r}_1)\rho(\mathbf{r}_2)[1 + h_{xc}(\mathbf{r}_1, \mathbf{r}_2)]}{r_{12}} d\mathbf{r}_1 d\mathbf{r}_2 \end{aligned} \tag{7.0.2}$$

And $\theta(\mu r_{12})$ can be seen as an approximation to the correlation hole $[1 + h^{\mu}_{xc}(\mathbf{r}_1, \mathbf{r}_2)]$. One could argue that since antisymmetry already ensures an exchange hole $[1+\theta]$ should only approximate the Coulomb hole h_c. This would correspond to using the regular two electron operator for the exchange terms and the modified operator for the Coulomb terms. This approach would however introduce self-interaction since the exchange and Coulomb terms would not cancel for $\mathbf{r}_1 \rightarrow \mathbf{r}_2$[1]. Using the same μ value for both exchange and

[1]This approach has been tested and for the potential energy of H_2 the results were of much poorer quality than the model where the same μ value is used for both exchange

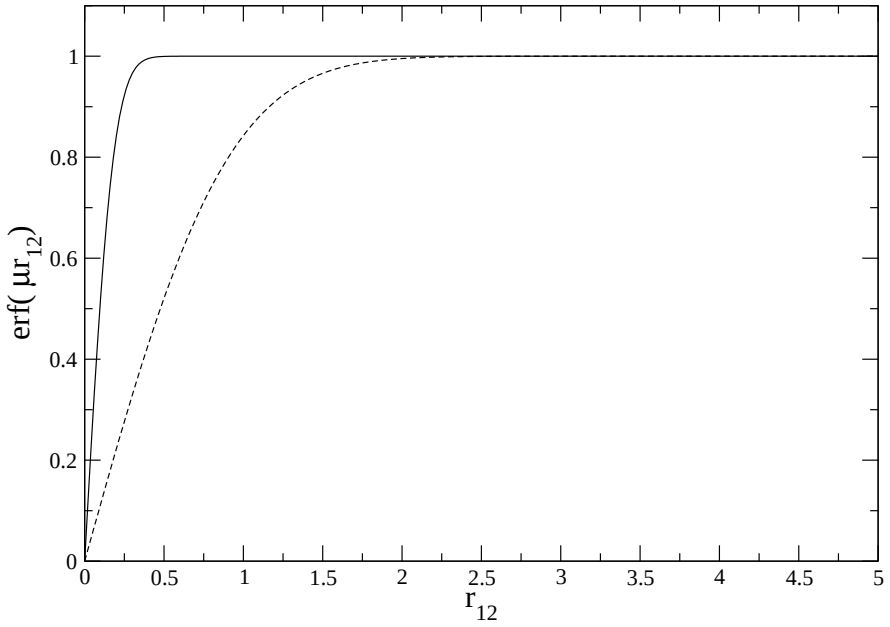

Figure 7.0.1: The error-function, erf(μr_{12}) for $\mu = 1$ (dashed line) and $\mu = 5$ (full line)

Coulomb terms the Coulomb hole model is of course self-interaction free.

7.1 Panas Corrected ERIs

The only computational difference between a normal ab initio method and a method corrected as proposed by I. Panas is the way the electronic repulsion part of the total electronic energy is calculated. Instead of the normal Coulomb operator, the modified operator of (6.0.1) is used. For the calculation of an electronic repulsion integral you get a more useful form of the modified Coulomb operator by making the substitution, $t = s \cdot r_{12}$, and using the definition of the error function one gets :

$$\frac{\theta(\mu \mathrm{r}_{12})}{\mathrm{r}_{12}} = \frac{2}{\mathrm{r}_{12}\sqrt{\pi}} \int_0^{\mathrm{r}_{12}\mu} \mathrm{e}^{-\mathrm{t}^2} \mathrm{dt} = \frac{2}{\sqrt{\pi}} \int_0^{\mu} \mathrm{e}^{-\mathrm{s}^2 \mathrm{r}_{12}^2} \mathrm{ds} \tag{7.1.3}$$

Using the Laplace transform of the unmodified Coulomb operator, equation (6.0.1) could be written as

$$\frac{2}{\sqrt{\pi}} \int_0^{\infty} \mathrm{e}^{-\mathrm{s}^2 \mathrm{r}_{12}^2} \mathrm{ds} \rightarrow \frac{2}{\sqrt{\pi}} \int_0^{\mu} \mathrm{e}^{-\mathrm{s}^2 \mathrm{r}_{12}^2} \mathrm{ds} \tag{7.1.4}$$

and Coulomb terms.

and the Panas correction is identified as a truncation of the Laplace transform of the Coulomb operator. Therefore the evaluation of Panas corrected (or regularized) integrals is basically calculated with the same effort as the normal ERIs. The evaluation is presented in AppendixB.1. The end result is that the regularized ssss integral takes the form

$$\mathrm{regERI} \;=\; 2\pi^{-7/2}\left(\frac{\mathrm{ab}}{\mathrm{a+b}}\right)^{3/2}\left(\frac{\mathrm{cd}}{\mathrm{c+d}}\right)^{3/2}\mathrm{K_{ab}K_{cd}}\cdot\sqrt{\tau}\mathrm{F}_0(\tau\mathrm{R}^2_{\mathrm{PQ}}) \tag{7.1.5}$$

All that has to be done to calculate the regularized integrals is to replace the normal reduced exponent $\eta = \frac{\alpha\beta}{\alpha+\beta}, \alpha = a+b, \beta = c+d$ by

$$\eta \to \tau = \eta\cdot\xi^2 = \frac{\eta\mu^2}{\eta+\mu^2} = \frac{1}{\frac{1}{\eta}+\frac{1}{\mu^2}} \tag{7.1.6}$$

and the Panas correction can be applied without increasing the computational effort. It is noticed that $\mu \to \infty$ restores the original repulsion integrals.

Integrals over basis functions of higher angular momentum, are calculated using a recurrence relation scheme. Following the McMurchie-Davidson [15] scheme the Gaussian charge distributions are expanded in Hermite Gaussian, and integrals of general order in the angular momentum can be expressed as derivatives of the zeroth order Boys function, as presented for the regular two electron integrals in AppendixA.2

$$\begin{aligned}\mathrm{g_{abcd}} \;=\; & 2\pi^{-7/2}\left(\frac{\mathrm{ab}}{\mathrm{a+b}}\right)^{3/2}\left(\frac{\mathrm{cd}}{\mathrm{c+d}}\right)^{3/2}\sum_{\mathrm{tuv}}\mathrm{E}^{\mathrm{ab}}_{\mathrm{tuv}}\sum_{\tau\nu\phi}(-1)^{\tau+\nu+\phi}\mathrm{E}^{\mathrm{cd}}_{\tau\nu\phi}\\ & \left(\frac{\partial}{\partial\mathrm{P_x}}\right)^{\mathrm{t}+\tau}\left(\frac{\partial}{\partial\mathrm{P_y}}\right)^{\mathrm{u}+\nu}\left(\frac{\partial}{\partial\mathrm{P_x}}\right)^{\mathrm{v}+\phi}\sqrt{\eta}\mathrm{F}_0(\eta\mathrm{R}^2_{\mathrm{PQ}})\end{aligned} \tag{7.1.7}$$

where $\sum_{tuv} E^{ab}_{tuv}$ are the expansion coefficients of the Gaussian distribution of order $n = t+u+v$ in Hermite Gaussians, formed by the product of two Gaussians centered on points a and b. Invoking the Panas correction in (7.1.6) the expression in (7.1.7) becomes

$$\begin{aligned}\mathrm{reg-g_{abcd}} \;=\; & 2\pi^{-7/2}\left(\frac{\mathrm{ab}}{\mathrm{a+b}}\right)^{3/2}\left(\frac{\mathrm{cd}}{\mathrm{c+d}}\right)^{3/2}\sum_{\mathrm{tuv}}\mathrm{E}^{\mathrm{ab}}_{\mathrm{tuv}}\sum_{\tau\nu\phi}(-1)^{\tau+\nu+\phi}\mathrm{E}^{\mathrm{cd}}_{\tau\nu\phi}\\ & \left(\frac{\partial}{\partial\mathrm{P_x}}\right)^{\mathrm{t}+\tau}\left(\frac{\partial}{\partial\mathrm{P_y}}\right)^{\mathrm{u}+\nu}\left(\frac{\partial}{\partial\mathrm{P_x}}\right)^{\mathrm{v}+\phi}\sqrt{\eta}\xi\mathrm{F}_0(\eta\xi^2\mathrm{R}^2_{\mathrm{PQ}})\end{aligned} \tag{7.1.8}$$

and the two linear combinations are identical, except that for each F_n in (7.1.7), generated by differentiation of F_0 n times, the corresponding term in (7.1.8) is multiplied by ξ^{2n+1}, and the argument to the nth order Boys function is multiplied by ξ^2.

To carry out calculations with the Panas correction an expression for μ is needed. To get an individual value of μ for each two-electron integral without using fitted parameters, Panas sought an expression for μ in terms of the basis set. In Appendix C it is shown how I. Panas ends up with expressing μ in the exponents of the Gaussian charge distributions involved in a given ERI :

$$\mu^2 = \frac{\alpha+\beta}{2} + \sqrt{\left(\frac{\alpha+\beta}{2}\right)^2 + \alpha\cdot\beta} \tag{7.1.9}$$

Panas makes another refinement though. Having grafted a Coulomb hole model onto the wave function and thereby constrained the approach of the electrons to each other, the kinetic energy must also be affected. He chooses to introduce the parameter f which, when chosen greater than one, will reduce the effect of the correction to V_{ee}, as would an actual correction to the kinetic energy, assuming that the Coulomb hole reduces the space taken up by the electrons. The need for a scaling of μ also seems reasonable when considering the simple expression for μ. Even if the expression has the right behavior, it is only based on the basis set, and it seems likely that some further calibration is needed. The modified Coulomb operator becomes,

$$\frac{1}{r_{12}} \;\rightarrow\; \frac{2}{\sqrt{\pi}}\left\{\int_0^{f\cdot\mu} \exp(-s^2 r_{12}^2)ds\right\} \tag{7.1.10}$$

the new expression for μ is,

$$\mu^2 = \frac{\alpha+\beta}{2} + \sqrt{\left(\frac{\alpha+\beta}{2}\right)^2 + \frac{\alpha\cdot\beta}{f^2}} \tag{7.1.11}$$

and the equivalent of (B.1.5) is

$$\eta \rightarrow \tau = \eta\cdot\xi^2 = \frac{\eta f^2\mu^2}{\eta + f^2\mu^2} = \frac{1}{\frac{1}{\eta}+\frac{1}{f^2\mu^2}} \tag{7.1.12}$$

Panas argues that a value of f of around 2.0 is a good choice.

7.2 Interpretation Of The Panas Model

The straightforward interpretation of the integral representation of the modified and unmodified Coulomb operators (7.1.4) is that the excess repulsion

of an uncorrelated model is simple thrown away as the integration is only carried out to a finite value. Throwing away part of V_{ee}, the total electronic energy of the Panas corrected model is expected to be lower than in the uncorrected ab initio model, as would be the case if the level of correlation was increased using standard ab initio models. This way of introducing dynamic correlation into a model is very different from the way it is usually done in ab initio models. Rather than introducing correlation by letting a number of configurations enter the wave function, the effects of correlation is mimicked by modifying the electronic repulsion operator directly. The slow convergence toward the true wave function of standard correlated ab initio methods can be characterized as the difficulty of making the wave function balance the singularity in the Coulomb operator, and therefore a faster convergence is expected if these demands are removed. This is exactly what the Panas correction sets out to do : $\frac{2}{\sqrt{\pi}}\int_0^{\mu} e^{-s^2 r_{12}^2} ds \rightarrow \frac{2\mu}{\sqrt{\pi}}$ as $r_{12} \rightarrow 0$. Assuming that μ depends on the quality of the wave function, the Panas correction can thus be characterized as making the treatment of electron repulsion fit the quality of the wave function, rather than employing the true Coulomb operator together with an approximate wave function as done in conventional ab initio methods. The expression that Panas suggests for μ (7.1.11) does not directly depend on the quality of the wave function but on the building blocks of the wave function - the basis set. This allows us to illustrate how the Panas correction affects the s-type repulsion integrals between two charge distributions of exponents α and β. Aside for some common constants the uncorrected and corrected integrals are given by $\sqrt{c}F_0(cR_{PQ}^2)$ and $\sqrt{\tau}F_0(\tau R_{PQ}^2)$ using the same notation as in section 7.1 : $c = \frac{\alpha\beta}{\alpha+\beta}$, $\tau = \frac{cf^2\mu^2}{c+f^2\mu^2}$, f=2, R_{PQ} being the distance between the center of the two charge distributions and μ calculated from (7.1.11). These functions are plotted in figure (7.2.2) in the case of relatively compact distributions($\alpha = \beta = 20$), and more diffuse distributions ($\alpha = \beta = 2$). For each of the two sets of curves, the lower one represents the modified potential. As expected the correction lowers the potential to mimic the potential present if the electrons were kept apart by correlation, and furthermore it is observed that the correction has no effect for large distances.

$$\left.\begin{array}{l}\sqrt{c}F_0(cR_{PQ}^2)\\ \sqrt{\tau}F_0(\tau R_{PQ}^2)\end{array}\right\} \rightarrow \sqrt{\frac{\pi}{4}}\frac{1}{R_{PQ}} \quad \text{as } R_{PQ} \rightarrow \infty \tag{7.2.13}$$

It is observed that for small R_{PQ} the difference between the modified and unmodified potentials is larger for the compact charge distributions ($\alpha = \beta = 20$) than for the more diffuse charge distributions ($\alpha = \beta = 2$). Furthermore, upon close inspection, it is observed that the Panas correction affects the diffuse charge distributions for larger R_{PQ} values than the compact charge

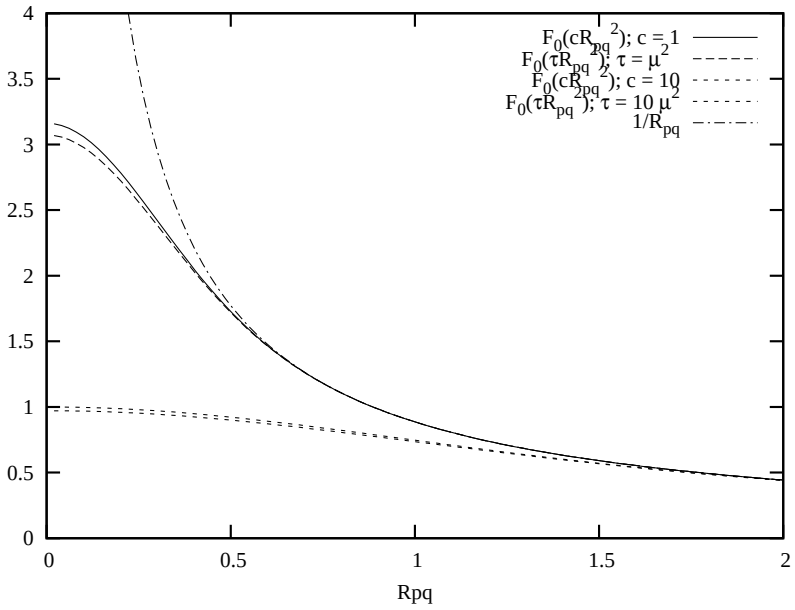

Figure 7.2.2: $\sqrt{c}F_0(cR_{PQ}^2)$ and $\sqrt{\tau}F_0(\tau R_{PQ}^2)$ for Gaussian distributions with exponents $\alpha = \beta = 20$ (upper two lines) and $\alpha = \beta = 2$ (lower two lines). The Coulomb potential from point charges ($1/R_{pq}$) is also shown.

distributions. Both observations support that the Panas correction has some of the wanted physics built into it. Since dynamic correlation is a short range effect the correction only should have an effect when electrons are likely to be close to each other. Hence,

- When electrons are located in compact charge distributions then the correction should have a relatively large effect, but the correction should die off quickly with the distance between the distributions.

- When electron are located in diffuse charge distributions the correction should have a relatively small effect, but the correction should have a longer range since the overlap of the distributions has a longer range.

7.3 Testing The Model.

In the following results from using the Panas Coulomb hole model are presented. When using the correction with some wave function, X, the method will be denoted regX. For example, regHF, is an abbreviation for the Hartree-Fock using the regularized two electron integrals, as proposed by I. Panas.

7.4 Ground State Energies And Basis Set Dependence

Using the Dalton program package [16], the ground state energies of He and Be are reported in table 7.4.1. The Panas correction is seen to lower the energy as expected. It is seen that the Panas correction only shows a slight dependence on the quality of the reference wave function but the dependence has the right behavior. Applying the correction to the MP2 wave function of He you get an energy lowering of the same order as when the correction is applied to the HF wave function. The contribution from the correction only drops slightly for the CAS wave functions and even for FCI wave function the contribution amounts to 75.8% of that gained from the HF wave function. The Panas correction is clearly not meant for use with MP2 and FCI wave functions but it is a reasonable assumption that some dependence on the quality of the reference wave function should be present and whether a refinement is needed or not will be discussed further in section 7.6.

One could also choose to use the Panas correction as a perturbation to the converged ab initio wave function. This has been tested for He and from table 7.4.2. The difference between the correlation energies from the two ways of using the correction is of the order 10^{-4}. Looking at the difference between the correlation energies obtained from the HF and CAS wave functions you get : $\Delta E^{pert}_{c,CAS}$-$\Delta E^{pert}_{c,HF} = 0.076$ and $\Delta E^{var}_{c,CAS}$-$\Delta E^{var}_{c,HF} = 0.061$. This underlines the conclusion made previously. Since the difference when going from a HF to a CAS wave function, using the modified coulomb operator in the optimization, is smaller than if you apply the correction to the optimized wave function, the CAS wave function must to some degree be affected by the corrected description of electron-electron interaction.

A final conclusion can be made from the numbers in table 7.4.1. The Panas correction seems to be quite basis set independent. As pointed out in section 7.2, this can be explained by the fact correlation is modeled by direct modification of the Coulomb operator, and having removed its singularity the need for a very flexible wave function is eliminated.

7.5 Excitation Energies

Here the vertical excitation energies of He and Ne are calculated using linear response. For He (table 7.5.3) HF, CASSCF and FCI wave functions are considered, while Ne (table 7.5.4) is treated with HF, CASSCF and CCSD. Large basis sets have been used in all cases, and the FCI (He) and CCSD

Table 7.4.1: Ground state energies (a.u.) for **He** and **Be**, with and without the Panas correction applied to reference wave functions of varying quality. The f-value of (7.1.11) is 2. The basis sets where no contraction is specified have been used uncontracted.

He

Basis set	HF	ΔE^{HF}_{Panas}	MP2	ΔE^{MP2}_{Panas}	CAS[a]	$\Delta E^{CAS\ a}_{Panas}$
$[9s \mid 7s]$	-2.8616267	-0.0227415	-2.8751044	-0.0209802	-2.8779385	-0.0207935
$[9s]$	-2.8616267	-0.0227415	-2.8751051	-0.0209800	-2.8779385	-0.0207935
$[12s]$	-2.8616280	-0.0227414	-2.8751066	-0.0209798	-2.8779397	-0.0207935
$[14s]$	-2.8616280	-0.0227415	-2.8751066	-0.0209799	-2.8779397	-0.0207935
$[14s10p10d]$	-2.8616280	-0.0227415	-2.8751066	-0.0209799	-2.8779397	-0.0207935
	FCI	ΔE^{FCI}_{Panas}				
$[14s10p10d]$	-2.9023613	-0.0172305				

Be

Basis set	HF	ΔE^{HF}_{Panas}	CASSCF[b]	$\Delta E^{CAS\ b}_{Panas}$	CASSCF	$\Delta E^{CAS\ c}_{Panas}$
$[14s9p \mid 7s47]$	-14.5729880	-0.0646824	-14.6168076	-0.0590725	-	-
$[16s11p6d]$	-14.5729890	-0.0646910	-14.6168083	-0.0590806	-14.6187913	-0.0587497
$[14s9p4d3f]$	-14.5729886	-0.0646911	-14.6168078	-0.0590806	-14.6187904	-0.0587812
$[18s12p11d]$	-14.5729893	-0.0646910	-14.6168087	-0.0590806	-14.6187967	-0.0587789

[a]Active space : 1s2s
[b]Active space : 2s2p
[c]Active space : 2s2p3s3p3d

Table 7.4.2: Correlation energy of He for HF and CAS wave functions, in an ano basis set[a] using the Panas correction in the optimization of the wave function (ΔE_c^{var}), and as a perturbation of the optimized wave function (ΔE_c^{pert}).

	E	ΔE_c^{pert}	ΔE_c^{var}
HF	-2.861626694770	-0.022648055843	-0.022741450756
CAS	-2.868637185119	-0.021712054076	-0.021800017075

[a] Basis set is that of Widmark *et al.* [17] using 6s- and 4p-functions.

(Ne) numbers are proof that these calculations have been performed near the basis set limit. A conclusion applying to both studies is that the calculated excitation energies are increased when going from the uncorrected ab initio method ($f = \infty$) to the correction suggested by I. Panas ($f \in [2, 3]$). This is the case for all the reference wave functions, and can be understood from the stabilization of the ground state from the introduction of the Coulomb hole, as mentioned previously. Again the correction is seen to be only slightly dependent of the quality of the ab initio method it is applied to. For He the ground state of the FCI wave function is lowered by : $E_{\Sigma_g^+,\text{regFCI}} - E_{\Sigma_g^+,\text{FCI}} = 3781.67\ \text{cm}^{-1}$, and this is roughly the same increase seen for all the excitation energies in the f=2.0 regFCI calculations.
HF excitation energies are generally too high, and therefore the regHF excitation energies are even worse. Small CAS wave functions give too small excitation energies for He, and applying the correction in these cases you get an improvement. For Ne the smallest CAS wave function give too large excitation energies leaving the Panas correction no chance for improving this. Though the main deficiency of a HF wave function for He is expected to be the lack of dynamic correlation it is obviously not possible to improve the excitation energies by the use of an effective dynamic correlation functional. This suggests that you need to work with a more flexible wave function as a small active space CASSCF, before a dynamic correlation correction can be expected to be a success. I will comment further on this in the next section.

7.6 Potential Energy Surfaces And Spectroscopic Constants

To see how the Panas correction behaves at different inter atomic distances, the potential energy surface of H_2 was calculated, see figure 7.6.1. Since there is an ionic contribution to the HF wave function at all inter atomic distances,

Table 7.5.3: HF,CASSCF and FCI vertical excitation energies of He in cm^{-1}. The basis is an extended uncontracted Widmark ano-basis, using 14s10p10d.

Transition	State	f	HF	CAS[a]	CAS[b]	CAS[c]	FCI	E(exp)[d]
$1s2s \leftarrow 1s^2(^1S)$	^3S	2	163789.35	159963.43	163537.79	163623.64	163572.81	
		$\sqrt{5}$	162899.25	159117.82	162787.70	162900.66	162853.45	
		2.5	162165.19	158423.32	162173.35	162309.79	162265.99	159850.32
		3	161239.69	157551.49	161406.91	161571.42	161532.98	
		∞	159008.14	155467.54	159578.91	159824.98	159802.42	
	^1S	2	174308.02	166962.21	170385.73	169985.62	169798.26	
		$\sqrt{5}$	173650.00	166180.08	169692.28	169309.12	169119.62	
		2.5	173035.66	165538.87	169125.36	168757.39	168566.05	166271.70
		3	172264.46	164735.45	168420.69	168068.86	167876.18	
		∞	170420.99	162822.15	166743.46	166447.00	166251.33	
$1s2p \leftarrow 1s^2(^1S)$	$^3P^o$	2	175735.76	169396.74	173158.97	172961.59	172830.98	
		$\sqrt{5}$	174909.60	168555.43	172415.44	172240.08	172109.83	
		2.5	174230.26	167865.06	171807.03	171650.90	171521.13	169081.19
		3	173376.35	166999.20	171051.97	170914.03	170787.01	
		∞	171329.82	164933.20	169246.70	169177.39	169055.38	
	$^1P^o$	2	179280.28	171651.22	175410.11	175016.04	174822.12	
		$\sqrt{5}$	178500.22	170833.52	174687.63	174311.68	174115.36	
		2.5	177859.61	170163.07	174096.86	173736.88	173538.72	171129.15
		3	177055.44	169322.89	173364.78	173018.95	172819.92	
		∞	175133.16	167321.50	171615.77	171327.37	171126.01	

[a]Active space : 1s2s
[b]Active space : 1s2s2p
[c]Active space : 1s2s2p3s3p3d
[d]Experimental values are from C. E. Moore [18]

Table 7.5.4: HF, CASSCF and CCSD calculations of excitation energies of Ne in cm^{-1}. The basis is an extended Widmark ano-basis : $[17s11p5d4f \mid 10s9p5d4f]$.

Transition	f	HF	CASSCF1[a]	CASSCF2[b]	CCSD	E(exp)[c]
$1s^22s^22p^53s(^3P) \leftarrow 1s^22s^22p^6(^1S)$	∞	145153.40	136778.95	137543.17		135890.67
	2	151553.53	142630.26	143546.05		135890.67
$1s^22s^22p^53s(^1P) \leftarrow 1s^22s^22p^6(^1S)$	∞	148143.07	138771.93	139471.16	134362.92	134820.60
	2	154161.98	144428.62	145300.79		134820.60
$1s^22s^22p^53p(^3S) \leftarrow 1s^22s^22p^6(^1S)$	∞	158959.49	151174.54	152277.11		148259.75
	2	166164.08	157546.36	158785.55		148259.75
$1s^22s^22p^53p(^1S) \leftarrow 1s^22s^22p^6(^1S)$	∞	163223.78	153662.05	154672.54	149572.86	148259.75
	2	169778.05	159759.83	160942.98		148259.75
$1s^22s^22p^54s(^3P) \leftarrow 1s^22s^22p^6(^1S)$	∞	171182.23	161347.28	162439.74		159536.57
	2	177789.23	167464.25	168715.83		159536.57
$1s^22s^22p^54s(^1P) \leftarrow 1s^22s^22p^6(^1S)$	∞	171825.08	161808.66	162878.97	157644.62	159381.94
	2	178342.51	167874.33	169109.39		159381.94

[a] Active space : 2s2p3s3p
[b] Active space : 2s2p3s3p3d
[c] Experimental values are from C. E. Moore [18].

Figure 7.6.1: HF and CAS ($1\sigma_g 1\sigma_u$) potential energy surface of H_2. An uncontracted ano-basis is used [$12s8p$].

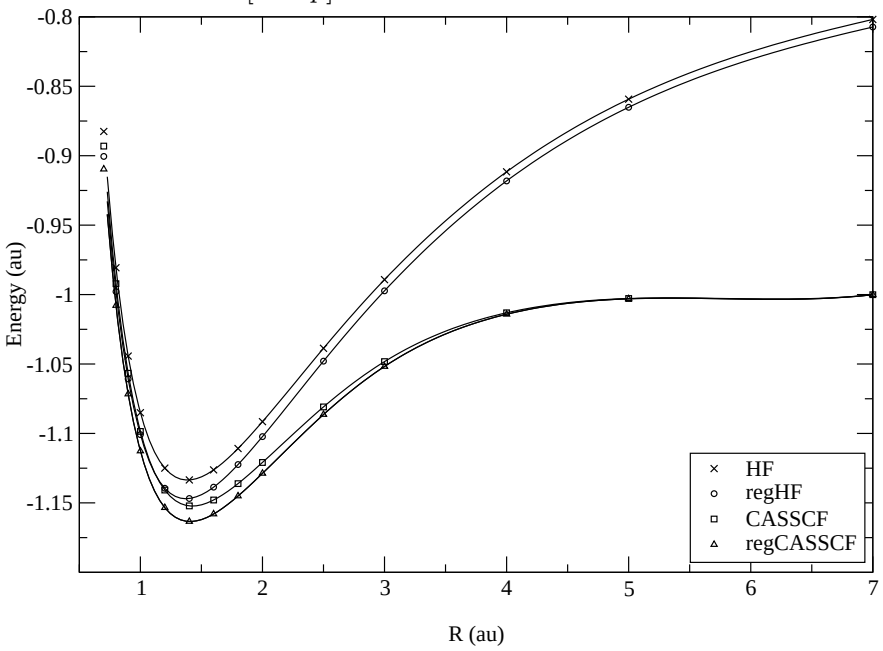

the Panas correction will have an effect at all distances. Being able to dissociate the molecule correctly, the CAS and regCAS curves coincide at large inter atomic distances and the effect of the Panas correction dies correctly off as the correlation energy of the isolated atoms is zero. The results of the geometry optimization of H_2 with HF, CAS and FCI wave functions are given in table 7.6.5. With an experimental equilibrium bond length of 0.74144Å it is seen that the HF approximation overestimates binding, and applying the Panas correction you get even worse results. The small CAS ($1\sigma_g 1\sigma_u$) underestimates binding in the H_2 molecule, and the corrected CAS produces a bond length close the experimental one. This situation is similar to the one seen for the excitation energies of He. For calculation of properties, the HF wave function seems to be incapable of benefiting from the introduction of a coulomb hole. A more flexible wave function like a small CAS is needed, even if static correlation effects are not expected to be important near the equilibrium geometry.

Using the Panas correction in geometry optimizations it will be favorable for electrons to be close to each other since this produce the largest effect from the correction. As a consequence bonds will shorten. This must be related to the fact that it has not been taken into account that the coulomb hole will also have an effect on the nuclear-electron attraction energy. As the

Table 7.6.5: Geometry-optimization of H_2. Units : E/au, r/Å, $\omega_e/\mathrm{cm}^{-1}$. Both basis sets used uncontracted.

Basis	$\frac{1}{f^2}$		HF	CAS[a]	FCI	EXP.
[14s]	0.00	E	−1.128554	−1.148788	−1.154817	–
		$r_{H\text{-}H}$	0.731783	0.755085	0.745948	0.741440
		$\omega_e(^1\Sigma_g^+)$	4575.30	4187.83	4281.90	4401.21
	0.25	E	−1.141559	−1.159452	−1.164715	–
		$r_{H\text{-}H}$	0.724994	0.745332	0.737703	0.741440
		$\omega_e(^1\Sigma_g^+)$	4654.69	4305.36	4386.22	4401.21
[14s8p]	0.00	E	−1.133599	−1.152217	−1.172213	–
		$r_{H\text{-}H}$	0.733494	0.754276	0.738803	0.741440
		$\omega_e(^1\Sigma_g^+)$	4585.40	4231.80	4483.59	4401.21
	0.25	E	−1.147109	−1.163424	−1.180975	–
		$r_{H\text{-}H}$	0.726666	0.744645	0.732753	0.741440
		$\omega_e(^1\Sigma_g^+)$	4666.01	4349.71	4521.10	4401.21

[a] Active space : $1\sigma_g 1\sigma_u$

Coulomb hole reduces the space taken by the electrons V_{ne} should also be reduced to counter balance the correction to V_{ee}. To make a correction for this, that might improve the performance of the regularized HF approach, one could attempt to deduce the modified one-electron density (ρ_1) by integration of the modified two-electron density (ρ_2) for the calculation of V_{ne}. This is not an easy task however since the correction enters the two-electron integrals and not directly the two-electron density. One could regard the Panas correction as a modification of the density

$$V_{ee}[\rho] = \iint \frac{\rho_2'(\mathbf{r}_1, \mathbf{r}_2)}{r_{12}} d\mathbf{r}_1 d\mathbf{r}_2 \tag{7.6.1}$$

with $\rho_2'(\mathbf{r}_1, \mathbf{r}_2) = \rho_2(\mathbf{r}_1, \mathbf{r}_2)\mathrm{erf}(\mu r_{12})$, but since μ depends on every exponent in the basis set there is no straight forward way of finding ρ_1' from ρ_2'.

The conclusion that spectroscopic constant obtained from HF theory does not benefit from the employment of a simple correlation functional has been reached by others as well. J. M. Pérez-Jordá *et al.* [19] use various density functionals together with Hartree-Fock and Generalized-Valence-Bond (GVB) wave functions to calculate spectroscopic constants (R_e, ω_e and D_e). They use the exact Hartree-Fock exchange, which makes their approach similar to that of I. Panas, and the following quote from their article agrees with the conclusion made here : *"... it becomes clear that correlation corrections to Hartree-Fock R_e or ω_e have little predictive value, unless the Hartree-Fock description of the molecular bond is qualitatively correct."*

7.7 Analysis Of Two-Electron Integrals

To investigate what kind of changes the integrals undergo from the correction a program was made to keep statistics on the absolute and relative differences of regularized and unregularized integrals. These are presented in table 7.7.1 for a calculation on H_2O. If the coulomb hole is expected to be a small perturbation to the wave function, the integrals are not expected to change dramatically, and the majority of the relative differences are of the order 10^{-2}-10. Some are seen to be of the order 10^3-10^4 though. Integrals purely over s-functions (not shown here) will only involve the zeroth order Boys function, and if an uncontracted basis is used you will only get positive integrals ($\mathrm{F}_0(x) \geq 0 \; \forall \; x \in [0, \infty[$), and as $\theta \cdot F_0(\alpha\theta^2 R_{PQ}^2) \leq F_0(\alpha R_{PQ}^2) \; \forall \; R_{PQ} \in [0, \infty[$, you are guaranteed to get relative differences of magnitude less than 1. The picture is more complicated for integrals over basis functions of angular momentum since these involve linear combinations of higher order Boys functions of which some

Table 7.7.1: Absolute and relative difference of the two-electron integrals in a H_2O calculation, using a cc-pVTZ basis.

Class. nr.	Interval	Abs. Diff.	Rel. Diff
1	10E-16 - 10E -8	79	0
2	10E -8 - 10E -7	82	0
3	10E -7 - 10E -6	429	5
4	10E -6 - 10E -5	3758	32
5	10E -5 - 10E -4	22193	392
6	10E -4 - 10E -3	96987	3077
7	10E -3 - 10E -2	177880	33795
8	10E -2 - 10E -1	45467	204318
9	10E -1 - 10E 0	3134	103938
10	10E 0 - 10E 1	50	4069
11	10E 1 - 10E 2	2	392
12	10E 2 - 10E 3	0	39
13	10E 3 - 10E 4	0	4
Sum		350061	350061

are negative. The linear combinations quickly become big and since each term in the linear combination is affected differently by the correction, depending on the exponents of the charge distributions, you could for example experience that two terms canceling each other in the unregularized scheme, suddenly contribute to the total value of the integral. It becomes even more complicated if contracted basis functions are used, but nevertheless, when comparing two integrals, one must still be able to order the uncorrected and corrected integral so that you can compare them for each order of the Boys functions entering the integral. This way you can get an idea how each term in the linear combination changes. The one-center integrals are expected to be effected the most by the correction and for some n'th order term you get ($R_{PQ} = 0,\ \tau = c \cdot \eta^2$)

$$\begin{aligned}
&\sqrt{c}c^n F_n(cR_{PQ}^2) - \sqrt{\tau}\tau^n F_n(\tau R_{PQ}^2) = \\
&\sqrt{c}c^n \frac{1}{2n+1} - \sqrt{c}\eta c^n \eta^{2n} \frac{1}{2n+1} = \frac{1}{2n+1}\sqrt{c}c^n(1-\eta^{2n+1}) = \\
&\sqrt{c}c^n F_n(cR_{PQ}^2)(1-\eta^{2n+1}) \\
&\Downarrow \\
&\text{rel. diff.} = (1-\eta^{2n+1}) \qquad (7.7.1)
\end{aligned}$$

The question is what values η can take. For point charges η becomes 1, and the relative difference is zero, as should be the case. If the two exponents of

the charge distribution are identical, μ becomes :

$$\begin{aligned}
\mu^2 &= \frac{\alpha+\beta}{2} + \sqrt{\left(\frac{\alpha+\beta}{2}\right)^2 + \frac{\alpha\cdot\beta}{\mathrm{f}^2}} \\
&= \alpha + \alpha\sqrt{\frac{1+\mathrm{f}^2}{\mathrm{f}^2}} \\
&\Downarrow \\
\eta^2 &= \frac{\mathrm{f}^2\mu^2}{c+\mathrm{f}^2\mu^2} = \frac{\mathrm{f}^2\alpha(1+\sqrt{\frac{1+\mathrm{f}^2}{\mathrm{f}^2}})}{\frac{1}{2}\alpha+\mathrm{f}^2\alpha(1+\sqrt{\frac{1+\mathrm{f}^2}{\mathrm{f}^2}})} \\
&= \frac{\mathrm{f}^2(1+\sqrt{\frac{1+\mathrm{f}^2}{\mathrm{f}^2}})}{\frac{1}{2}+\mathrm{f}^2(1+\sqrt{\frac{1+\mathrm{f}^2}{\mathrm{f}^2}})}
\end{aligned} \tag{7.7.2}$$

This means that for charge distributions of equal exponent the ratio of the uncorrected integral that is to be thrown away is independent of the size of the exponents. For f=2.0 this means that for integrals over s-type charge distributions with equal exponents, the relative difference between the regularized and unregularized integrals should be $1-\eta^1 = 0.028263$. This is in agreement with the results for He in a basis of s-functions (see table 7.7.2). When keeping β fixed the η^2-function can be plotted as a function of α. Figure 7.7.1 reveals that the value of η when the two exponents are equal, is actually a minimum (with magnitude determined by f), as η has the right properties in the limits $\alpha \to 0$ and $\alpha \to \infty$. It has hereby been established that for a fixed f-value, each order of the Boys function entering an electron repulsion integral can at most experience a change as described in 7.7.1 with η^2 given by 7.7.2. The relative difference function is seen in figure 7.7.2. This function is seen to be an increasing function, and already terms in fourth order in an integral, will be reduced by a factor of approximately 0.8. Off course using a different f-value the changes are less dramatic, but still for integrals over fairly compact Gaussians involving other than s- or p-functions a large absolute difference can be expected. In figure 7.7.3 the Boys functions of orders 0 to 4 are plotted. The regularization is seen to behave as predicted by (7.7.1) at $\mathrm{R_{pq}}$=0. The absolute difference seems to be fairly constant as n is increased meaning that the relative difference increase.

A fundamental property of the two-electron integral matrix is that it should be positive definite. If this is not the case a spurious two electron attraction can occur. Furthermore this property forms the basis for using the Cauchy-Schwarz inequality as a tool to screen away integrals that can safely be neglected without loss of accuracy. Having seen how the Panas correction

Table 7.7.2: Regularized and non-regularized integrals from a He calculation in an uncontracted s-basis.

ijkl	non − reg (ij|kl)	reg (ij|kl)	(nonreg − reg)/nonreg
1 1 1 1	0.705399131447E+01	0.685462113789E+01	0.282634564867E-01
2 1 1 1	0.470458468567E+01	0.457740869042E+01	0.270323532781E-01
2 1 2 1	0.321545590771E+01	0.312457600958E+01	0.282634564867E-01
2 2 1 1	0.468131864745E+01	0.458769961988E+01	0.199984309160E-01
2 2 2 1	0.333265665603E+01	0.325154154591E+01	0.243394740282E-01
2 2 2 2	0.374855864114E+01	0.364261141710E+01	0.282634564867E-01
3 1 1 1	0.244075512713E+01	0.237722390338E+01	0.260293312698E-01
3 1 2 1	0.168281437143E+01	0.163553242339E+01	0.280969480913E-01
3 1 2 2	0.177209896760E+01	0.172664799128E+01	0.256481027036E-01
3 1 3 1	0.883574985395E+00	0.858602102242E+00	0.282634564867E-01
3 2 1 1	0.315159293664E+01	0.310216016977E+01	0.156850100479E-01
3 2 2 1	0.227958732614E+01	0.223325950185E+01	0.203228995683E-01
3 2 2 2	0.266361556329E+01	0.259117916144E+01	0.271947659568E-01
3 2 3 1	0.122030316401E+01	0.119349091247E+01	0.219717954771E-01
3 2 3 2	0.193324019282E+01	0.187860014275E+01	0.282634564867E-01
3 3 1 1	0.288400439458E+01	0.285727821568E+01	0.926703820275E-02
3 3 2 1	0.212679845792E+01	0.209911589987E+01	0.130160702113E-01
3 3 2 2	0.261924518346E+01	0.256323662626E+01	0.213834724413E-01
3 3 3 1	0.114833692863E+01	0.113160590978E+01	0.145697821204E-01
3 3 3 2	0.196650706593E+01	0.191695500923E+01	0.251980059247E-01
3 3 3 3	0.213026272319E+01	0.207005413541E+01	0.282634564867E-01

Figure 7.7.1: η^2 as a function of α for fixed β (0.1, 0.5, 1.0, 2.0, 3.0, 4.0).

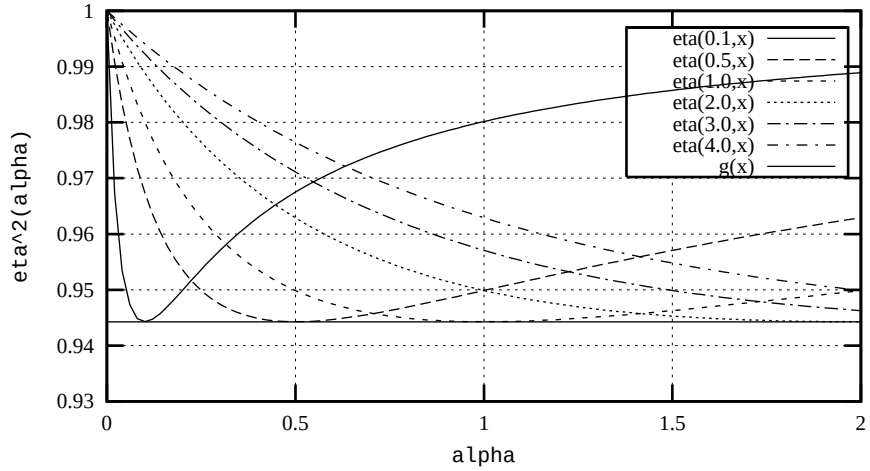

Figure 7.7.2: (1-η^{2n+1}) as a function of the order of the Boys functions entering the electronic repulsion integral. The upper curve is for f=2.0, the lower for f=2.5

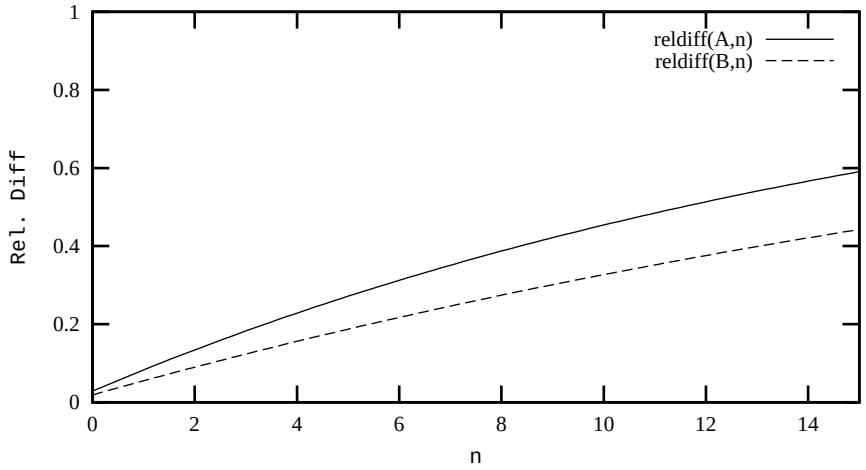

Figure 7.7.3: The regularized and unregularized Boys Functions of orders 0 to 4

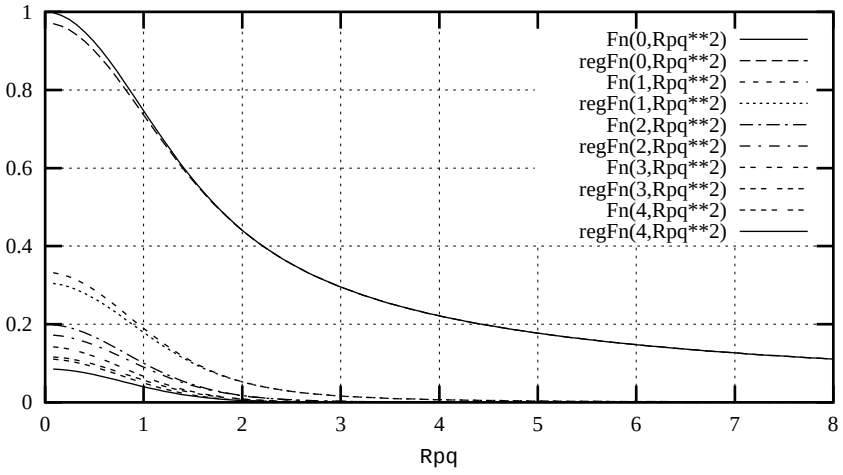

can sometime affect the integrals quite dramatically it should be investigated whether this property of the integral matrix is preserved. A large number of calculations were performed and in most cases the eigenvalues of the two electron integral matrix were all positive. It did however also happen that negative eigenvalues of rather significant magnitude appeared in the diagonalized matrix. This was for example the case in the simple example of using only an s-basis on the oxygen atom in water (table 7.7.3). It should be noted that the negative eigenvalues aren't present in the unregularized limit, and their existence in the regularized scheme is clearly unacceptable. Moreover the negative eigenvalue seem to be very hard to get rid of. Their are of course most dominant at $1/f^2$=0.25, but even at $1/f^2$=0.1 there is an eigenvalue with a value of -2.45·10^{-9}. From $1/f^2$=0.08 and toward the uncorrected method they disappear.

7.8 Summary

The following conclusion on the use of the Panas correction can be made : Testing the Panas proposal of a Coulomb hole model has revealed that

- The correction does not generally improve the properties obtained from HF theory. Small CAS wave function are improved but the correction shows limited dependence on the quality of the reference wave function.
- A deeper analysis of the density could reveal why the HF wave function does not benefit from the correction. An improvement of the method is expected if the modified one-electron density could evaluated and used in the calculation of V_{ne}.
- In certain cases the matrix of two-electron integrals is not positive definite.
- The relative difference between regularized and unregularized integrals can become large, and there might be a need to refine the expression for the 'cut-off' (μ) to depend on the angular momenta of the functions entering a given integral.

Table 7.7.3: Eigenvalues of the two-electron integral matrix for different values of f. The basis set is 7 uncontracted s-functions on Oxygen

Nr.	$1/f^2$=0	$1/f^2$=0.08	$1/f^2$=0.05	$1/f^2$=0.1	$1/f^2$=0.2	$1/f^2$=0.25
1	3.25312185E+02	3.23033782E+02	3.23872925E+02	3.22484027E+02	3.19843306E+02	3.18585393E+02
2	1.51278072E-01	1.25556795E-01	1.34673001E-01	1.19801889E-01	9.44332313E-02	8.35957528E-02
3	2.86363814E+00	2.71350474E+00	2.76784282E+00	2.67848961E+00	1.02043167E+00	9.71533457E-01
4	2.68378172E-05	1.25694546E-05	1.72101231E-05	9.85201262E-06	-2.70186485E-06	-2.08670571E-06
5	1.09623274E-03	6.17153253E-04	7.76241135E-04	5.23002084E-04	1.69317038E-04	5.52788152E-05
6	4.53272081E+01	4.46552467E+01	4.49015901E+01	4.44945647E+01	4.37303208E+01	4.33705486E+01
7	4.56304702E-10	4.06238799E-11	1.42302474E-10	-6.61799459E-12	-1.28600063E-10	-4.59251003E-11
8	1.13809538E-06	2.71480279E-07	5.22407940E-07	1.41568360E-07	-2.80698848E-07	-2.57710581E-07
9	1.38453360E-02	9.83851480E-03	1.12212840E-02	8.98812391E-03	5.46782109E-03	4.09095257E-03
10	1.53178427E+01	1.48103381E+01	1.49961125E+01	1.46893521E+01	1.41161801E+01	1.38477971E+01
11	1.89360026E-16	2.05943724E-15	-3.02326852E-15	-1.65847334E-15	3.81073198E-16	-8.01156721E-18
12	2.64677156E-13	-7.15352898E-14	3.28190564E-16	-5.47755317E-14	7.62827625E-15	1.76717888E-14
13	1.32265038E-07	2.03870655E-08	5.10353444E-08	-2.44674835E-09	-7.92293126E-10	-6.23101267E-09
14	1.64810558E-04	8.37677175E-05	1.10257022E-04	6.82878998E-05	1.14568754E-05	-2.02095300E-05
15	3.91669876E-02	3.13793938E-02	3.41320343E-02	2.96458141E-02	2.20398109E-02	1.88063674E-02
16	7.25598914E-17	-4.59247755E-17	-3.45546908E-16	-1.20617264E-15	1.01044366E-15	-1.08610410E-16
17	9.86064941E-17	4.53814335E-15	-6.80150196E-15	8.73135042E-16	-1.78683215E-15	3.93402756E-15
18	1.75533339E-12	-2.81465580E-13	8.17270754E-14	-1.19481877E-12	-5.45234311E-13	-2.23131177E-13
19	3.95996885E-08	2.64974966E-09	1.23465117E-08	5.46918409E-09	-2.93796963E-08	-6.47012550E-10
20	6.72236674E-06	2.35640926E-06	3.69552878E-06	1.61767326E-06	-1.63196871E-07	-4.04545419E-07
21	3.34750965E-01	3.03117093E-01	3.14592695E-01	2.95707093E-01	2.61270648E-01	2.45520256E-17
22	1.56411711E-17	4.51066222E-17	3.05703484E-18	-1.11176947E-16	4.41732645E-17	1.34082484E-18
23	3.75643975E-19	-7.54565719E-16	-4.23758114E-16	-1.10430634E-16	9.57837681E-16	9.85342635E-16
24	8.67583079E-17	-2.23391839E-15	4.64180372E-16	3.37319837E-16	-2.11056489E-15	2.46782754E-15
25	5.81849111E-12	-6.85548325E-13	7.14401900E-13	2.29662973E-12	-1.19945053E-13	8.77956204E-14
26	2.66835630E-09	-1.35479096E-10	6.48908492E-10	-3.67052337E-10	7.59212333E-09	4.46814135E-08
27	2.48744669E-03	1.63716550E-03	1.92455405E-03	1.46356605E-03	7.69372502E-04	5.07030629E-04
28	1.24672604E+00	1.14980149E+00	1.18506936E+00	1.12697250E+00	2.51642495E+00	2.44259909E+00

Chapter 8

Conclusion

The Coulomb hole model as proposed by I. Panas is abandoned on the basis of the tests summarized above. The model is not able to systematically improve on methods where dynamic correlation is not accounted for. Good result obtained with the Coulomb hole models can, as seen for the regCASSCF calculations, be due to fortunate error cancellations.
The idea of releasing HF and CACSF type wave functions from dealing with short range interacting electrons is however not abandoned, but simply throwing away part of the short range two electron potential introduces some unwanted effects like over binding of molecules and non positive definite two electron matrices. A better route is to replace the part of the two electron potential that is removed by using modified two electron operators by the potential from more efficient methods like DFT. This route is explored further in the next chapter.

Bibliography

[1] J. Olsen, B. O. Ross, P. Jørgensen, and H. J. Aa. Jensen. *J. Chem. Phys.*, 89:2185, 1988.

[2] E. Clementi. *Chem. Rev.*, 68:34, 1968.

[3] E. Clementi. *Int. J. Quant. Chem.*, 3:179, 1969.

[4] E. Clementi and G. Corongiu. *Int. J. Quant. Chem.*, 62:571, 1997.

[5] G. C. Lie and E. Clementi. *J. Chem. Phys.*, 60:1275, 1974.

[6] S. J. Chakravorty and E. Clementi. *Phys. Rev. A*, 39:2290, 1989.

[7] L. De Windt, D.W.M. Hofman, L. Pisani, and E. Clementi. *Int. J. Quant. Chem.*, 58:131, 1995.

[8] I. Panas. *Chem. Phys. Lett.*, 245:171, 1995.

[9] I. Panas and A. Snis. *Theor. Chem. Acc.*, 97:232, 1997.

[10] I. Panas. *Mol. Phys.*, 89:239, 1996.

[11] R. Colle and O. Salvetti. *Theor. Chem. Acc.*, 37:329, 1975.

[12] R. Colle and O. Salvetti. *Theor. Chim. Acta*, 79:1404, 1979.

[13] R. Colle and O. Salvetti. *J. Chem. Phys.*, 93:534, 1990.

[14] C. Lee, W. Yang, and R. G. Parr. *Phys. Rev. B*, 37:785, 1988.

[15] L. E. McMurchie and E. R. Davidson. *J. Comp. Phys.*, 49:3083, 1968.

[16] T. Helgaker, H. J. Aa. Jensen, P. Jørgensen, J. Olsen, K. Ruud, H. Ågren, K. L. Bak, V. Bakken, O. Christiansen, S. Coriani, P. Dahle, E. K. Dalskov, T. Enevoldsen, B. Fernandez, C. Hättig,

K. Hald, A. Halkier, H. Heiberg, H. Hettema, D. Jonsson, S. Kirpekar, R. Kobayashi, H. Koch, K. V. Mikkelsen, P. Norman, M. J. Packer, T. A. Ruden, T. Saue, S. P. A. Sauer, B. Schimmelpfennig, K. O. Sylvester-Hvid, P. R. Taylor, and O. Vahtras. Dalton release 1.2 (2001), an electronic structure program, http://www.kjemi.uio.no/software/dalton/dalton.html.

[17] P.O. Widmark, P.A. Malmqvist, and B. O. Roos. *Theor. Chem. Acc.*, 77:291, 1990.

[18] Charlotte E. Moore. Atomic energy levels, vol i (hydrogen through vanadium). Circular of the National Bureau of Standards 467, U.S. Government Printing Office, Washington, DC, 1949.

[19] J. M. Pèrez-Jordà, E. San-Fabiàn, and F. Moscardò. *Phys. Rev. A*, 45:4407, 1992.

Part III

Wave Function DFT Hybrid Models

Chapter 9

Merging Wave Function Theory and DFT.

9.1 Introduction.

From the previous chapter it became clear the simply removing certain parts of the short range two electron potential was not a generally applicable approach to mimic dynamic correlation in HF and MCSCF type wave functions. The classification of short range electronic interactions as the source of the slow convergence of wave function based methods, i.e the source of dynamic correlation, is nonetheless valid and the modified operator used by I. Panas [1,2] provides an easy way of removing short range interactions from the wave function treatment.
From the failure of the Coulomb hole models a natural next step is to not neglect parts of the two electron potential but instead replace it with a potential that more efficiently deals with dynamic correlation. DFT is of course an obvious candidate and the idea of merging wave function theory (WFT) with DFT is intriguing from both a DFT and WFT point of view. DFT is known to efficiently deal with short-range interaction electrons, for which the uniform electron gas is a good model system, but having problems describing long-range effect. Gradient corrected functionals can be seen as an attempt to deal with these issues, but the near degeneracy, improper asymptotic behavior and self-interaction problems have already been mentioned in Sec.4.5.6 as well known problems of DFT. Long-range interactions are on the other hand efficiently handled by Multi-reference wave functions that in turn are inefficient when it comes to dynamic correlation. The WFT DFT marriage seems ideal and actually has a long history.

As early as 1974 Lie and Clementi [3,4] defined a "HF with proper dissociation" reference wave function which basically was a small MCSCF wave function. They augmented the MCSCF energy with the energy from a reparameterization of the Gombas density functional [5] and fed this functional with a density that was a rescaled on the basis of the orbital occupation numbers. Rescaling the density does not completely rule out double counting of correlation but nevertheless the approach showed some promise.
The Colle and Salvetti functional [6, 7] of the two particle density has already been mentioned and its reparameterization in the LYP correlation functional [8] is a testament of its success in modeling dynamic correlation. In the context of this chapter the generalization of the Colle Salvetti functional to multi-configurational wave functions [9] should be mentioned.
A. Savin has been involved in numerous WFT DFT hybrid models. Here I mention the coupling of CI and DFT based on thresholds on the natural occupation numbers [10]. The method of Miehlich *et al.* [11] in which a model system is defined that excludes some of the low lying virtual orbitals of a CASSCF wave function. Finally a series of proposals based on a long-range short-range separation of the Coulomb operator [12–18]. The implementations of WFT DFT hybrid models presented in the following chapters are based on this idea.
The CI-DFT approach of Grimme and Waletzke in which a CI calculation is performed in the Kohn-Sham orbitals. Double counting is to some extend avoided by scaling the off-diagonal elements of the CI matrix by an exponential expression of the energy gap of the configuration state functions (CSFs) involved.
The combination of Valence Bond type wave functions with DFT of H. Stoll [19].
The combination of CASSCF type wave functions with functionals of the two particle density of McDouall [20]. For further reading this article has a short review of proposals previously mentioned in the literature, most of which have been mentioned here.

9.2 The Long-Range Short-Range Separation

The purpose of making a separation of the Coulomb operator into short-range and long-range parts

$$V_{ee} = V_{ee}^{lr} + V_{ee}^{sr} \tag{9.2.1}$$

is to allow DFT to treat the short-range interaction electrons while WFT treats the long-range interactions. From a practical point of view this should be done smoothly to not introduce any discontinuities in neither the DFT or

the wave function potential. Furthermore, for testing purposes, a parameter should be included to allow adjustment of the separation. At the same time such a separation is a way of addressing the double counting of correlation problem. A certain part of the interaction space is either treated by DFT or WFT, never both, and so double counting should be minimal.

The earliest proposal of such a separation is that of A. Savin [13] in which a Yukawa type potential is used.

$$\begin{aligned} V_{ee} &= V_{ee}^{lr} + V_{ee}^{sr} \\ &= \frac{1 - e^{-\mu r_{ij}}}{r_{ij}} + \frac{e^{-\mu r_{ij}}}{r_{ij}} \end{aligned} \tag{9.2.2}$$

From a practical point of view this choice of separation is not ideal when used with Gaussian basis sets since integrals evaluation becomes cumbersome. A better choice used extensively by A. Savin *et al.* [10, 14, 15] is based on the error function, already encountered in the Coulomb hole model of I. Panas (see Sec. 7).

$$V_{ee}^{lr} = W_{ee}^{\mathrm{erf},\mu}(r_{12}) = \frac{\mathrm{erf}(\mu r_{ij})}{r_{ij}} \tag{9.2.3}$$

The long-range part (erf, $W_{ee}^{\mathrm{erf}}(\mu r_{12})$) is shown for $\mu = 1$ in Fig.9.2.1. The long-range shor-range separation of this operator is however not complete in the sense that the long-range part, as seen on Fig.9.2.1, contributes significantly for small r_{12}. A sharper separation is obtained by augmenting the error function with an exponential term that cancels with the error function for $r_{12} \to 0$.

$$V_{ee}^{lr} = W_{ee}^{erfgau,\mu}(r_{12}) = \frac{\mathrm{erf}(\mu r_{12})}{r_{12}} - \frac{2\mu}{\sqrt{\pi}} e^{-\frac{1}{3}\mu^2 r_{12}^2} \tag{9.2.4}$$

This operator ($erfgau$) is also tested by Toulouse *et al.* [16–18] and a similar operator has also been used in a different context by Prendergast *et al.* [21]. For comparison between the two operators, the μ of $W_{ee}^{erfgau,\mu}$ is scaled by a constant so that both operators deviate from the true Coulomb interaction for approximately the same value of r_{12}. Note that $W_{ee}^{erfgau,\mu}$ does not contribute as much as $W_{ee}^{erf,\mu}$ for small r_{12} and that both operators are cuspless ($\frac{\partial W_{ee}^{X}}{\partial r_{12}}\Big|_{r_{12}=0} = 0$) while producing the correct Coulomb tail for large r_{12}.

The longe-range two electron operator is used by the WFT part of a WFT DFT hybrid and since the modified long-range two electron operators have been released from dealing with the short-range part of the interaction space

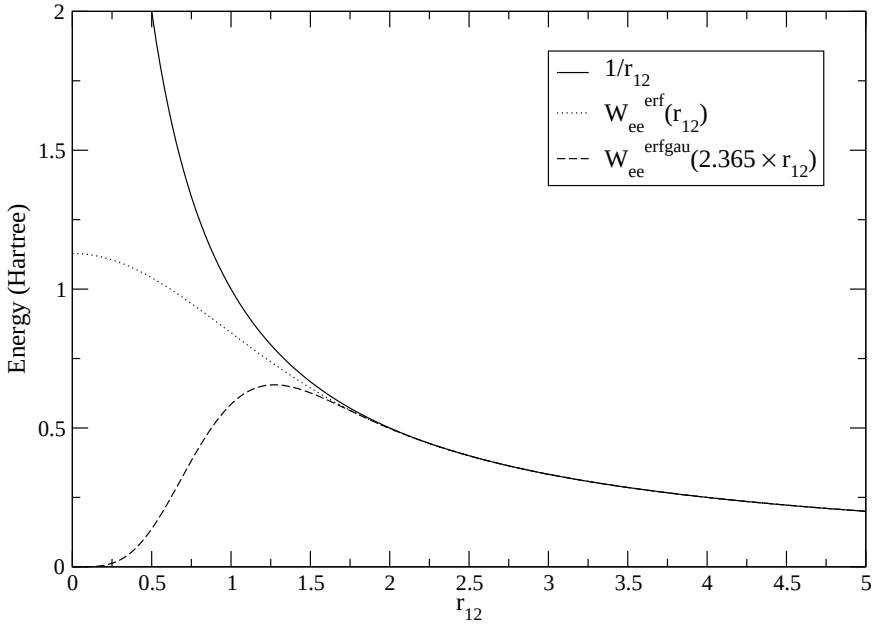

Figure 9.2.1: Modified two-electron operators used in this work. W_{ee}^{erf} is plotted for $\mu = 1$ while W_{ee}^{erfgau} is plotted for $\mu = 2.365$ to allow a better comparison of the two operators.

a new convergence behavior of the WFT part is expected. The wave function will not have to describe the Coulomb cusp and so it is expected that the basis set does not need to be as flexible as in usual CI or CC wave function expansions. Likewise a CI type wave function is expected to converge faster with respect to the expansion in Slater determinants or Configurations State Functions (CSFs).

The separation of the Coulomb operator in short and long-range parts through a function of the coupling parameter μ also presents a formal extension of Kohn-Sham DFT [22] to multi-reference wave functions. The adiabatic connection [23] can be used to connect the system with a fictitious (the long-range interacting) system with the true/fully interacting system. This is a generalization of the adiabatic connection used in Sec.4.5.5 for standard Kohn-Sham theory and is done in detail in Paper I (p.141). The result is an energy expression of the multi-reference wave function DFT hybrid model

$$E_{\text{hybrid}} = \langle \Psi^{\mu} \mid \hat{H}_{LR}^{\mu} \mid \Psi^{\mu} \rangle + J_{SR}^{\mu}[\rho] + E_{xc-SR}^{\mu}[\rho] \tag{9.2.5}$$

where $\hat{H}_{LR}^{\mu}$ is the usual Hamilton operator though using the long-range two-electron interaction ($W_{ee}^{erf,\mu}$ or $W_{ee}^{erfgau,\mu}$). J_{SR}^{μ} is the short-range Hartree

energy and E^{μ}_{xc-SR} the short-range exchange-correlation energy (see Paper I for further details). Moreover the adiabatic connection provides a recipe for constructing the short-range functionals needed in the hybrid methods as the difference between the Kohn-Sham exchange correlation energy and that of the fictitious long-range interacting system (see chapter 9.4).

9.3 Implementation of Long-range Integrals.

To evaluate two electron integrals using the long-range operator (erf and $erfgau$) it will be needed to calculate integrals using both the $\frac{\mathrm{erf}(\mu r_{12})}{r_{12}}$ and $-\frac{2\mu}{\sqrt{\pi}}\exp(-\frac{\mu^2}{3}r_{12}^2)$ operators. The evaluation of integrals using the erf operator has already been discussed in conjunction with the Panas Coulomb hole model (see Sec.7.1). Here we concentrate on calculation integrals with the $erfgau$ operator. The expressions for the Gaussian ssss integrals using the erf operator and the exp operator (that make up the $erfgau$ operator) are given in Appendix B.1 and B.2. These can be slightly rewritten to match the syntax of the DALTON source code and be shown to be proportional to :

$$\left(s_a s_b \left| \frac{\mathrm{erf}(\mu r_{12})}{r_{12}} \right| s_c s_d\right) \sim \left(\frac{1}{\alpha}+\frac{1}{\beta}+\frac{1}{\mu^2}\right)^{-1/2} F_0\left(-\frac{R_{PQ}^2}{\frac{1}{\alpha}+\frac{1}{\beta}+\frac{1}{\mu^2}}\right) \tag{9.3.1}$$

$$\left(s_a s_b \left| N\exp(-\frac{\mu^2}{3}r_{12}^2) \right| s_c s_d\right) \sim \left(\frac{1}{\alpha}+\frac{1}{\beta}+\frac{3}{\mu^2}\right)^{-3/2} \exp\left(-\frac{R_{PQ}^2}{\frac{1}{\alpha}+\frac{1}{\beta}+\frac{3}{\mu^2}}\right) \tag{9.3.2}$$

where $\alpha = a + b$ and R_{PQ} is the distance between the centers of the charge distributions formed by multiplication of s_a with s_b and s_c with s_d. All that is needed to calculate the integrals of higher momenta is the derivative of these ssss integrals.

$$\begin{aligned} &\frac{\partial}{\partial P_x} F_0\left(-\frac{R_{PQ}^2}{\frac{1}{p}+\frac{1}{q}+\frac{1}{\mu^2}}\right) \\ &= -2\left(\frac{1}{p}+\frac{1}{q}+\frac{1}{\mu^2}\right)^{-1} X_{PQ}\cdot F_1\left(-\frac{R_{PQ}^2}{\frac{1}{p}+\frac{1}{q}+\frac{1}{\mu^2}}\right) \end{aligned} \tag{9.3.3}$$

$$\begin{aligned} &\frac{\partial}{\partial P_x} \exp\left(-\frac{R_{PQ}^2}{\frac{1}{p}+\frac{1}{q}+\frac{3}{\mu^2}}\right) \\ &= -2\left(\frac{1}{p}+\frac{1}{q}+\frac{3}{\mu^2}\right)^{-1} X_{PQ}\cdot \exp\left(-\frac{R_{PQ}^2}{\frac{1}{p}+\frac{1}{q}+\frac{3}{\mu^2}}\right) \end{aligned} \tag{9.3.4}$$

The different pre-factors that come from differentiating the erf and exp terms mean that we cannot just add the zeroth order erf and exp integrals in a recurrence scheme for higher order integrals. We therefore do the following

1. Evaluate the charge distributions and determine their expansion in Hermite Gaussians

2. Enter a loop over blocks of basis functions and a loop over nuclei to evaluate both the erf zeroth order integrals (R(I,J), (9.3.1)) and the exp zeroth order integrals (E(I), (9.3.2)) at the same time.

3. For higher angular momenta do the following

```
DO I = 1,NUC
DO J = 1,JMAX
       A = A*1/(1/P+1/Q+1/MUSQ)
       B = B*1/(1/P+1/Q+3/MUSQ)
       R000(I,J) = A*R000(I,0) + B*E(I)
ENDDO
ENDDO
```

4. As a final step the total integrals are calculated by multiplying the pre-factors, the expansion coefficients and the $2X_{PQ}, 2Y_{PQ}, 2Z_{PQ}$ factors.

The extra memory needed for calculating the $erfgau$ integrals only amount to the memory needed to store the extra E(I) numbers (within each loop of blocks of basis functions). The recurrence relations for the exp terms are done simultaneously with the erf terms and therefore the extra time associated with the computation of the $erfgau$ integrals is minimal as seen if Fig.9.3 for H_2O.

Table 9.3.1: Timings for the two electron integral calculation in an H_2O calculation in the cc-pVQZ basis set.

Operator	Time
$\frac{1}{r_{12}}$	15.19s
$\frac{erf(\mu r_{12})}{r_{12}}$	15.11s
$\frac{erf(\mu r_{12})}{r_{12}} + N \cdot exp(-a \cdot r_{12}^2)$	15.49s

While the long-range integrals have been implemented very efficiently the short-range are evaluated in a “crude” manner for this initial implementation.

These are needed for computing the short-range Hartree energy (9.2.5) and are simply calculated by evaluating the regular two electron integrals using the full Coulomb operator and subtracting the set of long-range integrals. In a future more efficient implementation these integrals could be evaluated using density fitting techniques which would bring the scaling down from N^4 to N^3 [24,25]. A next step could be to use Fast Multipole Method techniques for computing the long-range integrals [26,27].

9.4 The short-range Density Functionals.

9.4.1 Short-range LDA

As mentioned the adiabatic connection provides a recipe for the construction of short-range density functionals as the difference between the exchange correlation energy in the Kohn-Sham limit ($\mu = 0$) and the exchange correlation energy at intermediate interaction μ. A first approximation to a short-range functional is provided by the Local Density Approximation (LDA). Toulouse *et al.* derive the short-range LDA functional in detail in [16].

The correlation energy for a system of intermediate long-range interaction (ε_c^μ) is obtained from Coupled-Cluster calculations with double excitations or from Fermi-hypernetted-chain (FHNC) calculations (see [16] for details) using the long-range two-electron operator. The short-range correlation energy per particle[1] ($\bar{\varepsilon}_c^\mu$)can then be expressed from the long-range correlation energy (ε_c^μ) and the usual LDA correlation energy (ε_c)

$$\bar{\varepsilon}_c^\mu(r_s) = \varepsilon_c(r_s)\left(1 - \frac{\varepsilon_c^\mu(r_s)}{\varepsilon_c^{\mu\to\infty}(r_s)}\right) \tag{9.4.1}$$

where r_s is the Wigner-Seitz radius ($r_s = (3/(4\pi\rho))^{1/3}$). This is seen to reduce to the usual LDA correlation energy in the limit $\mu \to 0$ and vanish at $\mu \to \infty$. Note that a practical implication of this is that the coupling between the short-range and long-range part is also put in the functional.

Toulouse it et al. computed the short-range correlation energy for a series of μ and r_s values and fitted this to the expression

$$\bar{\varepsilon}_c(r_s) = \frac{\varepsilon_c^\mu(r_s)}{1 + c_1(r_s)\mu + c_2(r_s)\mu^2} \tag{9.4.2}$$

[1]Related to the global correlation functional by : $\bar{E}_c^\mu[\rho] = \int \bar{\varepsilon}_c^\mu(\mathbf{r})\rho(\mathbf{r})d\mathbf{r}$

where the expressions for the coefficients c_1 and c_2 for both the erf and $erfgau$ operators are given in [16]. The short-range LDA (SRLDA) correlation functional is therefore basically rescaling of the VWN correlation functional [28].

The exchange energy functional can be computed analytically from the uniform electron gas with modified interaction. The end result given in [16] is

$$\bar{\varepsilon}^{\mu}_{x,\mathrm{erf}}(r_s) = -\left(\frac{18}{\pi^2}\right)^{1/3}\frac{1}{r_s}\left[\frac{3}{8} - A\left(\sqrt{\pi}\mathrm{erf}\frac{1}{2A} + (2A - 4A^3)e^{-1/(4A^4)} - 3A + 4A^3\right)\right] \tag{9.4.3}$$

$$\begin{aligned}\bar{\varepsilon}^{\mu}_{x,\mathrm{erfgau}}(r_s) &= \bar{\varepsilon}^{\mu}_{x,\mathrm{erf}}(r_s) \\ &- \left(\frac{18}{\pi^2}\right)^{1/3}\frac{1}{r_s}\left[A\left(\sqrt{\pi}\mathrm{erf}\frac{1}{2B} + (2B - 16B^3)e^{-1/(4B^4)} - 6B + 16B^3\right)\right]\end{aligned} \tag{9.4.4}$$

where $A = \mu/(2K_F), B = \mu/(2\sqrt{3}K_F)$ and $K_F = (3\pi^2\rho)^{1/3}$

The quality of the SRLDA is also investigated by Toulouse *et al.* [17,18] by comparing the exchange and correlation energy from the SRLDA functional and from accurate calculations of the exchange correlation energy along the adiabatic connection. It becomes clear that SRLDA is very accurate for large and intermediate μ values but fail near the Kohn-Sham end of the adiabatic connection ($\mu \to 0$). More specifically in this region SRLDA overestimates the exchange energy but underestimates the correlation energy. The observation of the behavior of the SRLDA functionals along the adiabatic connection can be understood from the very motivation for making the WFT DFT hybrid. Just like WFT has problems dealing with closely interacting electrons, DFT has problems describing long-range interactions (wrong asymptotic behavior and self-interaction has already been mentioned, Sec.4.5.6). Therefore for an intermediate or large value of μ the functionals only deals with electrons on a short-range scale and the uniform electron gas is a good approximation. Toulouse *et al.* even derive an expansion of the exchange and correlation energy in terms of the coupling parameter [18] and show that for large μ the leading terms of this expansion are indeed local functionals. SRLDA is therefore expected to perform well except for small μ. As it will be seen for larger systems, it is however not always possible to stay out of this region if the optimal WFT DFT mixing is to be achieved. Therefore it is of interest to search for short-range functionals that perform better in the small μ region.

9.4.2 Beyond Short-range LDA

The SRLDA correlation functional was shown to be underestimated the correlation energy energy by Toulouse *et al.* [17,18] and find that this error must be associated with the inhomogeneousity of the density. In inhomogeneous systems the electrons are correlated on a shorter distance than in the uniform electron gas and the failure of SRLDA for small μ values can be identified as long-range effects being spuriously transferred to the functional treatment. This is the motivation for improving the SRLDA functional by defining a local μ that is larger of equal to the global μ following the understanding that only truly short-range effects should be treated by LDA.

$$\mu^{\text{eff}}(\mathbf{r}) = \max(\mu^{\text{local}}(\mathbf{r}), \mu) \tag{9.4.5}$$

A number possibilities for choosing μ is suggested by Toulouse *et al.*. Here we will test the use of the inverse of the Wigner-Seitz radius as an estimate of the typical interaction length of the system.

$$\mu^{\text{local}}(\mathbf{r}) = \frac{1}{r_s} \tag{9.4.6}$$

It is noted that this idea cannot be transferred to the SRLDA exchange since this overestimated the exchange energy. Using an improved estimate for the short-range exchange is however needed together with the improved correlation functional since otherwise the errors of the short-range exchange functional would dominate the errors of the total $\text{SRLDA}_{\mu,\text{local}}$ functional. Here we test the μ^{local} correlation functional together with the short-range Hartree-Fock exchange.

A more natural extension to the SRLDA functional is to consider gradient corrections. Toulouse *et al.* performed this extension as well [17] and here I mentioned the Gradient Expansion Correction (GEA) to SRLDA and the extension of the PBE [29] functional to short-range interaction. Especially the PBE looks promising, providing good estimates of both the correlation and exchange energy of Be [17]. The use of this functional in the CI-DFT and MCSCF-DFT hybrid models is left for future research.

A third proposal of an improved SRLDA functional is the interpolation scheme of Toulouse *et al.* SRLDA is nearly exact for large μ and since functionals far better than LDA is known near the Kohn-Sham limit of the adiabatic connection, a μ dependent functional could therefore be constructed as an interpolation between an available functional in the Kohn-Sham limit and an LDA/exact functional in the large μ region. Two such proposal are made

in [18] of which I will mention the weighted interpolation for the exchange energy.

$$\bar{\varepsilon}_x^{\mu} = (\varepsilon_x^{\mathrm{KS-DFT}} - \bar{\varepsilon}_x^{\mathrm{LDA},\mu=0})w(\mu) + \bar{\varepsilon}_x^{\mathrm{LDA},\mu} \tag{9.4.7}$$

where $w(\mu)$ is the weight function that should cut off the contribution from Kohn-Sham functional as soon as LDA becomes near exact. This domain is well estimated by $1/r_s$ and Toulouse *et al.* suggest to use $w(\mu) = \mathrm{erfc}(r_s\mu)$. The μ dependent functional is now an available functional known from standard Kohn-Sham theory in the $\mu = 0$ limit (B3LYP, PBE,...), but the μ dependent SRLDA function for $\mu > 1/r_s$. The performance of this functional is also left for future investigations.

Chapter 10

The MCSCF-DFT model

The WFT DFT hybrid model has been implemented in a development version of DALTON as a hybrid between the MCSCF wave function and DFT. The hybrid model is however completely general and other short-range long-range separation and short-range functionals can easily be implemented. The details of the algorithm is given in Paper I (p.141). Double counting of correlation effects is avoided by the long-range short-range separation of the Coulomb operator (Sec.9.2) which has the following advantages :

1. This short-range DFT scheme can be defined with an adiabatic connection [30], making it in principle an exact theory, and it thus presents a straightforward generalization of Kohn-Sham DFT theory to multi-reference wave functions.

2. As a consequence such a scheme also allows us to switch continuously between the regular Kohn-Sham DFT and the pure wave function situation and thereby never loose control of the DFT WFT mixing.

3. Although the approximate functionals cannot be the same as in Kohn-Sham DFT (this would give double counting), one can use the same ideas as in standard DFT to construct them.

4. The wave function part of the problem has a non-singular two-electron operator and a short wave function expansion is therefore expected to be sufficient.

The choice of an MCSCF wave function as the WFT part of the hybrid is clear as MCSCF theory presents a more efficient way of recovering static correlation effect than CI which is used in previously presented WFT DFT hybrid models [10, 11, 13–15]. The MCSCF-DFT hybrid retains all the benefits of the MCSCF it is built on [31–36], meaning that it is :

a) second order since the energy is Taylor expanded to second order.

b) direct, in the sense that the Hessian is never evaluated explicitly, but projected onto a set of trial vectors generated iteratively.

c) step-restricted, since the "walk" on the energy hypersurface is restricted to a trust region. This region is dynamically updated to guarantee convergence.

d) spin-restricted with full implementation of spin symmetry and point group symmetries of D_{2h} and subgroups.

In Paper I a specific MCSCF-DFT hybrid model is tested. The long-range short-range separation is made using the $erfgau$ operator (see Sec.9.2.4) and the short-range LDA (see Sec.9.4.1) is used for the functional part. The following main conclusions are drawn from these investigations.

- In preliminary few electron calculations both the LDA and MCSCF energy ($\mu = 0$ and $\mu = \infty$ limits of the hybrid) is greatly improved by the WFT DFT mixing giving near exact energies for He and H_2 in cc-pVDZ and cc-pVTZ [37] basis sets.

- These calculations also indicate that the basis set requirements for the MCSCF-DFT hybrid is comparable to that of regular Kohn-Sham DFT. This can be understood from the fact that when comparing to the standard correlated methods (CC, CI, ...) the same flexibility in the basis set is not needed since the wave function part of the hybrid has been released from dealing with dynamic correlation.

- The occupation numbers of the 1s natural orbital of the regular MCSCF method compared to the MCSCF-DFT method showed that transfer of dynamical correlation effects from the wave function part of the hybrid to the DFT part meant that the 1s orbital is closer to being doubly occupied, indicating that a shorter wave function expansion of the MCSCF-DFT hybrid is to be expected.

- Calculations on Be and H_2O showed than when going to molecules with core electrons it becomes impossible to find a good value for the coupling parameter μ that gives a good description of both core and valence electrons. This can be understood from the different nature of core and valence electrons meaning that the correlation requirements are different for core and valence. To put it differently the optimal μ value is density dependent. However having a non-global μ in the wave

function part of the hybrid model is highly impractical and therefore better short-range functionals are needed that are able to give a better description of both core and valence, i.e take the shell structure into account. The functionals that go beyond LDA mentioned in Sec.9.4.2 are good candidates.

- A spin-off of this implementation is the quadratically convergent hybrid of Hartree-Fock and short-range DFT in cases where static correlation in not important. Being a mixture of Hartree-Fock and DFT it presents an interesting alternative to regular hybrid DFT like B3LYP.

Besides the investigations into developing better short-range functionals that will hopefully allow a WFT DFT hybrid method with a global (preferably small) μ value, it will also be of interest to extend the MCSCF-DFT algorithm to allow calculations of linear and non-linear response properties. Likewise the implementation of molecular gradients and Hessians is a natural extension to be able to perform geometry optimizations with the MCSCF-DFT method.

Chapter 11

The CI-DFT model

The following chapter presents the CI-DFT hybrid as implemented in a development version of DALTON [38]. In this scheme the DFT contributions are simply added as contributions to the CI energy and do not directly enter the CI wave function optimization, unlike the MCSCF-DFT model presented in chapter 10 where the MCSCF orbitals are subject to the full effect of the density functional under optimization. The CI optimization can of course be considered a special case of the more general MCSCF optimization and therefore for information on the DFT contributions to the CI gradient and Hessian I refer to chapter 10. Likewise the energy expressions presented in the following section are also general and apply to the MCSCF-DFT hybrid as well.

11.1 Implementation.

In the reduced space CI method the set of orbitals are devided into the inactive (the "nearly" doubly occupied) orbitals and the active orbitals. The CI energy can be written as

$$E^{CI} = V_{NN} + E_\eta + \mathrm{Tr}\left(\mathbf{F}^c \cdot \mathbf{D}^v\right) + \tfrac{1}{2}\sum_{uvxy}\left(uv \mid xy\right)\mathbf{P}_{uv,xy} \qquad (11.1.1)$$

where :

- u,v,x,y are indices that run over active orbitals.
- $\mathbf{P}_{uv,xy}$ is the two-electron density matrix.
- $\mathbf{D}$ denotes a one-electron density matrix. $\mathbf{D}^c$ being the core part, $\mathbf{D}^v$ the valence part.

- $\mathbf{F}^c$ is the core Fock matrix.

$$\mathbf{F}^c = \mathbf{h}_1 + \mathbf{G} \cdot \mathbf{D}^c \tag{11.1.2}$$
$$\mathbf{G} = \mathbf{J} - \mathbf{K} \tag{11.1.3}$$

  where $\mathbf{J}$ is the two-electron classical Coulomb repulsion. $\mathbf{K}$ is the two-electron non-classical exchange repulsion.

- E_η is the inactive energy containing the one electron energy (kinetic energy and nuclei-electron attraction energy) and the two-electron energy over the core-electrons.

$$E_\eta = \tfrac{1}{2}\mathrm{Tr}\left((\mathbf{F}^c + \mathbf{h}_1) \cdot \mathbf{D}^c\right) \tag{11.1.4}$$

- V_{NN} is the repulsion of the nuclei.

The third term in (11.1.1) describes the one-electron energy and the core-valence two-electron interaction while the fourth terms is the valence two electron interaction. The CI problem is linear as seen from the linearity of the energy in $\mathbf{D}^v$ and $\mathbf{P}^v$. The CI energy is thus entirely a function of the valence (one- and two-body) density matrices.

The goal is to formulate the CI-DFT energy in terms of the valence density as well, making it linear in the valence density. The WFT DFT energy is given in Eq.9.2.5 and adopting the core valence separation of the orbital set the CI-DFT energy can be written as.

$$E^{CI-DFT} = V_{NN} + E_\eta + \mathrm{Tr}\left(\left(\mathbf{F}^{c,lr} + \mathbf{J}^{c,sr}\right) \cdot \mathbf{D}^v\right) + \tfrac{1}{2}\sum_{uvxy} (uv \mid xy)^{lr} \mathbf{P}_{uv,xy} \tag{11.1.5a}$$
$$+ \tfrac{1}{2}\mathrm{Tr}\left(\mathbf{D}^v \cdot \mathbf{J}^{sr} \cdot \mathbf{D}^v\right) \tag{11.1.5b}$$
$$+ \left[E_{xc}^{sr}(\mathbf{D}) - E_{xc}^{sr}(\mathbf{D}^\mathbf{c})\right] \tag{11.1.5c}$$

where the inactive energy E_η now is

$$E_\eta = \tfrac{1}{2}\mathrm{Tr}\left(\left(\mathbf{F}^{c,lr} + \mathbf{h}_1\right) \cdot \mathbf{D}^c\right) + \tfrac{1}{2}\mathrm{Tr}\left(\mathbf{D}^c \cdot \mathbf{J}^{sr} \cdot \mathbf{D}^c\right) + E_{xc}^{sr}(\mathbf{D}^c) \tag{11.1.6}$$

$$\mathbf{F}^{c,lr} = \mathbf{h}_1 + \mathbf{G}^{lr} \cdot \mathbf{D}^c \tag{11.1.7}$$

and,

$$\mathbf{J}^{c,sr} = \mathbf{J}^{sr} \cdot \mathbf{D}^c \tag{11.1.8}$$

Two problems arise in the terms (11.1.5b) and (11.1.5c).

1. (11.1.5b) describes the short-range Coulomb contribution to the valence electrons and is seen not to be linear in $\mathbf{D}^v$
2. (11.1.5c) The exchange-correlation term does not factorize in core and valence components

$$E_{xc}^{sr}(\mathbf{D}^c + \mathbf{D}^v) \neq E_{xc}^{sr}(\mathbf{D}^c) + E_{xc}^{sr}(\mathbf{D}^v) \tag{11.1.9}$$

and therefore the exchange-correlation terms also is not linear in $\mathbf{D}^v$

This is addressed by expressing these terms in a reference density

$$\begin{aligned} &\mathbf{D}^{ref} = \mathbf{D}^c + \mathbf{D}^{v,ref} \\ &\Downarrow \\ &\mathbf{D} - \mathbf{D}^{ref} = \mathbf{D}^v - \mathbf{D}^{v,ref} = \delta \end{aligned} \tag{11.1.10}$$

ad.1) Using the reference density this term becomes

$$\begin{aligned} \tfrac{1}{2}\mathrm{Tr}\left(\mathbf{D}^v \cdot \mathbf{J}^{sr} \cdot \mathbf{D}^v\right) &= \tfrac{1}{2}\mathrm{Tr}\left(\left(\mathbf{D}^{v,ref} + \delta\right) \cdot \mathbf{J}^{sr} \cdot \left(\mathbf{D}^{v,ref} + \delta\right)\right) \\ &= \tfrac{1}{2}\mathrm{Tr}\left(\mathbf{D}^{v,ref} \cdot \mathbf{J}^{sr} \cdot \mathbf{D}^{v,ref}\right) + \mathrm{Tr}\left(\left(\mathbf{D}^{v,ref} \cdot \mathbf{J}^{sr}\right) \cdot \delta\right) + \mathcal{O}(\delta^2) \\ &= -\tfrac{1}{2}\mathrm{Tr}\left(\mathbf{D}^{v,ref} \cdot \mathbf{J}^{sr} \cdot \mathbf{D}^{v,ref}\right) + \mathrm{Tr}\left(\left(\mathbf{D}^{v,ref} \cdot \mathbf{J}^{sr}\right) \cdot \mathbf{D}^v\right) + \mathcal{O}(\delta^2) \end{aligned} \tag{11.1.11}$$

and (11.1.5b) is now approximated by a term in some reference density and a term linear in $\mathbf{D}^v$ as wanted.

ad. 2) This term is Taylor expanded around the reference density.

$$\begin{aligned} [E_{xc}^{sr}(\mathbf{D})] &= E_{xc}^{sr}(\mathbf{D})|_{\mathbf{D}=\mathbf{D}^{ref}} + \left.\frac{\partial E_{xc}^{sr}(\mathbf{D})}{\partial \rho}\right|_{\mathbf{D}=\mathbf{D}^{ref}} (\mathbf{D} - \mathbf{D}^{ref}) + \mathcal{O}(\delta^2) \\ &= E_{xc}^{sr}(\mathbf{D}^{ref}) + v_{xc}^{sr}|_{\mathbf{D}=\mathbf{D}^{ref}} (\mathbf{D}^v - \mathbf{D}^{v,ref}) + \mathcal{O}(\delta^2) \end{aligned} \tag{11.1.12}$$

Apparent possibilities for the reference density $\mathbf{D}^{ref}$ is the Hartree-Fock density or the density from a regular DFT calculation. The advantage of the latter would be that the DFT density in general will be better than the Hartree-Fock one, and in particular the core-density will be optimal for the subsequent CI-DFT hybrid.

Collecting the terms we can rewrite equations (11.1.5a)-(11.1.5c) to produce a CI-DFT energy that is now linear in the valence density.

$$\begin{aligned} E^{CI-DFT} &= V_{NN} + E_{\mu}^{CI-DFT} + \mathrm{Tr}\left(\left(\mathbf{F}^{c,lr} + \mathbf{J}^{c,sr} + \mathbf{J}^{v,ref,sr} + v_{xc}^{ref,sr}\right) \cdot \mathbf{D}^v\right) \\ &+ \tfrac{1}{2}\sum_{uvxy} (uv \mid xy)^{lr} \mathbf{P}_{uv,xy} \end{aligned} \tag{11.1.13}$$

with

$$\begin{aligned} E_{\mu}^{CI-DFT} &= \tfrac{1}{2}\mathrm{Tr}\left(\left(\mathbf{F}^{c,lr}+\mathbf{h}_1\right)\cdot\mathbf{D}^{c}\right)+\tfrac{1}{2}\mathrm{Tr}\left(\mathbf{D}^{c}\cdot\mathbf{J}^{sr}\cdot\mathbf{D}^{c}\right) \\ &- \tfrac{1}{2}\mathrm{Tr}\left(\mathbf{D}^{v,ref}\cdot\mathbf{J}^{sr}\cdot\mathbf{D}^{v,ref}\right)-v_{xc}^{ref,sr}\mathbf{D}^{v,ref}+E_{xc}^{sr}(\mathbf{D}^{ref}) \end{aligned} \tag{11.1.14}$$

$$\mathbf{F}^{c,lr} = \mathbf{h}_1 + \mathbf{G}^{lr}\cdot\mathbf{D}^{c} \tag{11.1.15}$$

$$\mathbf{J}^{c,sr} = \mathbf{J}^{sr}\cdot\mathbf{D}^{c} \tag{11.1.16}$$

$$\mathbf{J}^{v,ref,sr} = \mathbf{J}^{sr}\cdot\mathbf{D}^{v,ref} \tag{11.1.17}$$

$$v_{xc}^{ref,sr} = \left.\frac{\partial E_{xc}^{sr}(\mathbf{D})}{\partial\rho}\right|_{\mathbf{D}=\mathbf{D}^{ref}} \tag{11.1.18}$$

It should be noted that the trick of expressing the DFT contribution in terms of a reference density resembles that of J. Harris [39] used to simplify the interactions of weakly bound fragments in molecular DFT calculations. In this formulation the CI-DFT model can therefore be implemented by making the appropriate corrections to the inactive energy, the core Fock matrix and using the long-range two-electron integrals in the two-electron integrals over active indices. Having added the short-range valence Hartree and exchange correlation potential to the core Fock matrix enables us to make "CI macro iterations", in which we redo the CI-DFT calculation with an updated reference density. The macro iterations can therefore be continued until self-consistency has been reached to get a converged CI-DFT density. With a good starting reference density (like the Hartree-Fock density) the number of macro iterations is expected to be small.

11.2 Applications.

It was found in the MCSCF-DFT chapter (10) that the currently available short-range functionals do not enable us to define a good global value for the coupling parameter μ that gives a good description of both core and valence electrons in many electron systems. It is therefore pointless at this stage to do direct comparisons between CI-DFT and MCSCF-DFT calculations on many electron systems, and therefore comparisons will only be made on Helium and Beryllium. This section will furthermore try to add to the investigation done with MCSCF-DFT in Paper I (141) and present some calculations done with some functionals that try to improve on the LDA.

Figure 11.2.1: Ground state energy of He using the truncated CI-DFT, MCSCF-DFT and the FCI-DFT model using a cc-pVTZ basis set and the $erfgau$ two-electron operator.

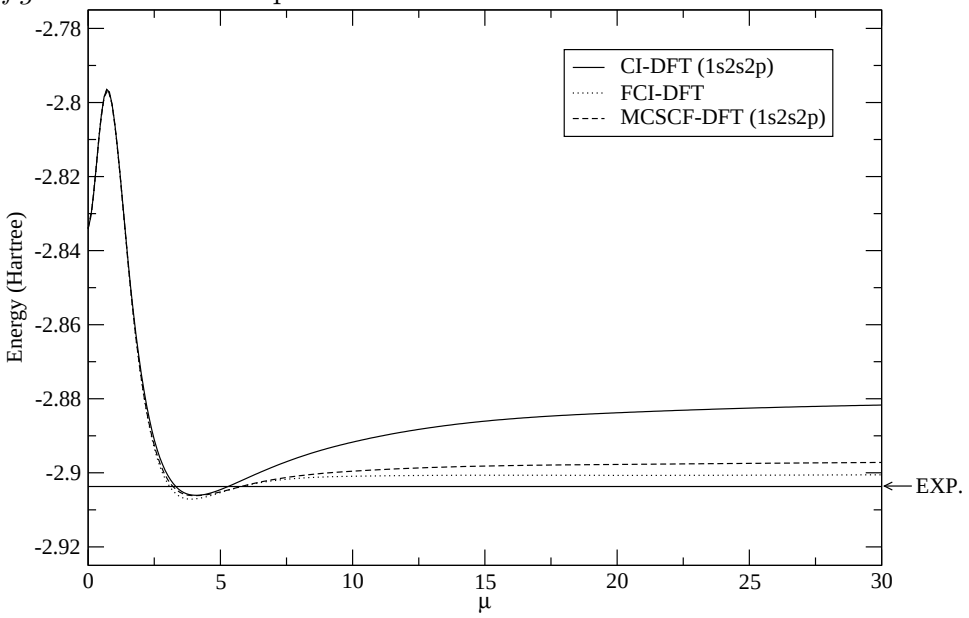

Figure 11.2.2: Contributions to the ground state energy of He in the truncated CI-DFT model, using the cc-pVTZ basis set and the $erfgau$ two-electron operator.

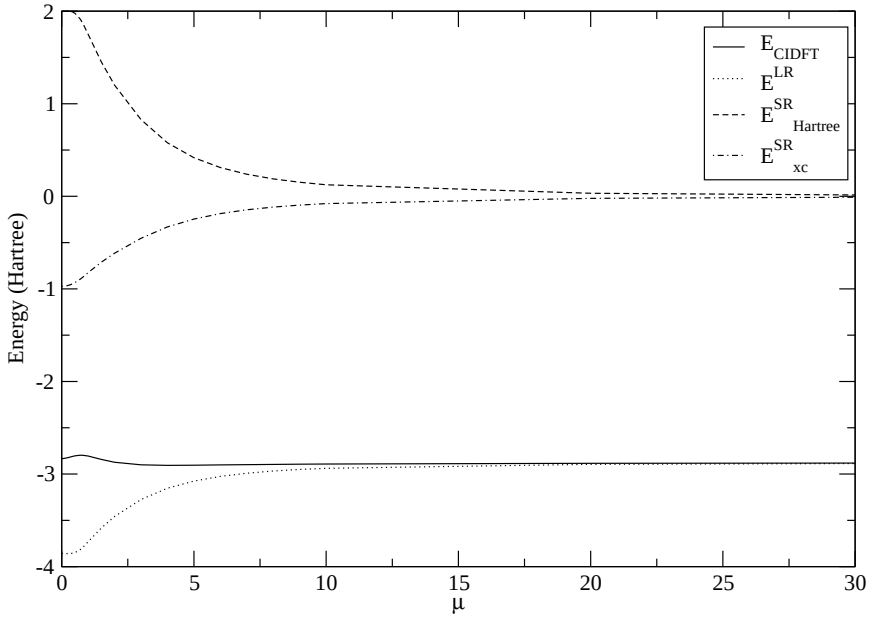

11.2.1 He

Like in Paper I (p.141) Helium is used as a good test for the quality of the short-range functionals. Helium is mainly dynamically correlated and the CI-DFT model should perform well. In Fig. 11.2.1 the μ-dependence of the ground state energy of He is shown for the truncated CI-DFT and MCSCF-DFT (with the 1s,2s,2p orbitals in the active space) models as well as the FCI-DFT model. It is seen that near the Kohn-Sham end of the adiabatic connection ($\mu \to 0$) the three curves are identical, as they should be since in this region the two-electron part of the energy is described by the density functional. The maximum of the curves in this region is also discussed in Paper I (p.141) and is nicely explained by Toulouse *et al.* [18] where it is shown that for values of μ close to zero the error of the short-range LDA functional grows with increasing μ, until $\mu \approx 1$ where the short-range LDA exchange becomes close to the true short-range exchange energy ($\mu \approx 2$ for the correlation energy) [18].
On the right-hand side of the optimal μ-value (~ 4) the CI-DFT, MCSCF-DFT, and FCI-DFT curves become different. Of course the FCI-DFT curve is below the truncated CI-DFT curve but it is also interesting that the MCSCF-DFT curve, having the same active space as the CI-DFT model, is a lot closer to the FCI-DFT curve than to the CI-DFT curve. This shows that when the two-electron interaction is described by the wave function part of the hybrid the optimized orbitals of the MCSCF-DFT model are far better at recovering the correlation energy. It is also nice to see that even though the MCSCF-DFT and FCI-DFT curves are much closer to the experimental ground state energy at the wave function end of the adiabatic connection ($\mu \to \infty$) all the three curves have the same optimal μ-value and optimal energy. This clearly indicates that the hybrid models take into account how much correlation is already accounted for in the wave function part and avoids double counting. The fact that the hybrid curves go below the experimental ground state energy is not a sign of double counting but a limitation of the short-range functional. Had we known the exact functional and done the FCI-DFT curve in a complete basis set the FCI-DFT curve would have been a straight line on top of the line indicating the experimental ground state energy. The FCI-DFT curve in Fig. 11.2.1 is not done in a complete basis set, as seen from the fact that the curve is 0.024 Hartree from the experimental line at $\mu \to \infty$, and therefore this FCI-DFT curve should not be a straight line, but instead have a minimum at the optimal μ.

From the curves on Fig. 11.2.1 it is clear that there is a smooth transfer of energy contributions from the functional part of the hybrid to the wave

function part as μ is increased from the optimal value to infinity. To further show this the three most important energy contributions that make up the CI-DFT energy are plotted in Fig. 11.2.2 along with the total CI-DFT energy. That is, the CI energy using the long-range part of the two-electron operator (E^{LR}), the short-range Hartree energy (E^{SR}_{Hartree}), and the short-range exchange correlation energy (E^{SR}_{xc}). These are the three energy contributions on the right-hand side of Eq. 9.2.5 in that order. It is seen that even as μ is increased from the optimal value and the CI-DFT curve starts to flatten out, the short-range Hartree and exchange correlation energies still contribute to the total energy. Actually even after long-range CI energy is getting indistinguishable from the curve of the total energy, the short-range Hartree and exchange correlation curves still contribute but to a high degree cancel with each other.

11.2.2 Be

For Helium only the $erfgau$ curves where shown. For Beryllium both the erf and the $erfgau$ curves are plotted in Fig. 11.2.3 using the truncated CI-DFT model with the 1s, 2s, and 2p orbitals in the active space. Note that the μ values of the $erfgau$ operator has not been scaled as otherwise done in Fig. 9.2.1, since here a comparison with the $erfgau$ curve of Helium will later be made. From the CI-DFT curves in Fig. 11.2.3 it is noticed that the $erfgau$ operators gives a lower energy than the erf operator with the $erfgau$ curve being closer to the B3LYP energy which in turn is close to the experimental ground state energy (-14.667 Hartree). This is explained by the cleaner short-range long-range separation of the $erfgau$ operator in which a larger part of the short-range interaction space is assigned to the density functional.

Unfortunately it is also observed that the optimal μ for Beryllium ($\mu \approx 10$) is far from the optimal value for Helium ($\mu \approx 4$). This system dependence of μ is also discussed in Paper I and is explained by the limitations of the simple short-range LDA ansatz. In Sec.9.4.2 various proposals for going beyond LDA were discussed. Here a few of proposals will be tested.

The SRLDA functional with local μ has been implemented and is tested on Beryllium in Fig. 11.2.4 with the CI-DFT model with the same active space as before (1s2s2p) and with two different short-range exchange functionals. The dotted curve is with short-range Hartree-Fock exchange and the dashed curve is with the usual short-range LDA exchange. The full curve is the usual CI-DFT with both exchange and correlation described by the short-range LDA (same curve as in Fig. 11.2.3). While it is clearly shown by

Figure 11.2.3: Ground state energy of Be in the truncated CI-DFT model, using the cc-pVTZ basis set and the erf and $erfgau$ two-electron operators.

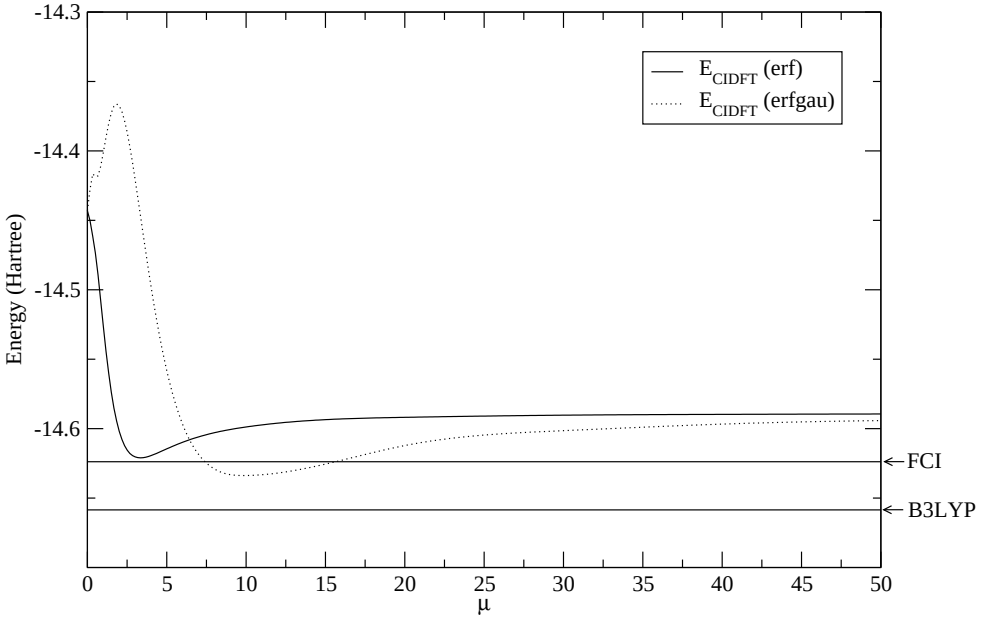

Figure 11.2.4: Ground state energy of Be in the truncated CI-DFT model, using the cc-pVTZ basis, the $erfgau$ two-electron operator, and three different short-range exchange and correlation functional combinations.

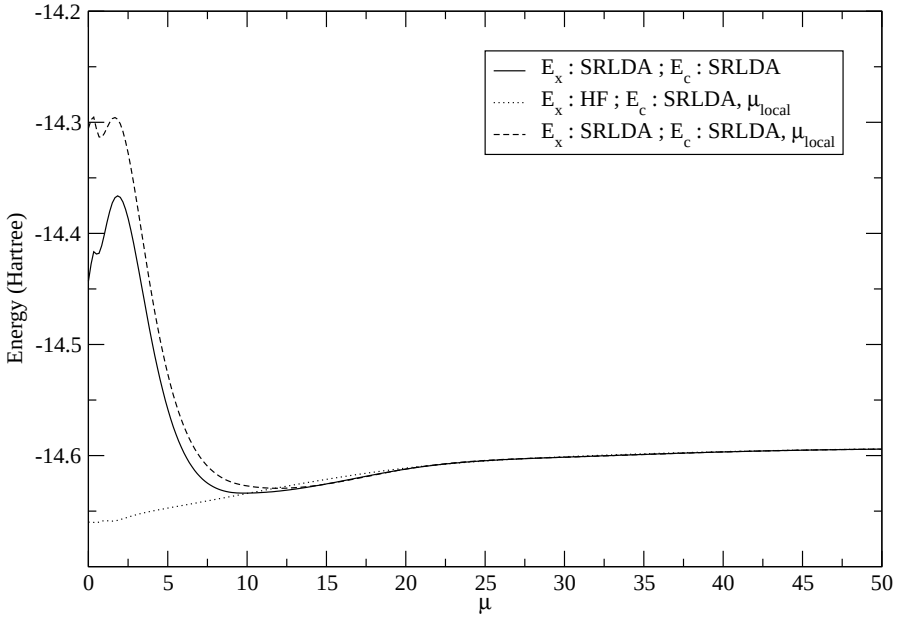

Toulouse *et al.* [17] that the local μ improves the short-range LDA functional and provides a near exact correlation energy for Helium it is evident from Fig. 11.2.4 that improving the correlation functional and keeping the usual short-range LDA exchange deteriorates the total exchange correlation functional. It is a well known fact that LDA to some degree rely on cancellation of errors and when improving the correlation functional this balance is shifted. Therefore the SRLDA with local μ functional is also tested with short-range Hartree-Fock exchange. This combination is however also seen to present no improvement, although the $\mu = 0$ energy accidentally is close to the experimental ground state energy. When adding the short-range Hartree-Fock exchange to the CI-DFT energy expression (Eq.11.1.13-11.1.14) we essentially get back the unmodified Coulomb and exchange interactions as if the CI had been done with the regular Coulomb operator. What the dotted curve in Fig. 11.2.4 represents is therefore the usual CI energy plus a correlation only contribution. Since the short-range correlation energy is always below or equal to zero the dotted curve has no minimum. Without a corresponding exchange functional the SRLDA with local μ correlation functional is abandoned.

A more promising idea for improving on the SRLDA functional is the extrapolation schemes mentioned in Sec. 9.4.2. At the time of writing this thesis these schemes have not been implemented but something related has been tested. As a first approximation to extending short-range VWN correlation to short-range LYP correlation, it is assumed that the rescaling (Eq. 9.4.2) that was done on the regular VWN functional [28] can also be applied to the LYP functional [8]. Letting A denote the denominator in Eq. 9.4.2 the short-range LYP correlation energy and potential become

$$E_c^{SR-LYP} \approx A \cdot E_c^{LYP} \tag{11.2.19}$$
$$V_c^{SR-LYP} \approx A \cdot V_c^{LYP} + dA \cdot E_c^{LYP} \tag{11.2.20}$$

The short-range LDA (Dirac) exchange was derived analytically and we therefore do not similarly have scaling factors that can be transferred to Becke exchange correction [40]. In stead the following is proposed

$$E_x^{SR-GGA} \approx A \cdot (E_x^{\text{Dirac}} + E_x^{\text{Becke}}) \tag{11.2.21}$$

where

$$A = \frac{E_x^{SR-LDA}}{E_x^{\text{Dirac}}} \tag{11.2.22}$$

and the potential becomes

$$V_x^{SR-B} \approx B \cdot (E_x^{\text{Dirac}} + E_x^{\text{Becke}}) + A \cdot (V_x^{\text{Dirac}} + V_x^{\text{Becke}}) \quad (11.2.23)$$

where

$$B = \frac{V_x^{SR-LDA}}{E_x^{\text{Dirac}}} - \frac{E_x^{SR-LDA} \cdot V_x^{\text{Dirac}}}{(E_x^{\text{Dirac}})^2} \quad (11.2.24)$$

The correct limits of E_x^{SR-LDA},

$$E_x^{SR-LDA} \rightarrow \begin{cases} E_x^{\text{Dirac}} & \text{for } \mu \rightarrow 0 \\ 0 & \text{for } \mu \rightarrow \infty \end{cases} \quad (11.2.25)$$

ensures the correct limits of E_x^{SR-B}

$$E_x^{SR-B} \rightarrow \begin{cases} E_x^{\text{Dirac}} + E_x^{\text{Becke}} & \text{for } \mu \rightarrow 0 \\ 0 & \text{for } \mu \rightarrow \infty \end{cases} \quad (11.2.26)$$

The total exchange correlation from this approximate scheme is the short-range BLYP functional. In Fig. 11.2.2 this a functional has been used in

Figure 11.2.5: Ground state energy of Be in the truncated CI-DFT model, using the cc-pVTZ basis, the $erfgau$ two-electron operator, and an approximate short-range BLYP functional.

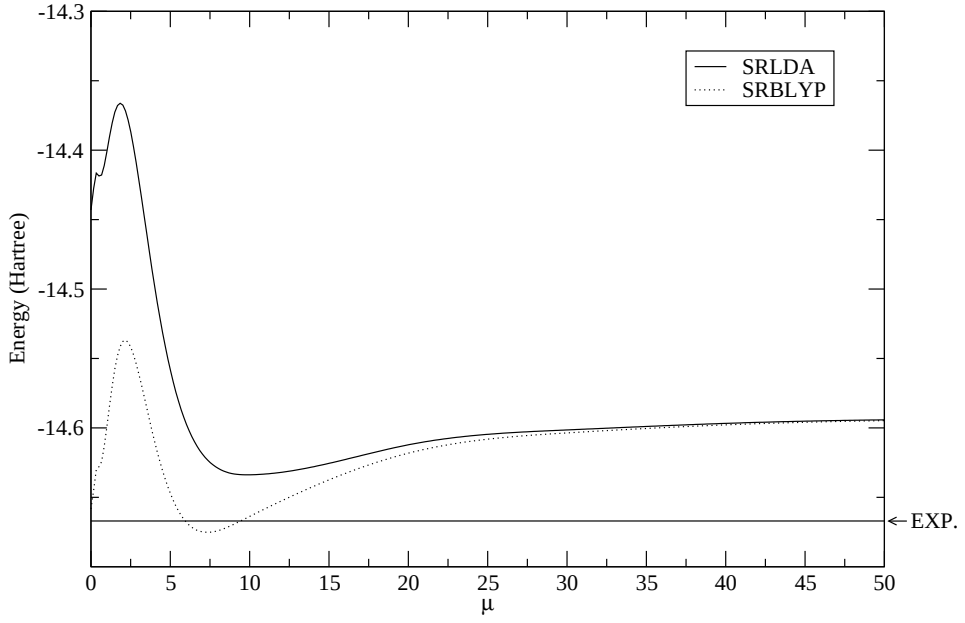

calculating the ground state energy of Beryllium in the truncated CI-DFT model using a cc-pVTZ basis set. One should of course be careful drawing

too many conclusions from using this approximate functional but the $\mu \to \infty$ limit is correctly the usual CI energy and the $\mu = 0$ limit is the usual BLYP energy which is close to the experimental energy (-14.667 Hartree). The CI-DFT now has a minimum which is much closer to the experimental energy than with the SRLDA functional. More importantly, the optimal μ value for the SRBLYP functional has been approximately decreased by 3 compared to the SRLDA functional and this indicates that with a better functional for small μ values the optimal μ is expected to be smaller. This is encouraging and is indeed what is wanted since a small μ value allows a better hybrid of WFT and DFT in which as much work as possible is done by the functional part of the hybrid.

Chapter 12

Conclusions

The hybrid method that merges wave function theory with density functional theory by means of short-range long-range separation of the Coulomb operator has been implemented in a development version of DALTON. The hybrid model has been implemented as the CI-DFT and MCSCF-DFT methods using either the erf

$$V_{ee}^{lr} = \frac{\mathrm{erf}(\mu r_{12})}{r_{12}} \tag{12.0.1}$$

or the $erfgau$

$$V_{ee}^{lr} = \frac{\mathrm{erf}(\mu r_{12})}{r_{12}} - \frac{2\mu}{\sqrt{\pi}} e^{-\frac{1}{3}\mu^2 r_{12}^2} \tag{12.0.2}$$

long-range two electron operators and using either the short-range LDA functional or more approximate functionals that go beyond LDA. The algorithms are completely general though and can easily be extended to using other two-electron operators and short-range functionals. The conclusions from the investigations can be summarized as :

1. In the systems tested the WFT DFT hybrid methods provide better estimates of the ground-state energies than both the regular DFT and WFT methods.

2. The tests indicate that both basis set requirements are lowered and that the need for long wave function expansions in multi-reference approaches to dynamic correlation has been removed from the WFT DFT hybrid by releasing the wave function from dealing with short-range interaction of the electrons. This is promising for performing large scale with the MCSCF-DFT model. An even more economical approach could be the Generalized Valence Bond DFT hybrid model.

3. Currently the limitations of using a short-range LDA type functional mean that it is impossible to achieve a good description of both core and valence electrons in many electron systems. Improving the functionals in the region of small μ values by taking advantage of the better quality of gradient corrected functionals looks very promising and could remove this obstacle.
   An alternative to improving the SRLDA functional in reduced space CI-DFT and MCSCF-DFT calculations is to treat the inactive core electrons by the regular B3LYP method in the Kohn-Sham spirit, and only perform the short-range long-range separation in the valence space. The motivation behind this procedure is that in this way the core electrons are described at a better level than with the SRLDA functional and the multi-configurational character is expected to mainly be associated with the valence electrons. At the time of writing this thesis the implementation of these ideas has begun but has not reached at state that allows any results to be reported.

4. Short-range gradient corrected functionals will also benefit from the short-range long-range separation. A well known problem with gradient corrected functionals is an incorrect asymptotic behavior. Assigning only short-range interactions to the functional this is not expected to be a serious problem for the WFT DFT hybrid in the region of intermediate and large μ values.

5. With the formulation of an MCSCF-DFT hybrid it will be possible to perform calculations on systems with multi-configurational characters. Systems that historically have been problematic to treat with regular DFT. Extending the method to allow calculations of frequency dependent response properties will likewise offer improvements over time-dependent DFT in cases with static correlation and in the description of excited states with for example double excitation character.

Bibliography

[1] I. Panas. *Chem. Phys. Lett.*, 245:171, 1995.

[2] I. Panas and A. Snis. *Theor. Chem. Acc.*, 97:232, 1997.

[3] E. Clementi and G. C. Lie. *J. Chem. Phys.*, 60:1275, 1974.

[4] E. Clementi and G. C. Lie. *J. Chem. Phys.*, 60:1288, 1974.

[5] P. Gombas. Pseudopotentials. In *Die Statiche Theorie des Atoms und ihre Anwendungen*. Springer Verlag, Vienna 1949, 1967.

[6] R. Colle and O. Salvetti. *Theor. Chem. Acc.*, 37:329, 1975.

[7] R. Colle and O. Salvetti. *Theor. Chim. Acta*, 79:1404, 1979.

[8] C. Lee, W. Yang, and R. G. Parr. *Phys. Rev. B*, 37:785, 1988.

[9] R. Colle and O. Salvetti. *J. Chem. Phys.*, 93:534, 1990.

[10] A. Savin. *Int. J. Quant. Chem. Symp.*, 22:59, 1988.

[11] B. Miehlich, H. Stoll, and A. Savin. *Mol. Phys.*, 91:527, 1997.

[12] A. Savin. On degeneracy, near-degeneracy and density functional theory. In J. M. Seminario, editor, *Recent Developments and Applications of Modern Density Functional Theory*, page 327. Elsevier, Amsterdam, 1996.

[13] A. Savin and H. J. Flad. *Int. J. Quant. Chem.*, 56:327, 1995.

[14] T. Leininger, H. Stoll, H.-J. Werner, and A. Savin. *Chem. Phys. Lett.*, 275:151, 1997.

[15] R. Pollet, A. Savin, T. Leininger, and H. Stoll. *J. Chem. Phys.*, 116:1250, 2002.

[16] J. Toulouse, A. Savin, and H. J. Flad. *manuscript*, 2004.

[17] J. Toulouse, F. Colonna, and A. Savin. *manuscript*, 2004.

[18] J. Toulouse, F. Colonna, and A. Savin. *manuscript*, 2004.

[19] H. Stoll. *Chem. Phys. Lett.*, 376:141, 2003.

[20] J. J. W. McDouall. *Mol. Phys.*, 101:361, 2003.

[21] D. Prendergast, M. Nolan, C. Filippi, S. Fahy, and J. C. Greer. *J. Chem. Phys.*, 115:1626, 2001.

[22] W. Kohn and L. J. Sham. *Phys. Rev. A*, 140:1133, 1965.

[23] O. Gunnarsson and B. I. Lundqvist. *Phys. Rev. B*, 13:4274, 1976.

[24] B. I. Dunlap, J. W. D. Connolly, and J. R. Sabin. *J. Chem. Phys.*, 71:3396, 1979.

[25] R. T. Gallant and Alain St-Amant. *Chem. Phys. Lett.*, 256:569, 1996.

[26] C. A. White and M. Head-Gordon. *J. Chem. Phys.*, 101:5693, 1994.

[27] H-Q. Ding, N. Karasawa, and W. A. Goddard. *J. Chem. Phys.*, 97:4309, 1992.

[28] S. J. Vosko, L. Wilk, and M. Nusair. *Can. J. Phys.*, 58:1200, 1980.

[29] J. P. Perdew, K. Burke, and M. Ernzerhof. *Phys. Rev. Lett.*, 77:3865, 1996.

[30] A. Savin, F. Colonna, and R. Pollet. *Int. J. Quant. Chem.*, 93:166, 2003.

[31] H. J. Aa. Jensen and P. Jørgensen. *J. Chem. Phys.*, 80:1204, 1984.

[32] H. J. Aa. Jensen and H. Ågren. *Chem. Phys. Lett.*, 110:140, 1984.

[33] H. J. Aa. Jensen and H. Ågren. *Chem. Phys.*, 104:229, 1986.

[34] H. J. Aa. Jensen, P. Jørgensen, and H. Ågren. *J. Chem. Phys.*, 87:451, 1987.

[35] H. J. Aa. Jensen, P. Jørgensen, H. Ågren, and J. Olsen. *J. Chem. Phys.*, 88:3834, 1988.

[36] H. J. Aa. Jensen. Electron correlation in molecules using direct second order mcscf. In G. L. Malli, editor, *Relativistic and Electron Correlation Effects in Molecules and Solids*, page 179. Plenum, New York, 1994.

[37] Jr. T. H. Dunning. *J. Chem. Phys.*, 90:1007, 1989.

[38] T. Helgaker, H. J. Aa. Jensen, P. Jørgensen, J. Olsen, K. Ruud, H. Ågren, K. L. Bak, V. Bakken, O. Christiansen, S. Coriani, P. Dahle, E. K. Dalskov, T. Enevoldsen, B. Fernandez, C. Hättig, K. Hald, A. Halkier, H. Heiberg, H. Hettema, D. Jonsson, S. Kirpekar, R. Kobayashi, H. Koch, K. V. Mikkelsen, P. Norman, M. J. Packer, T. A. Ruden, T. Saue, S. P. A. Sauer, B. Schimmelpfennig, K. O. Sylvester-Hvid, P. R. Taylor, and O. Vahtras. Dalton release 1.2 (2001), an electronic structure program, http://www.kjemi.uio.no/software/dalton/dalton.html.

[39] J. Harris. *Phys. Rev. B*, 31:1770, 1985.

[40] A. D. Becke. *Phys. Rev. A*, 38:3098, 1988.

Part IV

The One-center 4-Component Model

Chapter 13

Introduction

The work of Clementi *et al.* [1] was already mentioned in Sec.4 to show just how small an energy contribution the correlation is. The decomposition of energy contributions can be used once again to argue that the relativistic energy correction can likewise not be ignored if high accuracy is needed. From Fig.4.0.1 it was clear that the exchange energy was a considerable energy contribution that by far overshadowed the correlation energy. For atoms of nuclear charge $Z = 1..54$ Clementi *et al.* found that the relativistic energy correction becomes larger than the exchange energy for Z=50 while relativity becomes more important than correlation already at Z=12. In terms of ground state energies one can therefore conclude that for all but the lightest elements it becomes important to take relativistic effects into account and when approaching Z=12 it should even be considered as important as electron correlation. Of course in this part of the periodic table relativity is essentially a core effect, unlike correlation which will also affect valence properties.
That relativistic effects become increasingly important with increasing nuclear charge can be understand from the following simple arguments [2]. The average speed of the 1s-electron in atomic units is equal to the nuclear charge ($\langle v \rangle_{1s} = Z$). From special relativity we furthermore know that the mass of on electron traveling at the speed v is related to its rest mass (m_e) by

$$m^{1s} = \frac{m_e}{\sqrt{1 - \frac{v^2}{c^2}}} = \frac{m_e}{\sqrt{1 - \frac{Z^2}{c^2}}} \tag{13.0.1}$$

where $c \approx 137$, is the speed of light in atomic units. This factor $(1/\sqrt{1 - \frac{Z^2}{c^2}})$ increases dramatically as Z approaches the speed of light as seen on Fig.13.0.1. If the classical angular momentum

$$\mathbf{L} = \mathbf{r} \times (m\mathbf{v}) \tag{13.0.2}$$

Figure 13.0.1: Illustration of the relativistic mass correction as a function of nuclear charge.

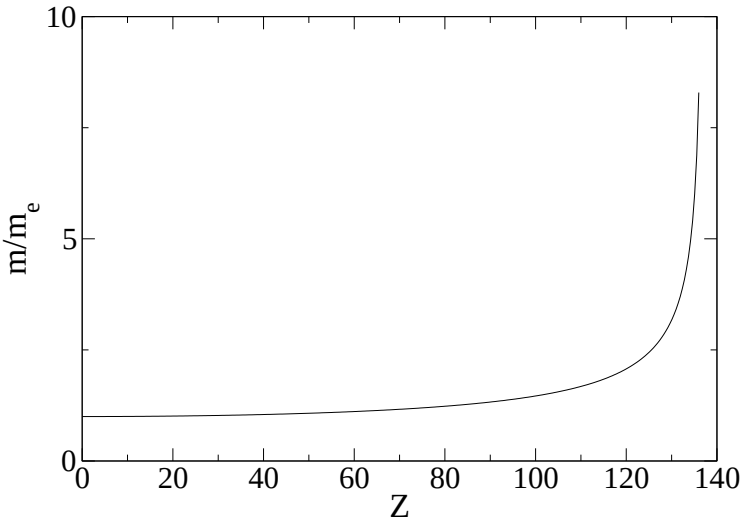

is to be preserved an increase in the mass must be accompanied by a contraction of the 1s-orbital. This contraction will propagate and produce a contraction of the outer s and p shells as well. The innermost d orbitals can likewise experience a relativistic contraction while the increased shielding of the nucleus due to these contractions will have the effect of an expansion of the outer d and f orbitals. A classic example of relativistic orbital contraction/expansion is the gap of the 5d 6s orbitals of Au, where a non-relativistic calculation would predict silver and gold to both absorb light in the ultraviolet region, i.e. having the color of silver, while a relativistic calculation decreases the 5d 6s gap of Au to predict an absorption in the 460nm region. The "take home message" is that - *the need to account for relativistic effect in calculations of both energies and properties becomes important whenever considering heavy elements and in general when calculating properties depending on the electronic density near the nuclear region.* This can be done in several ways. A simple way of incorporating some relativistic effects within an otherwise n.r. framework is replacing the core electrons by an effective potential based an relativistic atomic calculation. Since the relativistic effects are expected to be most pronounced near the nucleus, the use of such relativistic effective core potentials should account for a large fraction of the relativistic effects. Alternatively one can account for relativity by using Hamiltonians based on 1- and 2-component approximations to the Dirac equation [3–5], like the Douglas-Kroll [6, 7] and ZORA [8] Hamiltonians,

but while the reduced computational effort of these approximate methods is appealing, operators often become quite complicated. This in turn is the advantage of the 4-component formulation, in which operators have a much simpler structure. Though being better suited for describing relativity, methods formulated within the 4-component framework have only been applied in the last two decades, the reason being the computational effort required. Probably the most frequent argument from people being critical about the future of 4-component calculations is that the methods are only applicable to systems that are of no chemical interest. It is therefore important to prove that well founded approximation can bring the computational efficiency close to that of the n.r. approaches without jeopardizing the advantages of simple formalism and accuracy.

Many attempts to reduce the computational cost of the 4-component methods have focused on ways to avoid calculating the additional classes of integrals partially or entirely [9–13]. Complete neglect of integrals involving small component functions is generally not an applicable approach since the small component can be significantly occupied [14], but including the densities in an integral screening techniques based on the Cauchy-Schwartz inequality has proved to be an efficient way of neglecting integrals that contribute negligibly to the Fock matrix [11]. As will be seen in this chapter a large fraction of the additional integrals present in 4-component Dirac-Hartree-Fock (DHF) can be approximated or neglected which makes it possible to perform calculations with the one-center 4-component model on molecules of the same size as if the Douglass-Kroll or ZORA Hamiltonians are used.

Chapter 14

Dirac-Hartree-Fock Theory

The following section sets up the framework for doing 4-component Dirac-Coulomb Hartree Fock calculation. The notation closely follows that of T. Saue *et al.* [11]. We start from the relativistic one-electron Hamiltonian in the presence of the static potential from the Born-Oppenheimer reference frame of nuclei as proposed by P.A.M Dirac [3–5] in 1929

$$\hat{h}_D(i) = c\boldsymbol{\alpha} \cdot \mathbf{p}(i) + \beta mc^2 + V^N(i) \tag{14.0.1}$$

where $\mathbf{p} = -i\left[\frac{\partial}{dx}, \frac{\partial}{dy}, \frac{\partial}{dz}\right]$ is the momentum, $\boldsymbol{\alpha} = (\alpha_x, \alpha_y, \alpha_z)$ and where the components of $\boldsymbol{\alpha}$ as well as β are 4×4 matrices

$$\alpha_i = \begin{pmatrix} 0_2 & \sigma_i \\ \sigma_i & 0_2 \end{pmatrix} \ , \ \beta = \begin{pmatrix} I_2 & 0_2 \\ 0_2 & -I_2 \end{pmatrix} \tag{14.0.2}$$

where 0_2 and I_2 are the 2x2 null and unit matrices and σ_i are the Pauli matrices. To align the relativistic energy scale with the n.r. we do however not use β but $\beta' = \beta - \mathbf{I}_4$. $V^N(i)$ is the electrostatic potential on electron i from the N nuclei,

$$V^N(i) = -\sum_A^N \frac{\xi_A}{r_{iA}} \tag{14.0.3}$$

where $\xi_A(r_{iA}) = Z_A N_A \exp(-\eta_A r_{iA})$, and we model the distribution of the nuclear charge Z_A with a single Gaussian.

The Dirac Hamiltonian for a molecular system of n electrons is buildt by a sum of the one-electron Hamiltonians (14.0.1) and adding terms describing the electronic interactions (second term) as well as the repulsion between the N nuclei

$$\widehat{H}_D = \sum_{i=1}^{n} \hat{h}_D(i) + \sum_{i<j}^{n} \hat{g}(ij) + \sum_{A<B}^{N} \frac{Z_A Z_B}{R_{AB}} \tag{14.0.4}$$

Though getting an electron interaction that is not Lorentz invariant we settle for the usual n.r. Coulomb interaction $\hat{g}^{\text{Coulomb}}(i,j) = \frac{1}{r_{ij}}$. A better description is providing by the Breit interaction which is the sum of the Gaunt and Gauge terms,

$$\hat{g}^{\text{Breit}}(i,j) = -\left(\frac{\boldsymbol{\alpha}_i \cdot \boldsymbol{\alpha}_j}{2r_{ij}} + \frac{(\boldsymbol{\alpha}_i \cdot \mathbf{r}_{ij}) \cdot (\boldsymbol{\alpha}_j \cdot \mathbf{r}_{ij})}{2r_{ij}^3}\right) \tag{14.0.5}$$

but the use of this operator would require the evaluation of a huge number of integrals that are not expected to effect the properties of the valence region. Our choice of molecular Hamiltonian is therefore the Dirac-Coulomb Hamiltonian

$$\widehat{H}_{DC} = \sum_{i=1}^{n} \hat{h}_D(i) + \sum_{i<j}^{n} \frac{1}{r_{ij}} + \sum_{A<B}^{N} \frac{Z_A Z_B}{R_{AB}} \tag{14.0.6}$$

In the DHF approach we approximate the wave function by a single Slater determinant ($\Psi = \frac{1}{\sqrt{N!}} \mid \psi_1(1)\psi_2(2)\cdots\psi_N(N) \mid$) of orthonormal ($\langle \psi_i \mid \psi_j \rangle = \delta_{ij}$) molecular spinors, and we write the electronic Dirac-Coulomb energy as

$$E = \sum_{i=1}^{n} \langle \psi_i \mid \hat{h}_D \mid \psi_i \rangle + \frac{1}{2} \sum_{i,j=1}^{n} [(\psi_i\psi_i \mid \psi_j\psi_j) - (\psi_i\psi_j \mid \psi_j\psi_i)] \tag{14.0.7}$$

with the two-electron integrals written in Mulliken notation.
The presence of the 4×4 matrices in $\hat{h}_{DC}$ (14.0.1) must make the Molecular Orbitals (MO's) 4-spinors, and we expand these in a set of real atomic scalar functions (χ_i^X)

$$\psi_i = \begin{bmatrix} \psi_i^{L_\alpha} \\ \psi_i^{S_\alpha} \\ \psi_i^{L_\beta} \\ \psi_i^{S_\beta} \end{bmatrix} = \begin{bmatrix} \tilde{\boldsymbol{\chi}}^{L_\alpha} & 0 & 0 & 0 \\ 0 & \tilde{\boldsymbol{\chi}}^{S_\alpha} & 0 & 0 \\ 0 & 0 & \tilde{\boldsymbol{\chi}}^{L_\beta} & 0 \\ 0 & 0 & 0 & \tilde{\boldsymbol{\chi}}^{S_\beta} \end{bmatrix} \begin{bmatrix} \mathbf{c}_i^{L_\alpha} \\ \mathbf{c}_i^{S_\alpha} \\ \mathbf{c}_i^{L_\beta} \\ \mathbf{c}_i^{S_\beta} \end{bmatrix} = \tilde{\boldsymbol{\chi}}\mathbf{c}_i \tag{14.0.8}$$

where

$$\tilde{\boldsymbol{\chi}}^X = \begin{bmatrix} \chi_1^X \chi_2^X \cdots \chi_{N_X}^X \end{bmatrix} \ , \ \mathbf{c}_i^X = \begin{bmatrix} c_{1i}^X \\ c_{2i}^X \\ \vdots \\ c_{N_X i}^X \end{bmatrix} \ , \ X = L_\alpha, L_\beta, S_\alpha, S_\beta \tag{14.0.9}$$

The energy in (14.0.7) is now a function of the MO-coefficients and variational determination of the coefficients that minimize this energy, under the

constraint that the MO's remain orthonormal, yield the pseudo eigenvalue equation (the Dirac-Fock equation)

$$\mathbf{Fc} = \varepsilon \mathbf{Sc} \tag{14.0.10}$$

where $\mathbf{S}$ is the overlap matrix. $\mathbf{F}$ is the Fock matrix which can be split into one- and two-electron contribution ($\mathbf{F} = \mathbf{F}^{(1)} + \mathbf{F}^{(2)}$)

$$\mathbf{F}^{(1)} = \begin{bmatrix} \mathbf{V}^{L_\alpha L_\alpha} & -ic\mathbf{P}_z^{L_\alpha S_\alpha} & 0 & ic\mathbf{P}_-^{L_\alpha S_\beta} \\ -ic\mathbf{P}_z^{S_\alpha L_\alpha} & \mathbf{W}^{S_\alpha S_\alpha} & -ic\mathbf{P}_-^{S_\alpha L_\beta} & 0 \\ 0 & -ic\mathbf{P}_+^{L_\beta S_\alpha} & \mathbf{V}^{L_\beta L_\beta} & ic\mathbf{P}_z^{L_\beta S_\beta} \\ -ic\mathbf{P}_+^{S_\beta L_\alpha} & 0 & ic\mathbf{P}_z^{S_\beta L_\beta} & \mathbf{W}^{S_\beta S_\beta} \end{bmatrix} \tag{14.0.11}$$

with the elements

$$\mathbf{V}_{ij}^{XX} = \langle \chi_i^X \mid V^N \mid \chi_j^X \rangle \tag{14.0.12}$$

$$\mathbf{W}_{ij}^{YY} = \langle \chi_i^Y \mid V^N - 2c^2 \mid \chi_j^Y \rangle \tag{14.0.13}$$

$$ic(\mathbf{P}_\pm)_{ij}^{XY} = c\langle \chi_i^X \mid \frac{\partial}{\partial x} \mid \chi_j^Y \rangle \pm ic\langle \chi_i^X \mid \frac{\partial}{\partial y} \mid \chi_j^Y \rangle \tag{14.0.14}$$

$$ic(\mathbf{P}_z)_{ij}^{XY} = c\langle \chi_i^X \mid \frac{\partial}{\partial z} \mid \chi_j^Y \rangle \tag{14.0.15}$$

$$\text{where } X, Y \in \{L_\alpha, L_\beta, S_\alpha, S_\beta\} \tag{14.0.16}$$

$$\mathbf{F}^{(2)} = \mathbf{F}^J + \mathbf{F}^K \tag{14.0.17}$$

$$\mathbf{F}^J = \begin{bmatrix} \mathbf{J}^{L_\alpha} & 0 & 0 & 0 \\ 0 & \mathbf{J}^{L_\beta} & 0 & 0 \\ 0 & 0 & \mathbf{J}^{S_\alpha} & 0 \\ 0 & 0 & 0 & \mathbf{J}^{S_\beta} \end{bmatrix} \tag{14.0.18}$$

$$\mathbf{F}^K = \begin{bmatrix} -\mathbf{K}^{L_\alpha L_\alpha} & -\mathbf{K}^{L_\alpha S_\alpha} & -\mathbf{K}^{L_\alpha L_\beta} & -\mathbf{K}^{L_\alpha S_\beta} \\ -\mathbf{K}^{S_\alpha L_\alpha} & -\mathbf{K}^{S_\alpha S_\alpha} & -\mathbf{K}^{S_\alpha L_\beta} & -\mathbf{K}^{S_\alpha S_\beta} \\ -\mathbf{K}^{L_\beta L_\alpha} & -\mathbf{K}^{L_\beta S_\alpha} & -\mathbf{K}^{L_\beta L_\beta} & -\mathbf{K}^{L_\beta S_\beta} \\ -\mathbf{K}^{S_\beta L_\alpha} & -\mathbf{K}^{S_\beta S_\alpha} & -\mathbf{K}^{S_\beta L_\beta} & -\mathbf{K}^{S_\beta S_\beta} \end{bmatrix} \tag{14.0.19}$$

with elements

$$\mathbf{J}_{ij}^X = \sum_Y \sum_{kl} D_{kl}^{YY} (\chi_i^X \chi_j^X \mid \chi_k^Y \chi_l^Y) \tag{14.0.20}$$

$$\mathbf{K}_{ij}^{XY} = \sum_{kl} D_{kl}^{XY} (\chi_i^X \chi_l^X \mid \chi_k^Y \chi_j^Y) \tag{14.0.21}$$

$$\text{where } \; X, Y \in \{L_\alpha, L_\beta, S_\alpha, S_\beta\}$$

where the density matrix **D** has been introduced.

$$D_{kl}^{XY} = \sum_{i}^{n} c_{ki}^{X} c_{li}^{Y*} \tag{14.0.22}$$

Introducing time reversal symmetry as a way to reduce the work need to solve the eigenvalue problem (14.0.10) quaternion algebra is introduced [11]. The one- and two-electron Fock matrices have the structure

$$\begin{bmatrix} F^{\alpha\alpha} & F^{\alpha\beta} \\ F^{\beta\alpha} & F^{\beta\beta} \end{bmatrix} = \begin{bmatrix} A & B \\ -B^* & A^* \end{bmatrix} \tag{14.0.23}$$

which allows a unitary quaternion transformation ($\check{i}, \check{j}, \check{k}$ being the quaternion units)

$$\mathbf{U} = \frac{1}{\sqrt{2}} \begin{bmatrix} \mathbf{I} & \check{j}\mathbf{I} \\ \check{j}\mathbf{I} & \mathbf{I} \end{bmatrix} \tag{14.0.24}$$

to block diagonalize the Fock matrix

$$\mathbf{F}' = \mathbf{U}^{\dagger}\mathbf{F}\mathbf{U} = \begin{bmatrix} \mathbf{F}^{\alpha\alpha} + \mathbf{F}^{\alpha\beta}\check{j} & 0 \\ 0 & -\check{k}(\mathbf{F}^{\alpha\alpha} + \mathbf{F}^{\alpha\beta}\check{j})\check{k} \end{bmatrix} \tag{14.0.25}$$

This defines the quaternion Fock matrix (${}^{Q}\mathbf{F}$) and produces the quaternion Dirac-Fock pseudo eigenvalue equation which is solved iteratively

$${}^{Q}\mathbf{F}{}^{Q}\mathbf{c} = \left[\mathbf{F}^{\alpha\alpha} + \mathbf{F}^{\alpha\beta}\check{j}\right]\left[\mathbf{c}^{\alpha} - \mathbf{c}^{\beta*}\check{j}\right] = \varepsilon^{Q}\mathbf{S}\left[\mathbf{c}^{\alpha} - \mathbf{c}^{\beta*}\check{j}\right] = \varepsilon^{Q}\mathbf{S}{}^{Q}\mathbf{c} \tag{14.0.26}$$

14.1 Kinetic Balance - Choice Of Small Component Basis

Having seen that the wave function has a large and a small component we can write the one-electron Dirac-equation, corresponding to the Hamiltonian of (14.0.1), as two coupled equations

$$(V^N - E)\Psi^L + c(\boldsymbol{\sigma}\cdot\mathbf{p})\Psi^S = 0 \tag{14.1.27}$$

$$c(\boldsymbol{\sigma}\cdot\mathbf{p})\Psi^L + (V^N - E - 2mc^2)\Psi^S = 0 \tag{14.1.28}$$

From (14.1.28) we identify a coupling of the small and large component. Isolation of Ψ^S yields

$$\Psi^S = \frac{1}{2mc}B(E)(\boldsymbol{\sigma}\cdot\mathbf{p})\Psi^L \;; \quad B(E) = \left[1 + \frac{E - V^N}{2mc^2}\right]^{-1} \tag{14.1.29}$$

and in the n.r. limit we get

$$\lim_{c\to\infty} \Psi^S = \frac{1}{2mc}(\boldsymbol{\sigma}\cdot\mathbf{p})\Psi^L \tag{14.1.30}$$

For a hydrogenic large component wave function ($\Psi \sim e^{-Zr}$) this puts meaning to the names "large" and "small" components

$$\Psi^S \sim \frac{Z}{2mc}\Psi^L \sim \frac{Z}{274}\Psi^L \tag{14.1.31}$$

Choosing your small component part of the wave function as prescribed in (14.1.30) you get the right n.r. limit when the velocity operator works on the wave function (if we identify Ψ^L as the n.r. wave function, and $\mathbf{p} = m\mathbf{v}$).

$$\begin{aligned}\lim_{c\to\infty} \Psi^\dagger c\boldsymbol{\alpha}\Psi &= \left(\Psi^{L\dagger}\Psi^{S\dagger}\right)\begin{pmatrix} c\boldsymbol{\sigma}\Psi^S \\ c\boldsymbol{\sigma}\Psi^L \end{pmatrix} \\ &= \frac{1}{2m}\Psi^{L\dagger}\left[\boldsymbol{\sigma}(\boldsymbol{\sigma}\cdot\mathbf{p}) + (\boldsymbol{\sigma}\cdot\mathbf{p})\boldsymbol{\sigma}\right]\Psi^L \\ &= \frac{1}{m}\Psi^{L\dagger}\mathbf{p}\Psi^L \end{aligned} \tag{14.1.32}$$

Hence the kinetic energy has the right n.r. limit and (14.1.30) forms the basis for the *kinetic balance* condition. [15, 16]
To expand the MO's in scalar basis functions we must impose a coupling of the small- and large component basis similar to that of (14.1.30). We relate the set of small component basis functions to that of the large component by

$$\left\{\chi^S\right\} = \left\{(\boldsymbol{\sigma}\cdot\mathbf{p})\chi^L\right\} \tag{14.1.33}$$

Defining the Gaussian of exponent α and angular momentum $l = i + j + k$ as $G^\alpha_{ijk} = G^\alpha_i G^\alpha_j G^\alpha_k$ where for example $G^\alpha_i = x^i e^{-\alpha x^2}$, and expanding the MO's in these functions we get Gaussians of angular momentum lowered and incremented by one in the set of small component functions.

$$\chi^L = \{G^\alpha_l\} \Rightarrow \chi^S = \left\{G^\alpha_{l-1}, G^\alpha_{l+1}\right\} \tag{14.1.34}$$

The linear combination generated by differentiation of the large component function can be regarded as separate functions producing the *unrestricted kinetic balance* (UKB) scheme, in which there is approximately a factor of two between the number of large and small functions, or the linear combination can be regarded as a single Gaussian giving the *restricted kinetic balance* (RKB) scheme, in which there is a 1:1 ratio between the large and small functions.

The default procedure in DIRAC [17] is to use the restricted kinetic balance scheme, ensured by projecting out the "unphysical" solutions present in the free particle positronic spectrum. This projection ensures a 1:1 ratio between electronic and positronic orbitals.
Note that using the scheme described above one can use the usual non-relativistic basis sets where available for the large component. Of course some of the heavier elements are not included in these basis sets and relativistic Gaussian basis sets have been reported [18, 19].

14.2 Integral Logistics

Using the Coulomb operator we need to calculate three classes of integrals :

(i) LL integrals : X=Y=L in (14.0.20-14.0.21)
(ii) LS integrals : X=L,Y=S in (14.0.20-14.0.21)
(iii) SS integrals : X=Y=S in (14.0.20-14.0.21)

The integrals of class (i) are also calculated in the n.r. case. Taking the 8-fold index permutation symmetry

$$(ij \mid kl) = (ij \mid lk) = (ji \mid kl) = (ji \mid lk) =$$
$$(kl \mid ij) = (kl \mid ji) = (lk \mid ij) = (lk \mid ji)$$

into account the classes (ii) and (iii) scale as $\frac{1}{4}N_S^2N_L^2$ and $\frac{1}{8}N_S^4$ respectively, where the number of small component basis functions (N_S) is approximately twice the number of large functions (N_L). This produces about 25 times as many two-electron integrals as in the n.r. case which underlines the need to use a direct integral evaluation scheme and the usefulness of effective screening techniques as well as the possibility to only include the classes (ii) and (iii) after a certain number of iterations in the SCF procedure. The aim of the one-center approximation is to reduce this large factor between the number of two-electron integrals in the HF and DHF schemes without significant errors in the energy and wave function.

Chapter 15

One-center approximations

Despite the fact that the two-electron integrals involving the small component are numerous their contribution to the Fock matrix is often vanishing. Approximations to the evaluation of the relativistic two-electron integrals should involve the small component.

If we insert (14.1.29) in (14.1.27) get

$$\left[(V^N - E) + \frac{1}{2m}(\boldsymbol{\sigma}\cdot\mathbf{p})B(E)(\boldsymbol{\sigma}\cdot\mathbf{p})\right]\Psi^L = 0 \tag{15.0.1}$$

For $\mid V^N - E \mid < 2mc^2$ we can expand $B(E)$ in powers of $\frac{1}{2mc^2}$

$$B(E) \approx 1 - \frac{(E-V^N)}{2mc^2} - \frac{(E-V^N)^2}{2mc^4} - \cdots \tag{15.0.2}$$

After insertion of this expansion in (15.0.1), renormalization of Ψ^L and reordering, one can identify the Pauli Hamiltonian. Assuming a point nuclear potential it takes the form

$$\hat{h}^{\text{Pauli}} = T + V^N - \frac{1}{8m^3c^2}\mathbf{p}^4 + \frac{\pi Z}{2m^2c^2}\delta(\mathbf{r}) + \frac{Z}{2m^2c^2}\frac{\mathbf{s}\cdot\boldsymbol{\ell}}{r^3} \tag{15.0.3}$$

The three last terms can be considered corrections to the non-relativistic kinetic and potential energy $(T + V^N)$. The second and third terms are the mass-velocity and Darwin terms, collectively often called the scaler relativistic corrections. The third term is the spin-orbit correction, describing the interaction of the electron spin with the magnetic field generated by the movement of the electron. It depends on r to the third power and is therefore a very "local" property[1]. This locality has been utilized by B.A. Heß *et.*

[1]The two-electron spin-orbit interaction of the Breit-Pauli Hamiltonian has the same r-dependence

al [20], C. Marian *et. al* [21] and B. Schimmelpfennig *et. al* [22] to test the use of effective one-electron spin-orbit operators, neglecting all multi-center two- and one-electron contributions. Using the Atomic-Mean-Field-Integral code (AMFI, available in DALTON [23]) for evaluation of the one-center spin-orbit integrals while taking advantage of the high atomic symmetry, they have proved this to be an effective way of getting spin-orbit splittings in good agreement with experiment.

The success of the mean-field spin-orbit approach lets us expect that a way to reduce the computational effort of the 4-component approaches without jeopardizing the accuracy, must also be hidden somewhere within the 4-component framework. In 4-component theory the spin-orbit interaction is described through the LS class of integrals and applying the thinking of the mean-field approach we expect to be able to make good approximations not only to the SS, but also the LS class of integrals. Again it has to be stressed that simply neglecting the SS and LS integrals or even just neglecting the multi-center terms will not produce a good approximation. When the small component is significantly occupied this would mean that a considerable amount of electronic repulsion would be neglected and the electrostatics of the system would therefore be wrong. To make a comparison the Douglas-Kroll approximation does not have the LS and SS classes of integrals either but in this case the effect of the small component has been folded into the large component wave function by the Douglas-Kroll transformation. For this reason a 4-component calculation without the LS and SS integrals would perform worse than the Douglas-Kroll approach.

The key to reducing the computational effort associated with integral evaluation of 4-component methods is found in the highly localized nature of the small component density. This locality is nicely illustrated on Fig.15.0.1 where the large and small component density has been calculated using DIRAC and plotted in the Molekel[2] program. While the large component density extends to the entire molecule the small component density is localized on the atoms with negligible overlap between centers. One can say that : The superposition of atomic small component densities is a good approximation to the molecular small component density and as molecular formation does not distort the small component densities much we expect that interactions between small component charge centered on different atoms are either negligible or well approximated by simple Coulombic repulsion.

[2]http://www.cscs.ch/molekel/

Figure 15.0.1: Large and small component densities of Iodobenzene.

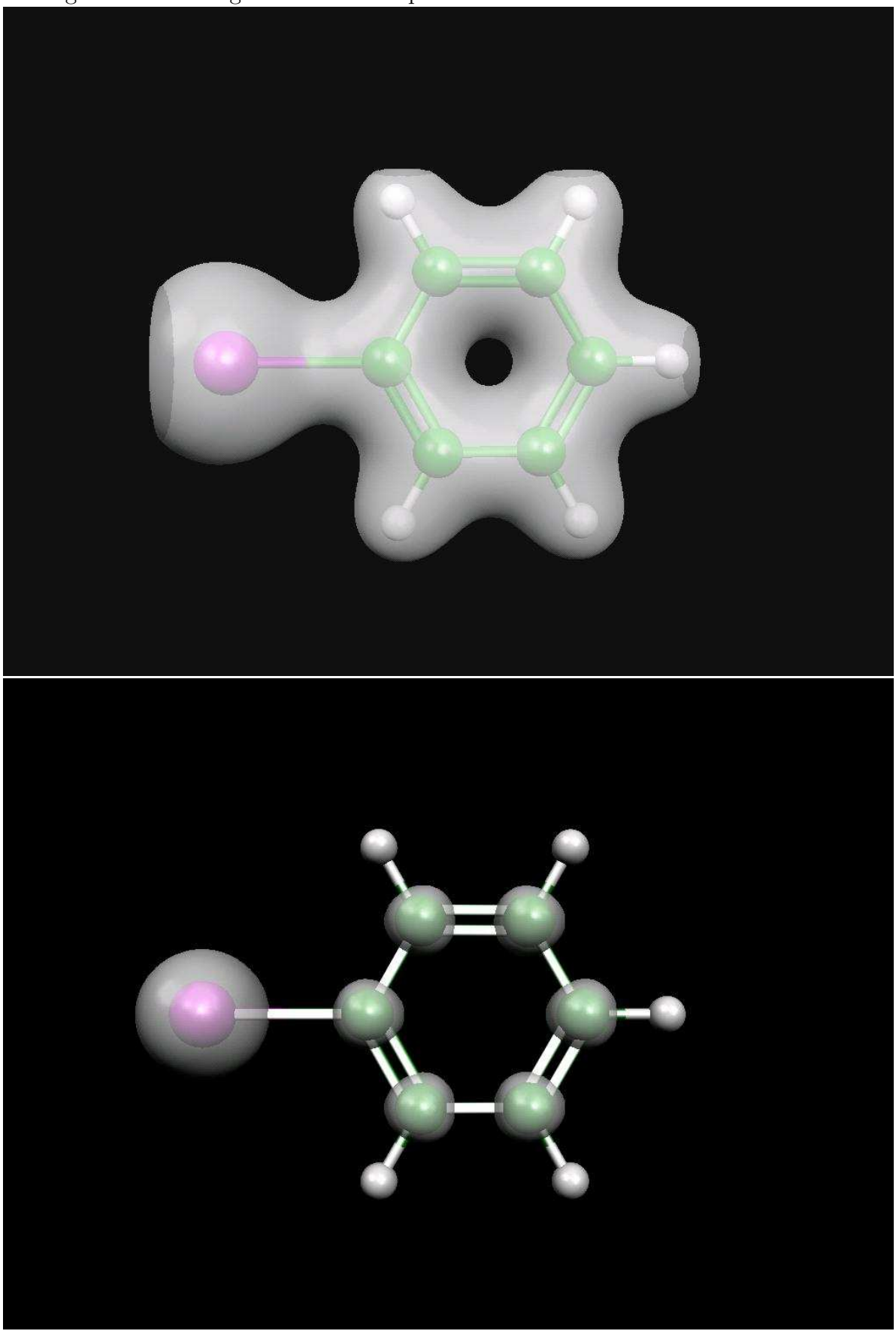

15.1 Notations and Integral Approximations.

The one-center models presented in the next section will all build on the approximations listed below. The notation used is somewhat "sloppy" but allows a simple definition of the models.

1. S_A is a batch of small component scalar functions centered on atom A. Likewise for L_A.

2. $(S_A S_B \mid S_C S_D)$ is the part of (14.0.20) where χ_i^X is centered on atom A and $X = S$ etc. For simplicity we skip the reference to spin.

3. $V^{ee}_{S_A S_B}$ is the contribution to the two-electron Fock matrix from all such elements in 2.

$$V^{ee}_{S_A S_B} \sim \sum_{C,D} D_{S_C S_D} (S_A S_B \mid S_C S_D)$$

   Giving the SS contributions to the electronic repulsion energy

$$E^{ee}_{SS} = \tfrac{1}{2} \sum_{A,B} D_{S_A S_B} V^{ee}_{S_A S_B}$$

4. In this notation the SS contribution to the two electron Fock matrix can be split in multi-center (first line) and one-center terms (second line).

$$\begin{aligned} V^{ee}_{S_A S_B} \quad &\sim \quad \sum_{C,D} D_{S_C S_D} (S_A S_B \mid S_C S_D)(1 - \delta_{AB})(1 - \delta_{CD}) \qquad (15.1.4) \\ &+ \quad \sum_{A \neq B} D_{S_B S_B} (S_A S_A \mid S_B S_B) + \sum_A D_{S_A S_A} (S_A S_A \mid S_A S_A) \qquad (15.1.5) \end{aligned}$$

5. In the one-center terms a further approximation can be made by replacing the contraction of the density with the with small component functions centered on the same atom by an effective charge.

$$\sum_{A \neq B} D_{S_B S_B} (S_A S_A \mid S_B S_B) \approx (S_A \mid \frac{q^S_B}{r_{1B}} \mid S_A) \qquad (15.1.6)$$

6. In the case where A=B (last term in Eq. 15.1.5) these terms can even be approximated calculating the repulsion energy from this term directly

and adding it to the total electronic energy instead of adding this term to the Fock matrix

$$\tfrac{1}{2}\sum_{A} D_{S_A S_A}(S_A \mid \frac{q_B^S}{r_{1B}} \mid S_A) \approx \tfrac{1}{2}\sum_{A\neq B}\frac{q_A^S q_B^S}{R_{AB}} \tag{15.1.7}$$

Furthermore charges and inter atomic distances are labeled as on figure 15.1.2.

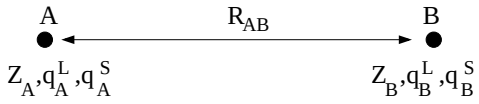

Figure 15.1.2: Notations used in the one-center approximations.

The discussion of how to obtain good estimates of the small component charges (q^S) is left for Sec. 15.6.

The following sections discuss some previously implemented models aswell as the models presented here. Appendix D.2 lists all currently implemented models in DIRAC.

15.2 Model I

The first model presented is the work of L. Visscher and T. de Jong [12, 13]. L. Visscher tested the effect of neglecting the entire SS-class of two-electron integrals and found that this is generally not a useful approach. While the one-center contributions to V_{SS}^{ee} are the most dominant they remain essentially the same in the molecule as in the atom and therefore do not influence the shape of the molecular potential energy surface. He therefore found that the addition of a simple distance dependent Coulombic repulsion correction to each point of the energy surface

$$\frac{1}{2}\sum_{A\neq B}\frac{q_A^s q_B^s}{R_{AB}} \tag{15.2.8}$$

approximated the multi-center contributions well and gave reliable bond distances and harmonic frequencies for the three heaviest halogen dimers while producing a speed-up factor of 3.
Visscher and de Jong [13] extended these ideas to get a reduction in the number of LS-class integrals as well. Again the method relies on the fact that

contributions to the potential energy from integrals over small component functions centered on different atoms are negligible. In contrast to the previously mentioned method the one-center SS-integrals are evaluated explicitly to improve the screening of the nuclei and thereby provide a more accurate wave function. The integral approximation in our notation is

$$\begin{aligned} V^{ee}_{S_A S_B} &\sim \sum_{C,D} D_{S_C S_D}(S_A S_B \mid S_C S_D)\delta_{AB}\delta_{CD} \\ &\sim \sum_{C} D_{S_C S_C}(S_A S_A \mid S_C S_C) \qquad (15.2.9) \\ V^{ee}_{L_A S_B} &\sim \sum_{C,D} D_{S_C S_D}(L_A L_B \mid S_C S_D)\delta_{CD} \\ &\sim \sum_{C} D_{S_C S_C}(L_A L_B \mid S_C S_C) \qquad (15.2.10) \end{aligned}$$

For consistency the corresponding multi-center nuclear-attraction integrals are neglected as well.

$$\begin{aligned} V^{ne}_{S_A S_B} &\sim \sum_{A,B}(S_A \mid -\sum_J \frac{Z_J}{r_J} \mid S_B)\delta_{AB} \\ &\sim \sum_{A}(S_A \mid -\sum_J \frac{Z_J}{r_J} \mid S_A) \qquad (15.2.11) \end{aligned}$$

The success of this approach shows that the terms neglected in (15.2.9-15.2.10) approximately cancel with the terms neglected in (15.2.11) since $(Z_J - q^L - q^S) \approx 0$. This will be seen to be the main approximation in all the one-center models presented here (see Sec. 15.5).
Equation (15.2.9) can be further reduced to just include one-center terms by using the approximation in Eq. 15.1.7 to produce the following SS energy contribution.

$$E^{ee}_{SS} \sim \tfrac{1}{2}\sum_A D_{S_A S_A} D_{S_A S_A}(S_A S_A \mid S_A S_A) + \tfrac{1}{2}\sum_{A\neq B} \frac{q^s_A q^s_B}{R_{AB}} \qquad (15.2.12)$$

Comparing to section 14.2 (page 98) the scaling is now reduced to being linear for the SS-class and cubic in the LS-class. Significant savings has hereby been achieved.
The errors introduced in the Coulomb repulsion are expected to be small, following the simple argument that for tight functions the overlap is insignificant and for diffuse functions having a considerable overlap, the contraction with a small density matrix element should give a vanishing contributions to

the Fock matrix. Approximations are also introduced in the exchange terms (14.0.21). The same arguments used for the Coulomb terms apply here. The largest contributions are expected from the K^{LL} block which we evaluate explicitly as in non-relativistic theory.
The model will be used in applications in this report for comparison with models II and III.

15.3 Model II

Assuming that the previous level of approximations (15.2.9-15.2.11) is a good one, we present here a way to take this approach even further. To make the DHF approach truly one-center in all integrals involving the small component we propose the following approximations.

$$\begin{aligned} V^{ee}_{S_A S_B} &\sim \sum_{C,D} D_{S_C S_D}(S_A S_B \mid S_C S_D)\delta_{AB}\delta_{CD}\delta_{AC} \\ &\sim \sum_{A} D_{S_A S_A}(S_A S_A \mid S_A S_A) \qquad (15.3.13) \\ V^{ee}_{L_A S_B} &\sim \sum_{C,D} D_{S_C S_D}(L_A L_B \mid S_C S_D)\delta_{AB}\delta_{CD}\delta_{AC} \\ &\sim \sum_{A} D_{S_A S_A}(L_A L_A \mid S_A S_A) \qquad (15.3.14) \end{aligned}$$

As before we make the corresponding approximations in the nuclear-attraction terms for consistency.

$$V^{ne}_{S_A S_B} \sim (S_A \mid -\sum_J \frac{Z_J}{r_J} \mid S_B)\delta_{AB}\delta_{AJ} \sim \sum_A (S_A \mid -\frac{Z_A}{r_A} \mid S_A) \qquad (15.3.15)$$

Assuming cancellation of the terms neglected this is clearly unsatisfactory in this case. This would mean neglecting integrals involving the large component which we can of course not trust to be as localized as the small component. Instead we compare the approximation (15.2.9-15.2.11) with (15.3.13-15.3.15) and identify what kind of interactions are additionally ne-

glected.

$$V^{ee}_{S_AS_B} \;:\; \sum_{A\neq B} D_{S_BS_B}(S_AS_A \mid S_BS_B) \tag{15.3.16}$$

(Going from (15.2.9) to (15.3.13))

$$V^{ee}_{L_AS_B} \;:\; \sum_{A\neq B} D_{S_AS_A}(L_BL_B \mid S_AS_A) + \sum_{A\neq B} D_{S_AS_A}(L_AL_B \mid S_AS_A) \tag{15.3.17}$$

(Going from (15.2.10) to (15.3.14))

$$V^{ne}_{S_AS_B} \;:\; \sum_{A\neq B}(S_A \mid -\frac{Z_B}{R_{AB}} \mid S_A) \tag{15.3.18}$$

(Going from (15.2.11) to (15.3.15))

Eq. 15.3.17 can be approximated by invoking the approximation in Eq. 15.1.6. Eq. 15.3.16 and 15.3.18 will not be added to the Fock matrix but approximated as energy corrections after applying the approximation in Eq. 15.1.7.
We therefore replace (15.3.16-15.3.18) by

$$E^{ee}_{SS} \;:\; \sum_{A\neq B} \frac{q^S_A q^S_B}{R_{AB}} \tag{15.3.19}$$

$$V^{ee}_{L_AS_B} \;:\; \sum_{A\neq B}(L_B \mid \frac{q^S_A}{r_A} \mid L_B) + \sum_{A\neq B}(L_A \mid \frac{q^S_A}{r_A} \mid L_B) \tag{15.3.20}$$

$$E^{ne}_{SS} \;:\; \sum_{A\neq B} -\frac{Z_B q^S_A}{R_{AB}} \tag{15.3.21}$$

The terms in (15.3.19) and (15.3.21) combine with the regular nuclear repulsion terms as modifications to nuclear charge.

$$E^{nn} \rightarrow \sum_{A\neq B} \frac{(Z_A - q^S_A)(Z_B - q^S_B)}{R_{AB}} \tag{15.3.22}$$

Likewise (15.3.20) combine with the large component contribution to the nuclear electron attraction terms.

$$\begin{aligned} V^{ne}_{L_AL_B} \;\rightarrow\; & \sum_A (L_A \mid -\frac{Z_A}{r_A} - \sum_{J\neq A} \frac{Z_J - q^S_J}{r_J} \mid L_A) \\ + \; & \sum_{A\neq B}(L_A \mid -\sum_J \frac{Z_J - q^S_J}{r_J} \mid L_B) \end{aligned} \tag{15.3.23}$$

In this way the locality of the small component charge as been exploited to produce a method where all multi center contributions to electron repulsion integrals involving the small component are estimated with no additional computational cost. The method simply amounts to modifying the nuclear charges in the appropriate nuclear-attraction and nuclear repulsion terms.

It should be noted that in (15.3.17) we only consider contributions to the J^L-part of the two-electron Fock matrix (14.0.18). We do of course neglect the contributions to J^S as well and following the same procedure this would give rise to corrections of the type

$$(S_A \mid \frac{q_A^L}{r_A} \mid S_B) \text{ and } (S_A \mid \frac{q_B^L}{r_B} \mid S_A)$$

As we make the correction through the nuclear attraction integrals we get the right "amount" of repulsion by adding the correction to the one-electron Fock matrix once since this is not multiplied by one half when calculating the total energy[3].

The scaling of this model has been reduced to being linear in the evaluation of LS- and SS-integrals since only the atomic contributions are evaluated. In AO-basis one-center two-electron integrals are unchanged during the wave function optimization and we can therefore benefit from writing these to disk at the start of the calculation. What has hereby been achieved is a DHF approach that only differs from a non-relativistic HF procedure, following a direct integral evaluation scheme, in the initial evaluation of one-center LS- and SS-integrals and the fetching of these from disk in each iteration. For molecules with many identical atoms, it is only necessary to calculate the one-center integrals for each atom type, since these are identical assuming that one is using the same basis set for each atom type. In large organic molecules the saving will be significant if you only have to evaluate the one-center LS and SS integrals for one carbon atom, one hydrogen atom, one oxygen atom etc. In the current implementation this is not utilized.

In the implementation of the one-center approximation described above, all corrections are made by adding constant numbers[4] to the nuclear charges in energy terms that all ready need to be calculated. Besides not increasing the computational effort, this allows us to use this approximate wave function for calculating properties without having to implement new integral types. For example the molecular gradient is calculated straightforward, and is actually done at the cost of a non-relativistic molecular gradient. The reason

[3]Calculating the total DHF energy as $E = \sum_{ij} D_{ij}(F_{ij}^{(1)} + \frac{1}{2}F_{ij}^{(2)})$

[4]Assuming that we use fixed small component charges (q_S). Other choices will be tested (see section 15.6)

is that since all multi-center two-electron integrals are estimated with modified nuclear-electron and nuclear-nuclear repulsion terms the contribution to molecular gradient from these terms are automatically included, and we are left with the one-center LS- and SS-integrals, which of course are geometry independent. This leaves us with only having to evaluate the geometry derivatives of the LL type two-electron integrals, just as in a non-relativistic calculation.

15.4 Model III

What model II does is to approximate a part of the two-electron Fock matrix by corrections to the one-electron Fock matrix. Though we expect to account for the right amount of electronic repulsion this way, and thereby get a reasonable total electronic energy, the wave function might be expected to suffer since terms from the LL and SS two-electron Fock matrix are added to the one-electron LL part. We therefore want to test the performance of an approximation where all multi-center contributions from both $(LL \mid SS)$, $(SS \mid LL)$ and $(SS \mid SS)$ integrals are calculated as two-index integrals. The approximation is written as,

$$\begin{aligned} V^{ee}_{S_A S_B} \sim & \sum_A D_{S_A S_A}(S_A S_A \mid S_A S_A) + \sum_{A\neq B}(S_A \mid \frac{q^S_B}{r_B} \mid S_A) + \\ & \sum_{A\neq B}(S_A \mid \frac{q^S_A}{r_A} \mid S_B) + \sum_{A\neq B\neq C}(S_A \mid \frac{q^S_C}{r_C} \mid S_B) \qquad (15.4.24) \\ V^{ee}_{X_A Y_B} \sim & \sum_A D_{Y_A Y_A}(X_A X_A \mid Y_A Y_A) + \sum_{A\neq B}(X_A \mid \frac{q^Y_B}{r_B} \mid X_A) + \\ & \sum_{A\neq B}(X_A \mid \frac{q^Y_A}{r_A} \mid X_B) + \sum_{A\neq B\neq C}(X_A \mid \frac{q^Y_C}{r_C} \mid X_B) \qquad (15.4.25) \end{aligned}$$

calculating the contributions to V^{ee}_{SS}, V^{ee}_{LS} (X=L,Y=S) and V^{ee}_{SL} (X=S,Y=L) separately and adding them to the appropriate blocks of the two-electron Fock matrix and not the one-electron Fock matrix as in model II. The only contributions not accounted for this way is from integrals over four functions centered on four different atoms. The error from these integrals is expected to be small. The errors associated with the approximation in (15.4.25) are clearly expected to be largest for the V^{ee}_{SL} contribution to the Fock matrix.

This model introduces no approximation in the V^{ne}-potential but reduces the evaluation of two-electron integrals involving the small component to the

one-center cases as in model II. Thus the scaling and computational effort of this model is approximately as in model II.

15.5 The Errors Of The One-Center Approximations

The errors introduced by Model I and Model II to the Fock matrix can be estimated by the terms ($A \neq B$),

$$\sum_{J \neq A,B} \left(S_A \mid \frac{q_J^S + q_J^L - Z_J}{r_J} \mid S_B \right) \tag{15.5.26}$$

It is clear that in the 'neutral atoms in molecules' picture these contributions should be small ($q_J^L + q_J^S \approx -Z_J$). In the general case, as for example a charged molecule, one must remember that the integrals in (15.5.26) will be multiplied with the D_{AC}^{SS} density matrix elements, giving a negligible energy contribution. However the integrals themselves can become large for diffuse basis functions, meaning that the contribution to the SS-block of the Fock matrix will not be negligible. This can lead to large errors in the positronic eigenvalue spectrum and can cause instabilities in the iterative Hartree-Fock procedure. This was also reported by de Jong and Visscher [13] who proposed a scheme to address these issues. Instead of discarding multi-center integrals these are expanded in one-center integrals. The scheme can therefore be described as projecting the multi-center terms onto the available set of one-center integrals. As that increases the complexity of especially the calculation of molecular gradients, we test the effect of simply projecting out the set of positronic solutions present in the external potential. Besides removing the instability of the iterative procedure we also reduce the dimension of the eigenvalue problem which further adds to the speed-up of the approximation. With this scheme a direct parallel can again be drawn to the Douglas-Kroll [6, 7] approach since the positronic solutions have been projected out and the small component is handled approximately (apart from the one-center parts).
The effects on energies and properties of projecting out the positronic solutions will be investigated.

Other concerns could be the errors introduced by neglecting the multi-center contributions to the non-classical exchange interaction and the most dominant non-scalar relativistic correction - the spin-orbit interaction. As argued by de Jong and Visscher [13] the delocalized nature of the exchange

contributions should insure that the approximations made to these terms are of little importance. Concerning the spin-orbit contributions, it has already been mentioned that this is a very local interaction, and the major part of the spin-orbit contribution is therefore described through the explicitly evaluated one-center LLSS integrals.

15.6 Implementation

Model I was implemented in DIRAC [17] by Visscher and de Jong [13]. In this work Model II and Model III have been implemented. All the corrections involve the integral code of DIRAC, and some effort has gone into implementing the models without interfering with the original integral routines. Therefore new routines were coded to calculate the corrections needed and adding them to the Fock matrix before solving the DHF eigenvalue problem. This also allows for easier updating and development of the models.

15.6.1 Which q^S to Use

Models I,II and III leave us with the freedom of choosing how to obtain the small component charges, q^S. One possibility is to perform accurate atomic calculations. and tabulate the small component charges for use with the one-center approximations. The advantage of using such charges is that they can be tabulated reused in each one-center calculation. Furthermore the tabulated charges are of course constant numbers and the one-center corrections will therefore be geometry independent.
However what we wish to approximate with the corrections at a given basis set level is the multi center contributions at that particular level. A better choice of small component charges should therefore reflect the quality of wave function, and as will be seen in section 15.9 we generally get better result when using the density based charges obtained from a Mulliken population analysis [24, 25]. For this purpose we interfaced a module written by O. Fossgaard and T. Saue for generating the Mulliken charges from the density in each DHF iteration. This scheme is expected to provide better energies, but being density based these charges are strictly not geometry independent. This is discussed in Sec. 15.7.

15.6.2 Which q^L to Use

Concerning the large component charges needed for model III we did try to use the ones obtained from a Mulliken analysis but found the need for

refinements. What the Mulliken population analysis does is to assign total charges to the atoms by splitting the off-diagonal elements of the matrix of charges in equal amounts between the atoms in question. Taking the diatomic molecule $(A-B)$ as an example we get contributions to the total charge from off-diagonal elements of the density and overlap matrix

	A	B
A	q_{AA}	q_{AB}
B	q_{BA}	q_{BB}

and $Q_A^{\text{Mulliken}} = q_{AA} + q_{AB}$. In the case where the charge of A and B differ significantly (for example like in HI) you get a misleading description of the charge distribution which will result in a misleading description of the repulsion approximated in model III. This problem is expected to be insignificant for the terms in (15.4.25) where q^S is used but certainly not when q^L is used. Instead we calculate all elements of the matrix and thereby have the possibility of distributing the off-diagonal elements on bonds and points between nuclei. Two choices of distributions have been implemented and are tested here. The first is to place all off-diagonal elements at the midpoint between the two atoms in questions. The second is to take into account how much each of the atoms contribute to the off-diagonal element q_{AB}. This is done by evaluating each component (x,y,z) of the matrix of dipole moment integrals.

	A	B
A	μ^x_{AA}	μ^x_{AB}
B	μ^x_{BA}	μ^x_{BB}

where $\mu^x_{AB} = \sum_{kl} D^{LL}_{kl} \langle \chi^A_k \mid x \mid \chi^B_l \rangle$. μ_{AB} provides an estimate of the center of the density on the bond between atom A and B, and placing the corresponding elements of the charge-matrix at these coordinates should produce a better distribution of q^L.
For both types of distribution we perform a test on the absolute value of the charge and skip this element if below a specified value.

15.7 Molecular Gradients

By writing the one-center LS- and SS-integrals to disk, they are reused in all steps in a geometry optimization and are therefore only calculated once in the entire optimization.

Currently molecular gradients are only available for models I and II. When using Mulliken small component charges in model II you have a dependence

on the density in the charges meaning that the charges are strictly not geometry independent ($\frac{dq_A^S}{dX_A} \neq 0$). This contribution to the molecular gradient is neglected in the current implementation and expected to be small following the argument that the small component density is to a good approximation unaffected by molecular formation and therefore fairly geometry independent. This is not the case for the density based large component charges used in model III which is the reason that the molecular gradient has not yet been implemented for this model. The performance of the model did not make this worthwhile.
In Sec 15.9.1 it is tested how the large and small component charges change during a geometry optimization and the numerical molecular gradient is calculated and compared to the approximate analytical gradient.

15.8 Extension to correlated wave functions.

Having formulated an efficient 4 component DHF model the next natural step is to extend the model to correlated methods. The extension to DFT is straightforward and requires no further considerations. Calculations with the one-center B3LYP model are presented for Iodobenzene.

Extending the one-center model to methods that rely on MO transformations like the MP2, CC, and MCSCF method requires some considerations. A simple approximation would be to assume that the contribution from the multi-center LS and SS integrals can be neglected in the MO transformation and describe these terms effectively by adding the approximate terms (Eq. 15.3.19-15.3.21) to the inactive Fock matrices. The performance of such a one-center 4-component MCSCF scheme will be left for future testing.

15.9 Testing the Models for Hartree-Fock.

15.9.1 Iodobenzene

I. Comparison of Model I and Model II
C_6H_5I is the molecule we investigated most intensively with the one-center models. It is a nice test case since the many centers and the presence of a "heavy"-atom should make the approximations perform well with respect to timings. Using an uncontracted n.r. cc-pVDZ [26] basis on Carbon and Hydrogen and an uncontracted Molfdir cc-pVDZ basis set on I (L-[17s13p7d]) [27] results are presented i table 15.9.1 using Model I and

Table 15.9.1: Dirac-Coulomb DHF and DFT calculations on Iodobenzene. Non-relativistic cc-pVDZ basis on C,H. Uncontracted MOLFDIR cc-pVDZ on I (L-[17s13p7d]). For Model II Mulliken charges are used. Numbers in upper half are at the geometry obtained with the full set of integrals. In lower half the geometry has been relaxed.

	Energy (au)	R_{C-I} (Å)	Norm mol. grad.	Dipole moment (db)	(N_{LS}, N_{SS})[1]	
All integrals	-7345.216513	2.116448	.000009	2.001829	10.8	27.8
Levy-Leblond	-7**147.533302**		.00**2006**	2.**195541**		
All integrals (no Pos.)[2]	-7345.21**9319**		.000009	2.00183**4**	10.2	28.2
Model I	-7345.216**065**		.000**223**	2.001**168**	4.46	2.78
Model I (no Pos.)[2]	-7345.21**8939**		.000**134**	2.001**174**	4.56	3.11
Model II	-7345.215**890**		.000**212**	2.00**0177**	0.33	0.65
Model II (no Pos.)	-7345.21**8764**		.000**123**	2.00**0183**	0.39	0.73
B3LYP	-7349.842436					
Model II + B3LYP	-7349.841**892**					
Levy-Leblond	-7147.533307	2.11**8233**	.000010	2.192085		
All integrals (no Pos.)[2]	-7345.219319	2.11645**0**	.000007	2.001832		
Model I	-7345.216065	2.116**884**	.000007	2.002221		
Model I (no Pos.)[2]	-7345.218939	2.11643**1**	.000008	2.000955		
Model II	-7345.215891	2.116**796**	.000007	2.001411		
Model II (no Pos.)	-7345.218765	2.11635**5**	.000006	2.000125		
EXP[3]		2.098				

[1] Time factors. Time used for LS-integrals (T_{LS}) is : $T_{LS} = N_{LS} \cdot T_{LL}$. Timings are from the first iteration (minimal screening)

[2] Positronic solutions projected out

[3] J. Brunvoll *et. al. Acta Chemica Scandinavica*, 44:23, 1990

Model II (only using Mulliken charges). The large computational effort associated with the full integrals evaluation scheme is evident. The time factors reported in the table are from the initial iteration where screening of the LS and SS integrals is not yet efficient. In the final iteration the time factors for the full DHF calculation are : $N_{LS} = 10.3; N_{SS} = 1.9$, as a proof that when the wave function is nearly converged screening is extremely effective on especially the SS integrals. During the optimization the time factors are closer to the those of the initial iteration and therefore the one-center models are still very useful in these iterations.

The large effort associated with evaluating LS and SS integrals is removed by the one-center approximations. Model II reduces the time factor for the LS-integrals to 0.33 and the time factor of the SS-integrals to 0.65, meaning the the LS and SS integrals in total only takes as much time as the LL integrals. In comparison, in model I, the LS and SS integrals takes about 10 times the time needed for the LL integrals. Projecting out the positronic solution does of course not affect the integral evaluation timings. It must be remembered though that the LS and SS-integrals have only been done 'on-the-fly' for the sake of comparing the timings. The additional advantage of model II is that the LS and SS-integrals can be written to disk and used conventionally throughout the optimization. Furthermore it is not utilized that the we only need to calculate the one-center integrals once of each atom type.

In spite of the huge savings associated with Model II the accuracy indeed seems to be preserved. The ground state energy using Model II is very close to the energy of Model I, which in turn is in agreement with the energy when using the full set of integrals to within 10^{-4} au. When using a no-pair approximation (projecting out all positronic solutions) the difference in energy of both Model I and Model II is increased to 10^{-3} au. but in nice agreement with the energy when using the no-pair approximation with the full set of integrals. The same arguments applies to both the norm of the molecular gradient and the dipole moment and when relaxing the geometry the Iodine carbon bond length predicted by the approximate one center models is in agreement with the full DHF calculation to within 10^{-4}Å. All in all the accuracy of Model II seems to be comparable to Model I, which is very promising considering the huge savings in the integral evaluation of Model II compared to Model I.

The 4-component B3LYP [28] result presented further adds to the advantages of Model II. The time used for the integral evaluation of the B3LYP and the B3LYP + one-center approximation is of course the same as for the

corresponding DHF models. The numerical integration of the exchange correlation potential will likewise be the same for the full 4-component B3LYP model and the B3LYP + Model II combination. To get a idea of the savings associated with B3LYP + Model II the total time needed for the first iteration of the B3LYP calculation was 1 hour and 6 minutes with the corresponding time for the B3LYP + Model II combination was 27 minutes. Still the accuracy of the Model II combination with B3LYP is of the same order as for Model II in combination with DHF (10^{-4}).

II. The importance of using Mulliken charges and comparing to Model III

To illustrate why Mulliken charges are favored and to make a comparison between all three one-center models another Iodobenzene calculation is presented in table 15.9.1. These calculations have been done in a far inferior

Table 15.9.2: Dirac-Coulomb SCF calculations on Iodobenzene using Model I,II and III. Non relativistic uncontracted cc-pVDZ basis set on C,H. Home made well-tempered basis set on I.

Model	Energy (au)
All integrals	-7216.901768
Model I	-7216.901**405**
Model II[a]	-7216.89**6270**
Model II[b]	-7216.901**336**
Model III[c]	-7216.9**17207**
Model III[d]	-7216.89**9428**
Model III[e]	-7216.90**2937**

[a]Using the tabulated small component charge on I (0.1895).

[b]Using atom centered Mulliken small component charge on I (0.1758).

[c]Using atom centered Mulliken small component charge on I (0.1758).

[d]Using Mulliken small component charge on I (0.1758) centered on atoms and midpoints between nuclei.

[e]Using Mulliken small component charge on I (0.1758) centered on atoms and points between nuclei determined by dipole moment.

basis set than those presented in table 15.9.1 but that does not affect the conclusions that can be drawn by comparing the one-center models to each other. It is clear why we favor the use of Mulliken small component charges for model II. The energy is far better than when using tabulated charges. It is easy to understand why. For the approximation in Eq. 15.1.6 and 15.1.7 to be as good as possible the small component charges q^S must reflect the quality of the basis set. The Mulliken charges do just that while the tabu-

lated charges are only a good approximation when we are close to the basis set limit.

The performance of model III is not as impressive as that of model II. The model where the charges have been distributed at points determined by the dipole moment give the best agreement. For the calculations with model III, we have used a single Gaussian to model the distribution of the charges in the "correction"-integrals (15.4.24-15.4.25) in stead of just being point charges. This only had cosmetic effects on the energy (the numbers when using point charges agree with the ones presented in the table to the sixth digit). As mentioned the error associated with model III is expected to mainly stem from the simple way the large component charges is distributed.

The motivation for proposing model III was to make a model that gave a more correct wave function since we do not fold part of the two-electron Fock matrix into the one-electron Fock matrix as in model I and II. In table 15.9.3 we investigate how much the convergence of the wave function is disturbed when switching off the integral approximation after convergence of the electronic gradient to a value specified by the keyword .SV1CNV (see section D.1) The leap in the value of electronic gradient after the first iteration shown for

Table 15.9.3: The effect of switching the integral approximations off after convergence of the one-center models. The one-center model is switched off after the first iteration shown for each model. Numbers are from the iodobenzene calculation.

	Energy	ERGVAL	FCKVAL	EVCVAL
Model I				
	-7.2169014052E+03	9.73E-08	-5.44E-04	1.08E-04
	-7.2169017969E+03	3.92E-04	7.99E+01	1.50E+00
	-7.2169017679E+03	-2.91E-05	4.68E-05	2.15E-04
Model II				
	-7.2169013659E+03	4.30E-08	5.02E-03	5.11E-05
	-7.2169017544E+03	3.89E-04	5.63E+01	1.53E+00
	-7.2169017677E+03	1.33E-05	-3.27E-03	1.78E-03
Model III				
	-7.2169172081E+03	-7.35E-08	1.78E-03	2.05E-05
	-7.2169017310E+03	-1.55E-02	5.03E+01	4.76E-01
	-7.2169017678E+03	3.68E-05	-1.14E-03	9.38E-04

each model is seen to be slightly smaller for model I than II. Model I seems to recover a bit faster as well. The electronic gradient of model III is not

as affected by switching off the approximation as model II even though the change in energy is bigger. Taking the electronic gradient as a measure of how much the approximate wave function differ from the full DHF one, we see that the desired effect is present in model III though not as big as hoped. It should be noted that the change in electronic gradient observed here is comparable to that seen when performing a conventional DHF calculation but switching the SS-integrals on when convergence to a specified threshold has been reached.

III. The molecular gradient of Model II

To underline the savings associated with the one-center models, the approximate timings for the geometry optimization on C_6H_5I are presented in table 15.9.4. The total CPU time needed in these calculations speak for themselves. The savings of model I and II when comparing to the full calculation

Table 15.9.4: Timings on the Iodobenzene geometry optimization on a single 250MHz R4400 SGI. Note that four iterations are made with model II due to harder convergence criteria.

Iter	Energy	Change	GradNorm	Index	StepLen	TrustRad
Full calculation						
0	-7216.901768	0.000000	0.000491	0	0.000963	0.500000
1	-7216.901768	0.000000	0.000211	0	0.000443	0.500000
2	-7216.901768	0.000000	0.000026	0	0.000062	0.500000
Total CPU time used in DIRAC: 2d13h10min						
Model I[a]						
0	-7216.901405	0.000000	0.000162			
1	-7216.901405	0.000000	0.000076			
2	-7216.901405	0.000000	0.000067			
3	-7216.901405	0.000000	0.000063			
Total CPU time used in DIRAC: ∼12h						
Model II						
0	-7216.901336	0.000000	0.000197	0	0.000632	0.500000
1	-7216.901336	0.000000	0.000055	0	0.000315	0.500000
2	-7216.901336	0.000000	0.000011	0	0.000088	0.500000
3	-7216.901336	0.000000	0.000004	0	0.000033	0.500000
Total CPU time used in DIRAC: 6h35min35s						

[a] Timings for this model is approximate because 5 geometry steps were rejected during this optimization. This average time pr. SCF iteration has been used to approximate the time used by these unsuccessful steps.

are tremendous and model II is seen to be twice as fast as model I. Convergence even seems to be better for model II than for model I.

The error associated with assuming that the small component Mulliken charges are geometry independent is investigated here. A direct comparison between the analytical and numerical gradient at the optimized geometry can be made and it is found that they are of the same order (analytical : 0.000212 ; numerical : 0.000194). This indicates that if the geometry dependence of the Mulliken charges constitute and error it is a small one. A further test that can be made is to follow how the Mulliken charges change during the geometry optimization. This is seen for a selected number of steps

Table 15.9.5: Large and Small component charges of C_6H_5I in a selected number of step in a geometry optimization.

It.1	Norm=0.221845	q_L	q_S
	C	-6.9**34753027568**	-0.00101**31034606**
	I	-51.9**2245559345**	-0.175813**8697014**
⋮			
It.9	Norm=0.000064	q_L	q_S
	C	-6.97783**0165195**	-0.001016194**0709**
	I	-51.88646**546524**	-0.175813635**1716**
It.10	Norm=0.000010	q_L	q_S
	C	-6.977833765261	-0.0010161951193
	I	-51.88646137094	-0.1758136352522

in the geometry optimization of Iodobenzene in table 15.9.1. While the large component charges change significantly (especially in the initial steps) the changes of the small component charges is at most of the order 10^{-7} in the initial iterations and 10^{-9} in the final iterations. It safe to conclude that the assumption that $\frac{dq_A^S}{dX_A} \approx 0$ is valid.

15.9.2 Hg_2Cl_2

With respect to relativistic effects on equilibrium geometries, an interesting application is Hg_2Cl_2. DHF and HF numbers have been reported by J.Thyssen [29]. A non-relativistic uncontracted ccpVDZ basis set was used

for chlorine and the Thallium basis set by Dyall [30] was used for Mercury[5]. The small component basis was generated with RKB. The numbers show

Table 15.9.6: Equilibrium geometry of Hg_2Cl_2. Model II numbers are from this work.

Bond	Distance/Å			
	HF	DHF[a]	Model II	EXP[b]
Hg-Hg	2.919	2.614	2.593	2.5955
Hg-Cl	2.469	2.354	2.351	2.3622

[a]HF and DHF numbers are taken from [29]. DHF numbers were calculated without the SS class of integrals but with the small component Coulombic correction of [12]

[b]Experimental numbers are from [31]

large relativistic contraction of the bonds, especially the Hg-Hg bond as noted by J. Thyssen [29]. It is interesting to see how well Model II performs. The DHF calculation was done without the SS-class of integrals but with the coulomb repulsion correction of (15.2.8). The full class of LS-integrals was used. Model II should be computationally cheaper since no LS- nor SS-integrals enter the gradient calculation, and still the overall result is closer to experiment. The difference in performance of the DHF and model II calculations must be due to the screening of the nucleus from the one-center SS-integrals, present in model II but not in the DHF calculation.

15.9.3 Coin-Dimers

The energy and polarizabilities of the coin-metal (Au,Ag,Cu) dimers were calculated in to also test the performance when calculating properties with the one-center approximations. Large basis sets have been used, as in the full 4-component DHF calculations of Saue and Jensen [32], which also shows up in the fact that the tabulated small component charges are close to the ones from Mulliken analysis.

The overall conclusions to make from tables 15.9.6 -15.9.8 are that model II does well in these cases. Total energies agree at the third digit and the polarizabilities are very close to the ones obtained with the conventional DHF scheme. Even at frequencies close to the poles there is a nice agreement. Here the curve is very steep making these polarizabilites harder to calculate.
From the Au_2-calculation the importance of including relativity is seen for the

[5]The Tl basis was used for Hg as a Hg basis set was not available at the time. Here this basis set re-used to allow a comparison with the numbers reported by J. Thyssen [29]

n.r. numbers calculated with the Levy-Leblond Hamiltonian. Furthermore we report the results when using model II without SS as well as without both SS and LS integrals. Within this model this means accounting for multi center terms of these classes but neglecting the one-center terms. The results underline the importance of the one-center integrals and can also be taken as proof that the improved scaling could not just have been reached by neglected LS and SS integrals without loosing accuracy.

15.9.4 Au_4

Calculations of total energies were carried out on linear Au_4 (table 15.9.10). Considering that more approximations have been made in model II than in model I, it is a surprise that model II gives the most correct energy. A few other conclusions can be made from these numbers.

In this case even the one-center integrals are too numerous to fit on disk and the real advantage of model II is therefore not put into use. This calculation would benefit from the possibility to only calculate the one-center integrals of each atom type. This would have reduced the time taken pr. iteration to 15min compared to more than 3h30min for the full DHF scheme. In the present implementation the savings are still considerable though.
Model III fails for this molecule. This reason is a completely wrong distribution of the large component charge. It is evident from table 15.9.11 that far too much, and even positive signed, charge is placed in the off-diagonal elements. This gives a wrong description of the electronic interactions and hence a wrong wave function.

Table 15.9.7: DHF calculations of total energies and polarizabilities of Au_2. A dual family basis set was used. Au:L-[24s20p14d10f]. Tabulated small component charges are used. However they are close to the Mulliken ones (0.50670 and 0.50664)

Model	Energy (au)	freq. (au)	α_{xx}	α_{zz}	α
Full	-38070.97145	0.00	65.668	114.231	81.856
		n.r.	117.797	173.437	136.344
		0.05	69.113	128.793	89.006
		0.10	93.658	304.329	163.882
		0.11	83.885	1118.095	428.622
		0.12	92.463	−224.744	−13.272
Model II	-38070.96**517**	0.00	65.665	114.218	81.850
		0.05	69.108	128.771	88.996
		0.10	93.462	304.043	163.655
		0.11	83.864	1111.332	426.353
		0.12	92.447	−225.451	−13.519
Model II (no SS)	-3807**5.51844**	0.00	65.621	114.130	81.791
		0.05	69.057	128.658	88.924
		0.10	95.332	304.134	164.933
		0.11	83.861	1166.598	444.773
		0.12	92.365	−220.090	−11.786
Model II (no SS,LS)	−**40133.07132**	0.00	18.262	63.906	33.477

Table 15.9.8: DHF calculations of total energies and polarizabilities of Ag_2. Dual family basis set are used Ag:L-[22s21p12d3f] For model II we use tabulated small component charge (0.141510)

Model	Energy (au)	freq.(au)	α_{xx}	α_{zz}	α
Full	-10629.25246	0.00	96.997	156.174	116.723
		0.05	109.052	193.213	137.106
		0.10	186.938	1282.243	552.040
		0.11	241.741	−1371.350	−295.956
		0.13	946.428	−204.637	562.739
		0.14	−1093.623	−127.348	−771.531
Model II	-10629.251**83**	0.00	96.993	156.177	116.721
		0.05	109.048	193.227	137.108
		0.10	186.929	1284.575	552.811
		0.11	241.729	−1367.935	−294.826
		0.13	946.380	−204.515	562.749
		0.14	−1093.561	−127.288	−771.470

Table 15.9.9: DHF calculations of total energies and polarizabilities of Cu_2. Dual family basis set are used Cu:L-[18s15p9d3f]. For model II we use tabulated small component charge (0.044070)

Model	Energy (au)	freq.(au)	α_{xx}	α_{zz}	α
Full	-3306.89855	0.00	81.887	123.749	95.842
		0.05	91.021	148.389	110.143
		0.11	171.796	1841.883	728.491
		0.12	225.363	−753.147	−100.807
		0.14	1005.803	−152.055	619.850
		0.15	−832.500	−95.057	−586.686
Model II	-3306.89855	0.00	81.874	123.657	95.802
		0.05	91.008	148.268	110.095
		0.11	171.728	1827.050	723.502
		0.12	225.166	−757.380	−102.350
		0.14	1000.714	−152.246	616.394
		0.15	−834.170	−95.000	−587.780

Table 15.9.10: Total DHF energies of linear Au_4 using the one-center models. Basis set is by T.Saue[a]

Model	Energy (au)	Time pr. It. for LL,LS,SS[b]
Full	-76141.900383	13min47s 1h12min 1h16min
I	-76141.8**87514**	13min31s 53min04s 49min22s
II	-76141.89**1425**	12min11s 19min31s 23min39s
III	-77**091.961331**	12min01s 17min17s 20min24s

[a] Basis set is by T.Saue [33] (L-[23s18p14d8f])
[b] On 4 UltraSparc III 750MHz processors.

Table 15.9.11: Matrix of large component charges in final model III iteration of Au_4.

	Column 1	Column 2	Column 3	Column 4
1	-1.176954D+04	1.117877D+04	1.150970D+03	-6.392136D+02
2	1.117877D+04	-1.176954D+04	-6.392136D+02	1.150970D+03
3	1.150970D+03	-6.392136D+02	-5.978185D+02	8.088084D+00
4	-6.392136D+02	1.150970D+03	8.088084D+00	-5.978185D+02

Chapter 16

Conclusions

Two approximate models for doing 4-component DHF calculations have been presented that both build on the same ideas of the model of L. Visscher *et al.* that the small component density is highly localized. Of these two model the model denoted Model II is very successful in reducing the computational cost associated with evaluating the LS and SS classes of integrals while providing energies and properties close to those of the full DHF calculations. Apart from the calculation or fetching of the relatively few one-center LS and SS integrals this 4-component model is comparable in cost to a regular HF calculation. The so called Model III requires some refinement to be successful.

Model II presents an alternative to methods employing approximate Hamiltonians like the ZORA [8] and Douglas-Kroll [6, 7] approaches in terms of computational cost. Model II still includes the relativistic effects included in the full 4-component DHF model and including spin-orbit effect via the one-center integrals the method bears similarities with the AMFI [22] method. However having formulated the approximation within the 4-component framework has the huge advantage of retaining the simple formalism and structure of 4-component theory.

Bibliography

[1] E. Clementi and G. Corongiu. *Int. J. Quant. Chem.*, 62:571, 1997.

[2] P. Pykkö. *Chem. Rev.*, 88:563, 1978.

[3] P A M Dirac. The quantum theory of the electron. *Proc. Roy. Soc. (London) A*, 117:610, 1928.

[4] P A M Dirac. The quantum theory of the electron. part ii. *Proc. Roy. Soc. (London) A*, 118:351, 1928.

[5] P A M Dirac. A theory of electrons and protons. *Proc. Roy. Soc. (London) A*, 126:360, 1930.

[6] B. A. Hess. *Phys. Rev. A*, 33:3742, 1986.

[7] U. Kaldor and B. A. Hess. *Chem. Phys. Lett.*, 230:1, 1994.

[8] E. Van Lenthe, E. J. Barends, and J.G. Snijders. *J. Chem. Phys.*, 99:4597, 1993.

[9] K. G. Dyall. *Chem. Phys. Lett.*, 196:178, 1992.

[10] L. Pisani and E. Clementi. *J. Comput. Chem.*, 15:466, 1994.

[11] K. Fægri T. Saue, T. Helgaker, and O. Gropen. *Mol. Phys.*, 91:937, 1997.

[12] L. Visscher. *Theor. Chem. Acc.*, 98:68, 1997.

[13] G. Theodoor de Jong and L. Visscher. *Theor. Chem. Acc.*, 107:304, 2002.

[14] T. Saue. *Principles and Applications of Relativistic Molecular Calculations.* Ph.d thesis, Department of Chemistry, Faculty of Mathematics and Natural Science, University of Oslo, 1996.

[15] R. E. Stanton and S. Havriliak. *J. Chem. Phys.*, 81:1910, 1984.

[16] K. G. Dyall, I. P. Grant, and S. Wilson. *J. Phys. B*, 17:493, 1984.

[17] T. Saue, V. Bakken, T. Enevoldsen, T. Helgaker, H. J. Aa. Jensen, J. Laerdahl, K. Ruud, J .Thyssen, and L. Visscher. "dirac, a relativistic ab initio electronic structure program , release 3.2 (2000)".

[18] K. G. Dyall and F. Fægri. *Theor. Chem. Acc.*, 94:39, 1996.

[19] K. G. Dyall and F. Fægri. *Theor. Chem. Acc.*, 105:252, 2001.

[20] B.A. Hess, C.M. Marian, U.Wahlgren, and O. Gropen. *Chem. Phys. Lett.*, 251:365, 1996.

[21] C.M. Marian and U.Wahlgren. *Chem. Phys. Lett.*, 251:357, 1996.

[22] B. Schimmelpfennig, L. Maron, U.Wahlgren, C. Teichteil, H. Fagerli, and O. Gropen. *Chem. Phys. Lett.*, 286:267, 1998.

[23] T. Helgaker, H. J. Aa. Jensen, P. Jørgensen, J. Olsen, K. Ruud, H. Ågren, K. L. Bak, V. Bakken, O. Christiansen, S. Coriani, P. Dahle, E. K. Dalskov, T. Enevoldsen, B. Fernandez, C. Hättig, K. Hald, A. Halkier, H. Heiberg, H. Hettema, D. Jonsson, S. Kirpekar, R. Kobayashi, H. Koch, K. V. Mikkelsen, P. Norman, M. J. Packer, T. A. Ruden, T. Saue, S. P. A. Sauer, B. Schimmelpfennig, K. O. Sylvester-Hvid, P. R. Taylor, and O. Vahtras. Dalton release 1.2 (2001), an electronic structure program, http://www.kjemi.uio.no/software/dalton/dalton.html.

[24] R. Mulliken. *J. Chem. Phys.*, 23:1833, 1955.

[25] R. Mulliken. *J. Chem. Phys.*, 23:2343, 1955.

[26] Jr. T. H. Dunning. *J. Chem. Phys.*, 90:1007, 1989.

[27] L. Visscher and K. G. Dyall. *J. Chem. Phys.*, 104:9040, 1996.

[28] T. Saue and T. Helgaker. *J. Comput. Chem.*, 23:814, 2002.

[29] J. Thyssen. *Development and applications of methods for correlated relativistic calculations of molecular properties.* Ph.d status report, Department of Chemistry, University of Southern Denmark, 1999.

[30] K. G. Dyall. *Theor. Chem. Acc.*, 99:366, 1998.

[31] N. J. calos and C. H. L. Kennard. *Z. Kristallogr.*, 187:305, 1989.

[32] T. Saue and H. J. Aa. Jensen. *J. Chem. Phys.*, 118:522, 2003.

[33] T. Saue. *Mol. Phys.*, 91:937, 1997.

Part V

Summary and Future Research

Chapter 17

Final Thoughts.

In this thesis I have tried to present computationally economic approaches to both correlation and relativistic effects in quantum chemical calculations of molecular properties. The goal was to make approximations within the standard methods for correlation (CI,MCSCF,CC,...) and within the 4-component method for relativity without loosing the accuracy of these models. Whenever making "shortcuts" in quantum chemistry there is a chance of loosing more than you gain - the Coulomb hole model of I. Panas is an example of that. To comment on the success of the approximations presented here the status of these models is summarized :

- Two new 4-component one-center models were presented as extensions to the previously reported one-center model of T. de Jong and L. Visscher [1]. Of these, Model II proved to be very successful in reducing the computational effort while still providing energies and properties in good agreement with the full 4-component DHF and DFT models. Future research involving Model II should focus on extending it to multi-reference methods (CI,MCSCF). Model III in its present state needs refinements but has the potential to be developed into a successful model.

  With Model II, I consider the goal of an efficient and accurate approximate 4-component DHF and DFT model accomplished.

- The CI-DFT and MCSCF-DFT hybrid models have been implemented using two different long-range two-electron operators and the short-range LDA functional along with some approximate gradient corrections to this functional. Few electron calculations give promising results and indicate that all the expected benefits of a wave function

DFT hybrid are seen. However many electron systems still present a problem for the current functionals.

The wave function DFT hybrid implementation is general and as such fulfills all the major requirements of a hybrid model. Double counting of correlation effects is avoided and the economy of the model will allow large scale calculations accounting for both static and dynamic correlation. At the time of writing this thesis accurate short-range functionals that allow an optimal hybrid of wave function theory and DFT for many electron systems has not been implemented. Such functionals have been proposed [2] and their implementation is straightforward and requires little work with the very general wave function DFT hybrid implementation in DALTON [3]. If sufficiently accurate short-range functionals are found the door is opened to a very exciting world of applications where molecular properties of systems can be investigated with the MCSCF-DFT hybrid model.

Considering the title of this thesis the ultimate goal would be the implementation of a one-center 4-component MCSCF-DFT hybrid model in DIRAC [4]. This would be a very general model accounting for both correlation and relativity at once. From the summary above it is clear that the building blocks for doing efficient 4-component calculations are present in the one-center models. Likewise are efficient methods for both dynamic and static correlation within reach and both these models could in principle be implemented within the 4-component MCSCF available in DIRAC [4] as implemented by J. Thyssen [5].

The extension of the MCSCF-DFT hybrid to allow calculations of response properties and molecular gradients and Hessian is also a task that can be accomplished with a foreseeable amount of work since it will mainly involve adjustments of already available modules. All in all I foresee a bright future for wave function DFT hybrid models in the calculation of molecular properties and I hope that more work in this direction will be continued within DALTON and DIRAC where this thesis leaves off.

Chapter 18

Dansk resumé

Denne afhandling opsummerer 4 års Ph.D studier og forskning ved Kemisk Institut, Syddansk University i Odense.

Det primære formål med mine studier har været at udvikle billige og velbegrundede approksimationer til de eksisterende metoder til beskrivelse af korrelations samt relativistiske effekter. Effekter der med normale beregningsmetoder er meget krævende og dyre.

Afhandlingen starter med en beskrivelse af de eksisterende metoder til beskrivelse af korrelations effekter og viser at korrelationsenergien konvergerer meget langsomt med hensyn til basis set samt ekspansionen in Slater determinanter for de multi-konfigurationelle CI og MCSCF metoder. Denne langsomme konvergens associeres med vekselvirkningen imellem elektroner på kort afstand.

Coulomb hul modellerne introduceres som mulige kandidater til effektiv beskrivelse af dynamiske korrelations effekter. Specielt undersøge Coulomb hul modellen foreslået af I. Panas [6]. Metoder der ikke beskriver den korrelerede bevægelse af elektronerne overestimerer to-elektron vekselvirkningen da elektronerne tillades at være tæt på hinanden. Coulomb hul modellen består i at fjerne en del af to-elektron potentialet i situationen hvor to elektroner er tæt på hinanden. Dette gøres ved at introducere en modificeret to-elektron operator og kan således beskrives som at et Coulomb hul modelleres ind i Hamilton operatoren. Metoden testes i en serie beregninger men kasseres da den introducere nogle ufysiske egenskaber. I geometri optimeringer bliver det således en fordel at overbinde atomerne i molekyler hvilket betyder en forværring af Hartree-Fock modellen når den modificerede to-elektron operator anvendes. En anden vigtig egenskab der ikke overholdes

i denne approksimative metode er at matricen af to-elektron integraler ikke er positiv definit.

Som alternativ til Coulomb hul modellerne introduceres bølgefunktion DFT hyrbid metoderne. Specielt fokuseres på metoden pioneret af A. Savin [2, 7–12] hvor en separation af to-elektron operatoren muliggør at vekselvirkninger på kort afstand beskrives ved et funktional af elektrontætheden mens vekselvirkninger over lang afstand beskrives med en bølgefunktion. Fordelen er en mere effektiv beskrivelse af dynamisk korrelation med en hurtigere konvergens af bølgefunktionen med hensyn til ekspansionen i Slater determinanter til følge. Metoden er implementeret som en CI-DFT og MCSCF-DFT hybrid og testes med funktionaler af LDA typen samt med få approksimative gradient korrigerede funktionaler. Konklusionen er at for systemer med få elektroner er LDA funktionalet tilstrækkeligt og hybrid metoderne viser lovende resultater. For mange-elektron systemer kræves dog bedre funktionaler for at en optimal hybrid kan opnås. Foreløbige beregninger med approksimative gradient korrigerede funktionaler ser lovende ud og andre funktionaler til løsning af disse problemer er blevet foreslået af Toulouse *et al.* [2, 11] og vil nemt kunne implementeres i DALTON. En mulig fremtidig udvidelse vil kunne inkludere muligheden for at beregne eksitationsenergier og andre linære samt ikke-linære respons egenskaber.

I sidste kapitel presenteres to modeller der har til hensigt at reducere beregningstiden for relativistiske 4-komponent metoder. Modellerne bygger videre på en model udviklet af T. de Jong og L. Visscher [1] og forsøger at reducere antallet af to-elektron integraler der involverer den lille komponent som er en konsekvens Dirac ligningen [13]. Disse integraler eksisterer ikke i den ikke-relativistiske teori og er yderst talrige. Det udnyttes at tætheden for den lille komponent af bølgefunktionen er meget kompakt og lokaliseret på atomerne i et molekyle. Alle integraler der involverer flere centre vil således være små af størrelse og kan derfor enten negligeres eller tilnærmes ved simpel Coulomb repulsion imellem punktladninger. Model II repræsenterer et godt kompromis imellem beregningstid og nøjagtighed. Kun et-center integraler over den lille komponent beregnes eksplicit og disse vil typisk kunne gemmes på disk. Antallet af integraler er derfor reduceret til det samme antal som i en ikke-relativistisk beregning. Kun et-center integraler over den lille komponent beregnes eksplicit og disse vil typisk kunne gemmes på disk. Antallet af integraler er derfor reduceret til det samme antal som i en ikke-relativistisk beregning, mens modellen stadig giver energier og egenskaber i god overensstemmelse med den fulde 4-komponent beregning. Der presenteres resultater med et-center 4-komponent DHF samt DFT modellen, mens

en udvidelse til 4-komponent MCSCF metoden overlades til fremtidig forskning.

Den overordnede konklusion er at byggestenene nu foreligger til udvikling af en et-center 4-komponent MCSCF DFT hybrid metoder der vil kunne beskrive både statiske og dynamiske korrelationseffekter samt relativistiske effekter. MCSCF-DFT hybrid metoden spås en lys fremtid så snart bedre funktionaler foreligger og et hav af anvendelser og undersøgelser vil kunne foretages med denne metode i fremtiden.

Bibliography

[1] G. Theodoor de Jong and L. Visscher. *Theor. Chem. Acc.*, 107:304, 2002.

[2] J. Toulouse, F. Colonna, and A. Savin. *manuscript*, 2004.

[3] T. Helgaker, H. J. Aa. Jensen, P. Jørgensen, J. Olsen, K. Ruud, H. Ågren, K. L. Bak, V. Bakken, O. Christiansen, S. Coriani, P. Dahle, E. K. Dalskov, T. Enevoldsen, B. Fernandez, C. Hättig, K. Hald, A. Halkier, H. Heiberg, H. Hettema, D. Jonsson, S. Kirpekar, R. Kobayashi, H. Koch, K. V. Mikkelsen, P. Norman, M. J. Packer, T. A. Ruden, T. Saue, S. P. A. Sauer, B. Schimmelpfennig, K. O. Sylvester-Hvid, P. R. Taylor, and O. Vahtras. Dalton release 1.2 (2001), an electronic structure program, http://www.kjemi.uio.no/software/dalton/dalton.html.

[4] T. Saue, V. Bakken, T. Enevoldsen, T. Helgaker, H. J. Aa. Jensen, J. Laerdahl, K. Ruud, J .Thyssen, and L. Visscher. "dirac, a relativistic ab initio electronic structure program , release 3.2 (2000)".

[5] J. Thyssen. *Development and Applications of Methods for Correlated Relativistic Calculations of Molecular Properties.* Ph.d thesis, Department of Chemistry, University of Southern Denmark - Odense University, 2001.

[6] I. Panas and A. Snis. *Theor. Chem. Acc.*, 97:232, 1997.

[7] A. Savin. On degeneracy, near-degeneracy and density functional theory. In J. M. Seminario, editor, *Recent Developments and Applications of Modern Density Functional Theory*, page 327. Elsevier, Amsterdam, 1996.

[8] A. Savin and H. J. Flad. *Int. J. Quant. Chem.*, 56:327, 1995.

[9] T. Leininger, H. Stoll, H.-J. Werner, and A. Savin. *Chem. Phys. Lett.*, 275:151, 1997.

[10] R. Pollet, A. Savin, T. Leininger, and H. Stoll. *J. Chem. Phys.*, 116:1250, 2002.

[11] J. Toulouse, A. Savin, and H. J. Flad. *manuscript*, 2004.

[12] J. Toulouse, F. Colonna, and A. Savin. *manuscript*, 2004.

[13] P A M Dirac. The quantum theory of the electron. *Proc. Roy. Soc. (London) A*, 117:610, 1928.

Part VI

Papers and Manuscripts.

Chapter 19

Summary of Papers.

Paper I

In this paper we present the theory and implementation of a generic second order restricted step hybrid model between a multi-configuration self-consistent field wave function (MCSCF) and density functional theory (DFT). As in the CI-DFT hybrid models previously presented by others [1–7] double counting of correlation effects is avoided by splitting the two-electron operator into short-range and long-range parts, thereby allowing all short-range interactions to be treated by DFT while the long-range interaction is assigned to the MCSCF wave function treatment. For the DFT part a short-range LDA functional is implemented and tested on the calculation of ground state energies of He, Be, and H_2O. The implementation is completely general and will allow the use of any improved functionals that will be developed in the future.
The conclusion is that MCSCF DFT hybrid presents an improvement over both regular Kohn-Sham DFT and regular MCSCF theory where decreased basis set and wave function expansion requirements make the hybrid model economical. However the currently available short-range functionals do not provide an optimal MCSCF DFT hybrid for many electron systems and better functionals are needed before high quality large scale calculations are possible.
Status : *submitted to Journal of Chemical Physics.*

Manuscript I

In this paper the One-Center 4-component DHF and DFT model and its applications is presented. This is also presented in detail in Part IV (p.90)

of the thesis and therefore this manuscript has been left out of the thesis.

The evaluation and subsequent handling of a large number of two-electron integrals involving the small components of the 4-spinors is the major cause of the larger computation times of relativistic 4-component calculations compared to both 1- and 2-component approximate alternatives to the Dirac equation and to non-relativistic calculations based on the Schrödinger equation. In the One-Center models we use the fact that the small component density is highly localized. That is, the small component density located between different centers in a molecule is negligible

$$D^{S_A S_B} \approx D^{S_A S_B} \delta_{AB} = D^{S_A S_A}$$

Using this fact we extend the models previously reported by T. de Jong and L. Visscher [8] and propose approximations for the multi-center SS and LS classes of integrals that require little computational effort. One-center SS and LS are explicitly evaluated but will in most cases fit on disk meaning that the number of integrals that need to be evaluated in each SCF iteration is the same as in non-relativistic Hartree-Fock calculations. The One-Center model can therefore be considered an economical 4-component alternative to the 2-component based Douglas-Kroll [9, 10] and ZORA [11] approaches.
Preliminary calculations on C_6H_5I, Hg_2Cl_2, Au_2, Ag_2, Cu_2, and Au_4 show that the accuracy on ground-state energies, equilibrium geometries and frequency dependent polarizabilities is intact in the One-Center model.
Status : *Nearly done!*

In preparation.

- M. Patzschke, J. K. Pedersen and H. J. Aa. Jensen : The excitation energies of Bi(V)-compounds.

Bibliography

[1] A. Savin. On degeneracy, near-degeneracy and density functional theory. In J. M. Seminario, editor, *Recent Developments and Applications of Modern Density Functional Theory*, page 327. Elsevier, Amsterdam, 1996.

[2] A. Savin and H. J. Flad. *Int. J. Quant. Chem.*, 56:327, 1995.

[3] T. Leininger, H. Stoll, H.-J. Werner, and A. Savin. *Chem. Phys. Lett.*, 275:151, 1997.

[4] R. Pollet, A. Savin, T. Leininger, and H. Stoll. *J. Chem. Phys.*, 116:1250, 2002.

[5] J. Toulouse, A. Savin, and H. J. Flad. *manuscript*, 2004.

[6] J. Toulouse, F. Colonna, and A. Savin. *manuscript*, 2004.

[7] J. Toulouse, F. Colonna, and A. Savin. *manuscript*, 2004.

[8] G. Theodoor de Jong and L. Visscher. *Theor. Chem. Acc.*, 107:304, 2002.

[9] B. A. Hess. *Phys. Rev. A*, 33:3742, 1986.

[10] U. Kaldor and B. A. Hess. *Chem. Phys. Lett.*, 230:1, 1994.

[11] E. Van Lenthe, E. J. Barends, and J.G. Snijders. *J. Chem. Phys.*, 99:4597, 1993.

Paper I

Part VII

Appendices.

Appendix A

Electronic Repulsion Integrals Of S-Type Gaussians

A.1 Solution Of A Gaussian ssss-ERI

In this appendix an electron repulsion integral over normalized s-type Gaussian functions ($\mathrm{s_a} = \left(\frac{\mathrm{a}}{\pi}\right)^{3/2} \mathrm{e}^{-\mathrm{ar}^2}$) is solved. The evaluation closely follows that of V. R. Saunders [1].

$$(s_a s_b \mid s_c s_d) = \left(\frac{ab}{\pi^2}\right)^{3/2} \left(\frac{cd}{\pi^2}\right)^{3/2} \int_{-\infty}^{\infty}\int_{-\infty}^{\infty} \frac{e^{-ar_1^2} e^{-br_1^2} e^{-cr_1^2} e^{-dr_1^2}}{r_{12}} \mathrm{d}\mathbf{r}_1 \mathrm{d}\mathbf{r}_2 \quad \text{(A.1.1)}$$

After applying the Gaussian Product Theorem the integral is reduced to :

$$(\mathrm{s_a s_b} \mid \mathrm{s_c s_d}) = \pi^{-3} \left(\frac{\mathrm{ab}}{\mathrm{a+b}}\right)^{3/2} \left(\frac{\mathrm{cd}}{\mathrm{c+d}}\right)^{3/2} \mathrm{K_{ab} K_{cd}} \int_{-\infty}^{\infty}\int_{-\infty}^{\infty} \frac{\Omega_\alpha(\mathrm{r_{1P}})\Omega_\beta(\mathrm{r_{2Q}})}{\mathrm{r_{12}}} \mathrm{d}\mathbf{r}_1 \mathrm{d}\mathbf{r}_2 \quad \text{(A.1.2)}$$

with

$$\mathrm{K_{ab}} = \exp\left[-\frac{\mathrm{ab}}{\mathrm{a+b}} \times \mathrm{R_{AB}^2}\right] \quad , \qquad \tilde{\mathrm{P}} = \frac{\mathrm{a}\tilde{\mathrm{A}} + \mathrm{b}\tilde{\mathrm{B}}}{\mathrm{a+b}}$$

$$\Omega_\alpha(\mathrm{r_{1P}}) = \left(\frac{\alpha}{\pi}\right)^{3/2} \exp\left[-\alpha \times \mathrm{r_{1P}^2}\right] \quad , \quad \alpha = \mathrm{a+b} \qquad \text{(A.1.3)}$$

where $\tilde{\mathrm{A}}$ is the point of origin of $\mathrm{s_a}$ etc. The integral in (A.1.2) is solved using the Laplace transform of the coulomb operator

$$\frac{1}{r_{12}} = \frac{2}{\sqrt{\pi}} \int_0^\infty \mathrm{e}^{-r_{12}^2 t^2} \mathrm{dt} = \frac{1}{\sqrt{\pi}} \int_0^\infty \mathrm{e}^{-r_{12}^2 s} \frac{\mathrm{ds}}{\sqrt{s}} \qquad \text{(A.1.4)}$$

enabling us to write the integral in (A.1.2) as

$$\begin{aligned} \mathrm{ERI} &= \frac{1}{\sqrt{\pi}}\pi^{-6}(\alpha\beta)^{3/2}\left(\frac{ab}{a+b}\right)^{3/2}\left(\frac{cd}{c+d}\right)^{3/2}\mathrm{K_{ab}K_{cd}} \\ &\quad \int_0^\infty \iint \exp\left[-\alpha r_{1P}^2 - \beta r_{1Q}^2 s r_{12}^2\right] s^{1/2}\mathrm{d}\mathbf{r}_1\mathrm{d}\mathbf{r}_1\mathrm{ds} \\ &= \frac{1}{\sqrt{\pi}}\pi^{-6}(\alpha\beta)^{3/2}\left(\frac{ab}{a+b}\right)^{3/2}\left(\frac{cd}{c+d}\right)^{3/2}\mathrm{K_{ab}K_{cd}} \\ &\quad \int_0^\infty \mathrm{I_x I_y I_z}\cdot \mathrm{s}^{-1/2}\mathrm{ds} \end{aligned} \tag{A.1.5}$$

where

$$\mathrm{I_x} = \int_{-\infty}^{\infty}\int_{-\infty}^{\infty}\exp\left[-\alpha(\mathrm{x_1}-\mathrm{P}_x)^2 - \beta(\mathrm{x_2}-\mathrm{Q}_x)^2 - s(\mathrm{x_1}-\mathrm{x_2})^2\right]\mathrm{dx_1 dx_2}$$
$$\text{etc.} \tag{A.1.6}$$

Now let $\mathrm{u} = \mathrm{x_1} - \mathrm{P_x}$, $\mathrm{v} = \mathrm{x_2} - \mathrm{Q_x}$ and $\mathrm{R_{PQ,x}} = \mathrm{P_x} - \mathrm{Q_x}$. This substitution transforms $\mathrm{I_x}$ to

$$\begin{aligned} \mathrm{I_x} &= \int_{-\infty}^{\infty}\int_{-\infty}^{\infty}\exp\left[-\alpha\mathrm{u}^2 - \beta\mathrm{v}^2 - \mathrm{s}(\mathrm{u}-\mathrm{v}+\mathrm{R_{PQ,x}})^2\right]\mathrm{dudv} \\ &= \exp(-\mathrm{sR_{PQ,x}^2})\int_{-\infty}^{\infty}\exp\left[-(\alpha+\mathrm{s})\mathrm{u}^2 - 2\mathrm{usR_{PQ,x}}\right] \\ &\quad \int_{-\infty}^{\infty}\exp\left[-(\beta+\mathrm{s})\mathrm{v}^2 + 2\mathrm{s}(\mathrm{u}+\mathrm{R_{PQ,x}})\mathrm{v}\right]\mathrm{dudv} \end{aligned} \tag{A.1.7}$$

Using $\int_{-\infty}^{\infty}\exp(-\mathrm{ax}^2+\mathrm{bx})\mathrm{dx} = \sqrt{\frac{\pi}{a}}\exp\left(\frac{\mathrm{b}^2}{4\mathrm{a}}\right)$, to integrate the last integral in (A.1.7) over v, one gets (after some rearrangement).

$$\begin{aligned} \mathrm{I_x} &= \sqrt{\frac{\pi}{\beta+\mathrm{s}}}\exp\left(-\mathrm{sR_{PQ,x}^2}\cdot\frac{\beta}{\beta+\mathrm{s}}\right) \\ &\quad \int_{-\infty}^{\infty}\exp\left[-\frac{(\alpha\beta+(\alpha+\beta)\mathrm{s})}{\beta+\mathrm{s}}\mathrm{u}^2 - \frac{2\mathrm{s}\beta\mathrm{R_{PQ,x}}}{\beta+\mathrm{s}}\mathrm{u}\right]\mathrm{du} \end{aligned} \tag{A.1.8}$$

integrating over u, in the same manner produces :

$$\begin{aligned} \mathrm{I_x} &= \sqrt{\frac{\pi}{\beta+\mathrm{s}}}\sqrt{\frac{\pi(\beta+\mathrm{s})}{(\alpha\beta+(\alpha+\beta)\mathrm{s})}} \\ &\quad \exp\left[-\mathrm{sR_{PQ,x}^2}\cdot\frac{\beta}{\beta+\mathrm{s}} + \frac{4\mathrm{s}^2\beta^2\mathrm{R_{PQ,x}^2}/(\beta+\mathrm{s})^2}{4(\alpha\beta+(\alpha+\beta)\mathrm{s})/(\beta+\mathrm{s})}\right] \\ &= \pi(\alpha\beta+(\alpha+\beta)\mathrm{s})^{-1/2}\exp\left[-\frac{\mathrm{s}\alpha\beta\mathrm{R_{PQ,x}^2}}{(\alpha\beta+(\alpha+\beta)\mathrm{s})}\right] \end{aligned} \tag{A.1.9}$$

The substitution $\eta = \frac{\alpha\beta}{\alpha+\beta}$ makes I_x take the simple from :

$$I_x = \pi(\alpha+\beta)^{-1/2}(\eta+s)^{-1/2} \cdot \exp\left[-\frac{s\eta R_{PQ,x}^2}{\eta+s}\right] \tag{A.1.10}$$

Integration in the y- and z-directions produce similar results for I_y and I_z allowing us to write (A.1.5) as :

$$\begin{aligned} ERI &= \\ &\frac{1}{\sqrt{\pi}}\pi^{-6}(\alpha\beta)^{3/2}\left(\frac{ab}{a+b}\right)^{3/2}\left(\frac{cd}{c+d}\right)^{3/2} K_{ab}K_{cd} \cdot \pi^3 \cdot (\alpha+\beta)^{-3/2} \\ &\int_0^\infty (\eta+s)^{-3/2}\exp\left[-\frac{\eta s}{\eta+s}R_{PQ}^2\right] \cdot s^{-1/2}ds \\ = \; &\frac{1}{\sqrt{\pi}}\pi^{-3}\left(\frac{ab}{a+b}\right)^{3/2}\left(\frac{cd}{c+d}\right)^{3/2} K_{ab}K_{cd} \cdot \eta^{3/2} \\ &\int_0^\infty (\eta+s)^{-3/2} \cdot \exp\left[-\frac{\eta s}{c+s} \cdot R_{PQ}^2\right] \cdot s^{-1/2}ds \end{aligned} \tag{A.1.11}$$

With the substitution $t^2 = \frac{s}{\eta+s}$ you get :

$$\begin{aligned} ds &= \frac{2\sqrt{s}(\eta+s)^{3/2}}{\eta}dt \\ s &= 0 \Rightarrow t = 0 \\ s &= \infty \Rightarrow t = 1 \end{aligned} \tag{A.1.12}$$

transforming (A.1.11) into :

$$ERI = \frac{2}{\sqrt{\pi}}\pi^{-3}\left(\frac{ab}{a+b}\right)^{3/2}\left(\frac{cd}{c+d}\right)^{3/2} K_{ab}K_{cd} \cdot \sqrt{\eta}\int_0^1 e^{-\eta R_{PQ}^2 t^2}dt \tag{A.1.13}$$

With the definition of the zeroth order Boys function, $F_0(x) = \int_0^1 e^{-xt^2}dt$, we end up with the solution to a Gaussian ssss-integral being proportional to this function, with the squared distance of the origins of the two Gaussian charge distributions, as its argument.

$$(s_a s_b \mid s_c s_d) = 2\pi^{-7/2}\left(\frac{ab}{a+b}\right)^{3/2}\left(\frac{cd}{c+d}\right)^{3/2} K_{ab}K_{cd}\sqrt{\eta}F_0(\eta R_{PQ}^2) \tag{A.1.14}$$

A.2 ERI's For Higher Angular Momenta.

Integrals over Gaussians of higher angular momentum can be evaluated using recurrence relations. Following the McMurchie-Davidson [2] scheme the

Gaussian charge distributions are expanded in Hermite Gaussian. Considering just the x-direction, the charge distribution Ω_{ij}, formed by multiplication of to Gaussians $G_i(x_A)$ and $G_j(x_B)$, has degree i + j and can be expanded exactly in the Hermite Gaussians of degree $t \leq i + j$

$$\Omega_{ij} = \sum_{t=0}^{ij} E_t^{ij} \Lambda_t \tag{A.2.1}$$

where the Hermite Gaussians of exponent p and centered on **P** are defined as

$$\Lambda_t(x, p, P) = (\partial/\partial P_x)^t exp(-p x_P^2) \tag{A.2.2}$$

The expansion coefficients E_t^{ij} can easily be computed using recurrence relations

$$\begin{aligned} E_t^{i+1,j} &= \frac{1}{2p} E_{t-1}^{ij} + X_{PA} E_t^{i,j} + (t+1) E_{t+1}^{ij} \\ E_t^{i,j+1} &= \frac{1}{2p} E_{t-1}^{ij} + X_{PB} E_t^{i,j} + (t+1) E_{t+1}^{ij} \end{aligned} \tag{A.2.3}$$

with the starting coefficient being the pre-exponential factor

$$E_0^{00} = K_{ab}^x \tag{A.2.4}$$

The ease with which the Hermite Gaussians of all degrees are integrated (here just the x component)

$$\int_{-\infty}^{\infty} \Lambda_t(x) dx = (\partial/\partial P_x)^t \int_{-\infty}^{\infty} exp(-p x_P^2) dx = \delta_{t0} \sqrt{\frac{\pi}{p}} \tag{A.2.5}$$

allow us to write the solution to an electronic repulsion integral over non spherical charge distributions (of all angular momenta). Ignoring the pre-exponential factors and the normalization factors of the individual Cartesian Gaussians forming the Cartesian Gaussian charge distribution, we can write the integral over the charge distributions as

$$\begin{aligned} g_{abcd} = (G_a(\mathbf{r}_1) G_b(\mathbf{r}_1) \mid G_c(\mathbf{r}_2) G_d(\mathbf{r}_2)) = \iint \frac{\Omega_{ab}(\mathbf{r}_1) \Omega_{cd}(\mathbf{r}_2)}{r_{12}} d\mathbf{r}_1 d\mathbf{r}_2 = \\ \sum_{tuv} E_{tuv}^{ab} \sum_{\tau\nu\phi} E_{\tau\nu\phi}^{cd} \iint \frac{\Lambda_{tuv}(\mathbf{r}_1) \Lambda_{\tau\nu\phi}(\mathbf{r}_2)}{r_{12}} d\mathbf{r}_1 d\mathbf{r}_2 \end{aligned} \tag{A.2.6}$$

where $E_{tuv}^{ab} = E_t^{ij} E_u^{kl} E_v^{mn}$. Expanding the Hermite Gaussians as in (A.2.2) we are left with an integral over to s-type Gaussian, with the solution known

from Appendix A.1 to involve the zeroth order Boys function. Using the same notation as in Appendix A.1, $\eta = \frac{\alpha\beta}{\alpha+\beta}$, $\alpha = \mathrm{a} + \mathrm{b}$ and $\beta = \mathrm{c} + \mathrm{d}$, we get

$$\mathrm{g_{abcd}} = 2\pi^{-7/2} \left(\frac{\mathrm{ab}}{\mathrm{a}+\mathrm{b}}\right)^{3/2} \left(\frac{\mathrm{cd}}{\mathrm{c}+\mathrm{d}}\right)^{3/2} \sum_{\mathrm{tuv}} \mathrm{E}^{\mathrm{ab}}_{\mathrm{tuv}} \sum_{\tau\nu\phi} \mathrm{E}^{\mathrm{cd}}_{\tau\nu\phi}$$
$$\left(\frac{\partial}{\partial \mathrm{P_x}}\right)^{\mathrm{t}} \left(\frac{\partial}{\partial \mathrm{P_y}}\right)^{\mathrm{u}} \left(\frac{\partial}{\partial \mathrm{P_z}}\right)^{\mathrm{v}} \left(\frac{\partial}{\partial \mathrm{Q_x}}\right)^{\tau} \left(\frac{\partial}{\partial \mathrm{Q_y}}\right)^{\nu} \left(\frac{\partial}{\partial \mathrm{Q_z}}\right)^{\phi} \sqrt{\eta}\mathrm{F}_0(\eta \mathrm{R}^2_{\mathrm{PQ}}) \tag{A.2.7}$$

From differentiation of the Boys function

$$\begin{aligned} \frac{\partial}{\partial \mathrm{P_x}}\mathrm{F}_0(\alpha \mathrm{R}^2_{\mathrm{PQ}}) &= \int_0^1 \frac{\partial}{\partial \mathrm{P_x}} \mathrm{e}^{-\alpha \mathrm{R}^2_{\mathrm{PQ}} \mathrm{t}^2} \mathrm{dt} = -2\alpha \mathrm{X_{PQ}} \int_0^1 \mathrm{e}^{-\alpha \mathrm{R}^2_{\mathrm{PQ}} \mathrm{t}^2} \mathrm{t}^2 \mathrm{dt} \\ -2\alpha \mathrm{X_{PQ}} \mathrm{F}_1(\alpha \mathrm{R}^2_{\mathrm{PQ}}) &= -\frac{\partial}{\partial \mathrm{Q_x}} \mathrm{F}_0(\alpha \mathrm{R}^2_{\mathrm{PQ}}) \end{aligned} \tag{A.2.8}$$

we note that the Boys function only depends on the relative separation of the two centers of the charge distributions, and we can write (A.2.7) as

$$\begin{aligned} \mathrm{g_{abcd}} &= 2\pi^{-7/2} \left(\frac{\mathrm{ab}}{\mathrm{a}+\mathrm{b}}\right)^{3/2} \left(\frac{\mathrm{cd}}{\mathrm{c}+\mathrm{d}}\right)^{3/2} \sum_{\mathrm{tuv}} \mathrm{E}^{\mathrm{ab}}_{\mathrm{tuv}} \sum_{\tau\nu\phi} (-1)^{\tau+\nu+\phi} \mathrm{E}^{\mathrm{cd}}_{\tau\nu\phi} \\ &\left(\frac{\partial}{\partial \mathrm{P_x}}\right)^{\mathrm{t}+\tau} \left(\frac{\partial}{\partial \mathrm{P_y}}\right)^{\mathrm{u}+\nu} \left(\frac{\partial}{\partial \mathrm{P_x}}\right)^{\mathrm{v}+\phi} \sqrt{\eta}\mathrm{F}_0(\eta \mathrm{R}^2_{\mathrm{PQ}}) \end{aligned} \tag{A.2.9}$$

Appendix B

Electronic Repulsion Integrals Using Modified 2-el. Operators.

B.1 Solution of a Gaussian ssss-ERI Using The $\frac{\mathrm{erf}(\mu r_{12})}{r_{12}}$ Operator.

Evaluation of ERIs using the operator

$$\frac{\mathrm{erf}(\mu \mathrm{r}_{12})}{\mathrm{r}_{12}} = \frac{2}{\mathrm{r}_{12}\sqrt{\pi}} \int_0^{\mathrm{r}_{12}\mu} \mathrm{e}^{-\mathrm{t}^2} \mathrm{dt} = \frac{2}{\sqrt{\pi}} \int_0^{\mu} \mathrm{e}^{-\mathrm{s}^2 \mathrm{r}_{12}^2} \mathrm{ds} \tag{B.1.1}$$

is essentially the same as for the reguler ERIs. The evaluation runs as in Appendix A.1 until Eq.A.1.11. Hence, we can write the regularized electron repulsion integral as :

$$\begin{aligned} \mathrm{regERI} \;=\; & \frac{1}{\sqrt{\pi}} \pi^{-3} \left(\frac{ab}{a+b}\right)^{3/2} \left(\frac{cd}{c+d}\right)^{3/2} \mathrm{K_{ab}K_{cd}} \cdot \eta^{3/2} \\ & \int_0^{\mu} (\eta + \mathrm{s})^{-3/2} \cdot \exp\left[-\frac{\eta \mathrm{s}}{\eta + \mathrm{s}} \cdot \mathrm{R_{PQ}^2}\right] \cdot \mathrm{s}^{-1/2} \mathrm{ds} \end{aligned} \tag{B.1.2}$$

The substitutions $\mathrm{t}^2 = \frac{\mathrm{s}}{\eta + \mathrm{s}}$ and writing $\xi = \frac{\mu}{\sqrt{\eta + \mu^2}}$, equivalent to Eq.A.1.12, takes the regularized repulsion integral to the form

$$\mathrm{regERI} = \frac{2}{\sqrt{\pi}} \pi^{-3} \left(\frac{\mathrm{ab}}{\mathrm{a+b}}\right)^{3/2} \left(\frac{\mathrm{cd}}{\mathrm{c+d}}\right)^{3/2} \mathrm{K_{ab}K_{cd}} \cdot \sqrt{\eta} \int_0^{\xi} \mathrm{e}^{-\eta \mathrm{R_{PQ}^2 t^2}} \mathrm{dt} \tag{B.1.3}$$

With yet another substitution,$u = \frac{1}{\xi}t$, and writing $\tau = \eta \cdot \xi^2 = \frac{\eta\mu^2}{\eta+\mu^2}$, we arrive at

$$\begin{aligned} \mathrm{regERI} &= \frac{2}{\sqrt{\pi}}\pi^{-3}\left(\frac{\mathrm{ab}}{\mathrm{a+b}}\right)^{3/2}\left(\frac{\mathrm{cd}}{\mathrm{c+d}}\right)^{3/2}\mathrm{K_{ab}K_{cd}}\cdot\sqrt{\tau}\int_0^1 \mathrm{e}^{-\tau \mathrm{u}^2\mathrm{R}_{\mathrm{PQ}}^2}\mathrm{du} \\ &= 2\pi^{-7/2}\left(\frac{\mathrm{ab}}{\mathrm{a+b}}\right)^{3/2}\left(\frac{\mathrm{cd}}{\mathrm{c+d}}\right)^{3/2}\mathrm{K_{ab}K_{cd}}\cdot\sqrt{\tau}\mathrm{F}_0(\tau\mathrm{R}_{\mathrm{PQ}}^2) \end{aligned} \tag{B.1.4}$$

All that has to be done to calculate the regularized integrals is to replace the normal reduced exponent η by

$$\eta \rightarrow \tau = \eta \cdot \xi^2 = \frac{\eta\mu^2}{\eta+\mu^2} = \frac{1}{\frac{1}{\eta}+\frac{1}{\mu^2}} \tag{B.1.5}$$

and the Panas correction can be applied without increasing the computational effort. It is noticed that $\mu \rightarrow \infty$ restores the original repulsion integrals.

B.2 Solution of a Gaussian ssss-ERI Using The $\frac{2\mu}{\sqrt{\pi}}\exp(-\frac{\mu^2}{3}r_{12}^2)$ Operator.

Evaluation of ERIs over s-type Gaussians using this operator is even simpler than in the $\frac{1}{r_{12}}$ and $\frac{\mathrm{erf}(\mu r_{12})}{r_{12}}$ case since if will not involve the Boys function. The evaluation runs as for the regular ssss ERI : the Gaussian product rule is invoked taking the integral to

$$\begin{aligned} \mathrm{ERI} &= \pi^{-6}\frac{2\mu}{\sqrt{\pi}}(\alpha\beta)^{3/2}\left(\frac{ab}{a+b}\right)^{3/2}\left(\frac{cd}{c+d}\right)^{3/2}\mathrm{K_{ab}K_{cd}} \\ &\quad \iint \exp\left[-\alpha r_{1P}^2 - \beta r_{1Q}^2 - \frac{\mu^2}{3}r_{12}^2\right]\mathrm{d}\mathbf{r}_1\mathrm{d}\mathbf{r}_2 \qquad \text{(B.2.1)} \\ &= \pi^{-6}\frac{2\mu}{\sqrt{\pi}}(\alpha\beta)^{3/2}\left(\frac{ab}{a+b}\right)^{3/2}\left(\frac{cd}{c+d}\right)^{3/2}\mathrm{K_{ab}K_{cd}} \\ &\quad I_x I_y I_z \qquad \text{(B.2.2)} \end{aligned}$$

with I_x defined as

$$\mathrm{I_x} = \int_{-\infty}^{\infty}\int_{-\infty}^{\infty}\exp\left[-\alpha(\mathrm{x}_1-\mathrm{P}_x)^2 - \beta(\mathrm{x}_2-\mathrm{Q}_x)^2 - \frac{\mu^2}{3}(\mathrm{x}_1-\mathrm{x}_2)^2\right]\mathrm{dx}_1\mathrm{dx}_2 \tag{B.2.3}$$

To solve the I_x, I_y, I_z integrals the exact same procedure is used as in Eqs. A.1.8 - A.1.10. The result is :

$$\mathrm{I_x} = \pi(\alpha+\beta)^{-1/2}\left(\eta+\frac{\mu^2}{3}\right)^{-1/2}\cdot\exp\left[-\frac{\frac{\mu^2}{3}\eta}{\eta+\frac{\mu^2}{3}}\mathrm{R^2_{PQ,x}}\right] \tag{B.2.4}$$

where $\eta = \frac{\alpha\beta}{\alpha+\beta}$ as previously

$$\begin{aligned}
\mathrm{ERI} &= \pi^{-7/2}2\mu\left(\frac{ab}{a+b}\right)^{3/2}\left(\frac{cd}{c+d}\right)^{3/2}\mathrm{K_{ab}K_{cd}}\cdot\eta^{3/2} \\
&\quad (\eta+\frac{\mu^2}{3})^{-3/2}\cdot\exp\left[-\frac{\eta\frac{\mu^2}{3}}{\eta+\frac{\mu^2}{3}}\cdot R^2_{PQ}\right] \\
&= \pi^{-7/2}2\mu\left(\frac{ab}{a+b}\right)^{3/2}\left(\frac{cd}{c+d}\right)^{3/2}\mathrm{K_{ab}K_{cd}} \\
&\quad \left(\frac{\eta}{\eta+\frac{\mu^2}{3}}\right)^{3/2}\cdot\exp\left[-\frac{\eta\frac{\mu^2}{3}}{\eta+\frac{\mu^2}{3}}\cdot R^2_{PQ}\right]
\end{aligned} \tag{B.2.5}$$

with the substitution $\tau = \frac{\eta\frac{3}{\mu^2}}{\eta+\frac{3}{\mu^2}}$ the ERI with the *exp* operator takes a form familiar from the regular and Panas regularized integrals

$$\mathrm{ERI} = \pi^{-7/2}2\mu\left(\frac{ab}{a+b}\right)^{3/2}\left(\frac{cd}{c+d}\right)^{3/2}\mathrm{K_{ab}K_{cd}}\cdot\tau^{3/2}\cdot\exp\left[-\tau R^2_{PQ}\right] \tag{B.2.6}$$

Appendix C

An Expression For μ In The Panas Model.

Panas [3] sought an expression for μ in Eq.B.1.1 in terms of the basis set. μ is written as

$$\mu^2 = \alpha + \beta + \varepsilon \tag{C.0.1}$$

for some ε. This allows us to write the modified Coulomb operator as

$$\begin{aligned}\frac{\theta(\mu r_{12})}{r_{12}} &= \frac{2}{\sqrt{\pi}}\int_0^{\mu}\exp(-\mathrm{s}^2\mathrm{r}_{12}^2)\mathrm{ds} \\ &= \frac{2\mu}{\sqrt{\pi}}\int_0^{1}\exp(-\mu^2\mathrm{s}^2\mathrm{r}_{12}^2)\mathrm{ds} \\ &= \frac{2\mu}{\sqrt{\pi}}\int_0^{1}\exp(-\beta\mathrm{s}^2\mathrm{r}_{12}^2)\exp(-\alpha\mathrm{s}^2\mathrm{r}_{12}^2)\exp(-\varepsilon\mathrm{s}^2\mathrm{r}_{12}^2)\mathrm{ds}\end{aligned} \tag{C.0.2}$$

and the modified electronic repulsion integral as

$$\begin{aligned}\frac{2\mu}{\sqrt{\pi}}\int_0^{1}\iint \exp\left[-\alpha\mathrm{r}_{1\mathrm{P}}^2 - \beta\mathrm{s}^2\mathrm{r}_{12}^2\right]\exp\left[-\varepsilon\mathrm{s}^2\mathrm{r}_{12}^2\right] \\ \times\exp\left[-\beta\mathrm{r}_{2\mathrm{Q}}^2 - \alpha\mathrm{s}^2\mathrm{r}_{12}^2\right]\mathrm{d}\mathbf{r}_1\mathrm{d}\mathbf{r}_2\mathrm{ds}\end{aligned} \tag{C.0.3}$$

Assuming that the electrons interact with one pinned at the center of the charge distribution you get

$$\begin{aligned}\frac{2\mu}{\sqrt{\pi}}\int_0^{1}\iint \exp\left[-\alpha\mathrm{r}_{1\mathrm{P}}^2 - \beta\mathrm{s}^2\mathrm{r}_{1\mathrm{Q}}^2\right]\exp\left[-\varepsilon\mathrm{s}^2\mathrm{R}_{\mathrm{PQ}}^2\right] \\ \times\exp\left[-\beta\mathrm{r}_{2\mathrm{Q}}^2 - \alpha\mathrm{s}^2\mathrm{r}_{\mathrm{P}2}^2\right]\mathrm{d}\mathbf{r}_1\mathrm{d}\mathbf{r}_2\mathrm{ds}\end{aligned} \tag{C.0.4}$$

The integration over $\mathbf{r}_1$ and $\mathbf{r}_2$ can be carried out to obtain

$$\frac{2\mu}{\sqrt{\pi}}\int_0^1 \exp\left[-\frac{\alpha\beta \mathrm{s}^2}{\alpha+\beta \mathrm{s}^2}\mathrm{R}_{\mathrm{PQ}}^2\right]\times\left(\frac{\pi}{\alpha+\beta \mathrm{s}^2}\right)^{3/2}\exp\left[-\varepsilon \mathrm{s}^2\mathrm{R}_{\mathrm{PQ}}^2\right] \times\exp\left[-\frac{\alpha\beta \mathrm{s}^2}{\alpha \mathrm{s}^2+\beta}\mathrm{R}_{\mathrm{PQ}}^2\right]\times\left(\frac{\pi}{\alpha \mathrm{s}^2+\beta}\right)^{3/2}\mathrm{ds} \quad \text{(C.0.5)}$$

To proceed α and β are taking sufficiently small

$$2\left(\frac{\varepsilon}{\pi}\right)^2\int_0^1\left(\frac{\pi}{\alpha+\beta \mathrm{s}^2}\right)^{3/2}\times\exp\left[-\varepsilon \mathrm{s}^2\mathrm{R}_{\mathrm{PQ}}^2\right]\left(\frac{\pi}{\alpha \mathrm{s}^2+\beta}\right)^{3/2}\mathrm{ds} \quad \text{(C.0.6)}$$

Next Panas assumes that $\varepsilon \mathrm{R}_{PQ}^2$ is of such a size that the exponential in the integrant only contributes for small s. However taking s small the integral becomes

$$\frac{2\pi^{5/2}}{(\alpha\cdot\beta)^{3/2}}\sqrt{\varepsilon}\int_0^1\exp\left[-\varepsilon \mathrm{s}^2\mathrm{R}_{\mathrm{PQ}}^2\right]\mathrm{ds}=\frac{2\pi^{5/2}}{(\alpha\cdot\beta)^{3/2}}\sqrt{\varepsilon}\mathrm{F}_0(\varepsilon\mathrm{R}_{\mathrm{PQ}}^2) \quad \text{(C.0.7)}$$

A requirement for ε is that the approximate expression in C.0.7 should produce the regular expression for the regularized integral (B.1.4). This is the case if $\varepsilon=\tau$ and an expression for μ is

$$\begin{aligned}
&\varepsilon=\tau\\
&\Downarrow\\
&\mu^2-\alpha-\beta=\frac{1}{\frac{1}{\alpha}+\frac{1}{\beta}+\frac{1}{\mu^2}}\\
&\Downarrow\\
&\mu^2=\frac{\alpha+\beta}{2}+\sqrt{\left(\frac{\alpha+\beta}{2}\right)^2+\alpha\cdot\beta}
\end{aligned} \quad \text{(C.0.8)}$$

Appendix D

The One-Center Models In Dirac.

D.1 Specification of The Models.

The one-center models are specified in the '**HAMILTONIAN' directive of the DIRAC input file with the keyword .ONECAP. This keyword additionally takes a number (JNTV1C) to specify which model to use (I, II, or III), what charges to use (for model I and II) and how to distribute them (model III). For model I and II you can also manually specify what small component charges to use with the keyword '.SCQSET'. This keyword takes two numbers to specify element number and small component charge.

Even when doing calculations with the full set of integrals a useful application of the one-center models is to use them in the initial SCF iterations. The number of iterations needed with the full integral evaluation scheme is then expected to be small. The convergence threshold for the one-center models is specified with the keyword '.SV1CNV' (see figure D.1.1). When convergence to this threshold [1] has been reached, the one-center model will be switched off and the full set of integrals (or what was specified with the '.INTFLG' keyword) will be used.

By default the one-center LS and SS integrals are calculated on the fly. In many cases the one-center integrals will fit on disk which will speed up the calculation as the integrals then only need to be evaluated once, even in geometry optimizations. This is controlled with the '.DIRECT' keyword in the '**GENEREL' directive. '.DIRECT' takes three bits specifying which integral to calculate on the fly and which to write to disk (see figure D.1.1).

[1] This threshold applies to whatever convergence criteria has been specified : Electronic gradient, total energy or absolute change in Fock matrix.

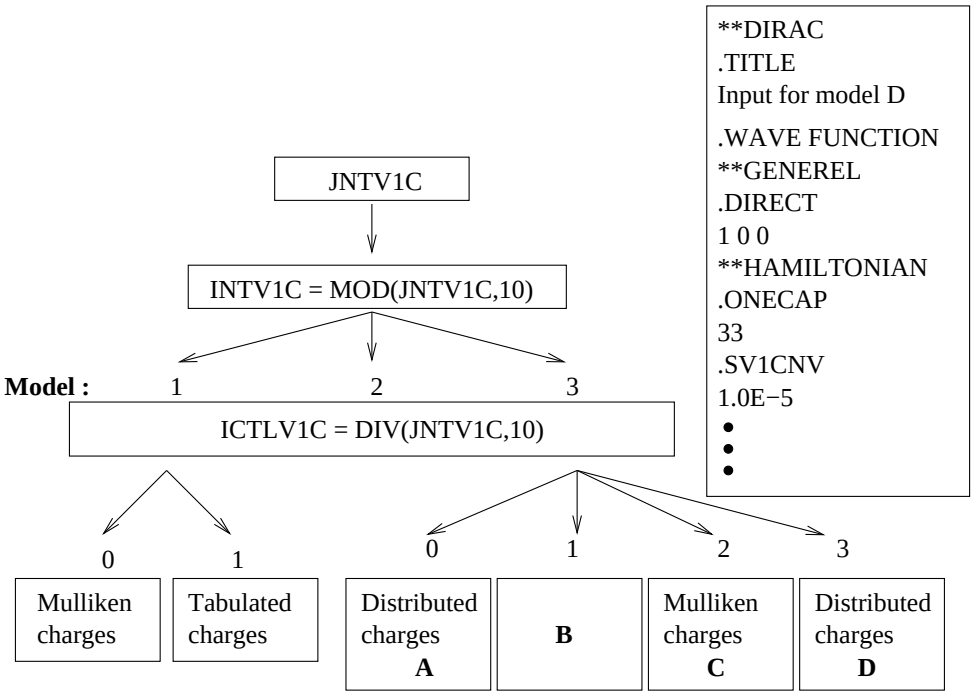

A : Charges distributed on nuclei and on point between nuclei determined by dipole moment.
B : Option not available. No tabulated large component charges.
C : Atom centered Mulliken charges.
D : Charges distributed on nuclei and at midt−point between nuclei.

Figure D.1.1: Specification of one-center models.

D.2 Implemented One-Center Models.

Currently Implemented One-Center Approximations.

Explicitly evaluated in **All Models**

Kinetic energy	:	$c\cdot\vec{\alpha}\cdot\vec{p}$
Large component one-electron interactions	:	$\langle L \mid \frac{-Z}{r} \mid L\rangle$
Large component two-electron interactions (n.r)	:	$(LL \mid LL)$

Model (INTV1C)	$\langle S_A \mid \frac{-Z_B}{r_B} \mid S_C\rangle$	$(L_AL_B \mid S_CS_D)$	$(S_AS_B \mid S_CS_D)$	Main Errors
1	$\langle S_A \mid \frac{-Z_A}{r_A} \mid S_A\rangle \rightarrow F_1$ $\langle S_A \mid \frac{-Z_B}{r_B} \mid S_A\rangle \rightarrow F_1$ $O\,[\sim\langle S_A \mid \frac{-Z_B}{r_B} \mid S_C\rangle(1-\delta_{AC})]$	$(L_AL_A \mid S_AS_A) \rightarrow F_2$ $(L_AL_A \mid S_BS_B) \rightarrow F_2$ $(L_AL_B \mid S_AS_A) \rightarrow F_2$ $(L_AL_B \mid S_CS_C) \rightarrow F_2$ $O\,[(L_AL_B \mid S_CS_D)(1-\delta_{CD})]$	$(S_AS_A \mid S_AS_A) \rightarrow F_2$ $(S_AS_A \mid S_BS_B) \rightarrow F_2$ $O\,[(S_AS_B \mid S_CS_D)(1-\delta_{AB})(1-\delta_{CD})]$	'Point/(single Gaussian)'– q^S distributions $\sum_B(S_A \mid \frac{q^L_B+q^S_B-Z_B}{r_B} \mid S_C) \approx 0$
2	$\langle S_A \mid \frac{-Z_A}{r_A} \mid S_A\rangle \rightarrow F_1$ $-\frac{Z_B q^S_A}{R_{AB}} \rightarrow F_0$ $O\,[\sim\langle S_A \mid \frac{-Z_B}{r_B} \mid S_C\rangle(1-\delta_{AC})]$	$(L_AL_A \mid S_AS_A) \rightarrow F_2$ $(L_A \mid \frac{q^S_B}{r_B} \mid L_A) \rightarrow F_1$ $(L_A \mid \frac{q^S_A}{r_A} \mid L_B) \rightarrow F_1$ $(L_A \mid \frac{q^S_C}{r_C} \mid L_B) \rightarrow F_1$ $O\,[(L_AL_B \mid S_CS_D)(1-\delta_{CD})]$	$(S_AS_A \mid S_AS_A) \rightarrow F_2$ $\frac{q^S_Aq^S_B}{R_{AB}} \rightarrow F_0$ $O\,[(S_AS_B \mid S_CS_D)(1-\delta_{AB})(1-\delta_{CD})]$	'Point/(single Gaussian)'– q^S distributions F_2 elements added to F_1 $\sum_B(S_A \mid \frac{q^L_B+q^S_B-Z_B}{r_B} \mid S_C) \approx 0$
3	$\langle S_A \mid \frac{-Z_B}{r_B} \mid S_C\rangle \rightarrow F_1$	$(L_AL_A \mid S_AS_A),(S_AS_A \mid L_AL_A) \rightarrow F_2$ $(L_A \mid \frac{q^S_B}{r_B} \mid L_A),(S_A \mid \frac{q^L_B}{r_B} \mid S_A) \rightarrow F_2$ $(L_A \mid \frac{q^S_A}{r_A} \mid L_B),(S_A \mid \frac{q^L_A}{r_A} \mid S_B) \rightarrow F_2$ $(L_A \mid \frac{q^S_C}{r_C} \mid L_B),(S_A \mid \frac{q^L_C}{r_C} \mid S_B) \rightarrow F_2$ $O\,[(L_AL_B \mid S_CS_D)(1-\delta_{AB})]$ + $O\,[(L_AL_B \mid S_CS_D)(1-\delta_{CD})]$	$(S_AS_A \mid S_AS_A) \rightarrow F_2$ $(S_A \mid \frac{q^S_B}{r_B} \mid S_A) \rightarrow F_2$ $(S_A \mid \frac{q^S_A}{r_A} \mid S_B) \rightarrow F_2$ $(S_A \mid \frac{q^S_C}{r_C} \mid S_B) \rightarrow F_2$ $O\,[(S_AS_B \mid S_CS_D)(1-\delta_{CD})]$	'Point/(single Gaussian)'– q^L distributions $(L_AL_B \mid S_CS_D)(1-\delta_{AB})$
4	$\langle S_A \mid \frac{-Z_B}{r_B} \mid S_C\rangle \rightarrow F_1$	$(L_A \mid \frac{q^S_A}{r_A} \mid L_A) \rightarrow F_1$ $(L_A \mid \frac{q^S_B}{r_B} \mid L_A) \rightarrow F_1$ $(L_A \mid \frac{q^S_A}{r_A} \mid L_B) \rightarrow F_1$ $(L_A \mid \frac{q^S_C}{r_C} \mid L_B) \rightarrow F_1$ $O\,[(L_AL_B \mid S_CS_D)(1-\delta_{CD})]$	$(S_A \mid \frac{q^S_A}{r_A} \mid S_A) \rightarrow F_2$ $(S_A \mid \frac{q^S_B}{r_B} \mid S_A) \rightarrow F_2$ $(S_A \mid \frac{q^S_A}{r_A} \mid S_B) \rightarrow F_2$ $(S_A \mid \frac{q^S_C}{r_C} \mid S_B) \rightarrow F_2$ $O\,[(S_AS_B \mid S_CS_D)(1-\delta_{CD})]$	'Point/(single Gaussian)'– q^S distributions F_2 elements added to F_1 $(X_AX_B \mid S_CS_D)(1-\delta_{CD})$
2*	$\langle S_A \mid \frac{-Z_A}{r_A} \mid S_A\rangle \rightarrow F_1$ $-\frac{Z_Bq^S_A}{R_{AB}} \rightarrow F_0$ $O\,[\sim\langle S_A \mid \frac{-Z_B}{r_B} \mid S_C\rangle(1-\delta_{AC})]$	$(L_A \mid \frac{q^S_A}{r_A} \mid L_A) \rightarrow F_1$ $(L_A \mid \frac{q^S_B}{r_B} \mid L_A) \rightarrow F_1$ $(L_A \mid \frac{q^S_A}{r_A} \mid L_B) \rightarrow F_1$ $(L_A \mid \frac{q^S_C}{r_C} \mid L_B) \rightarrow F_1$ $O\,[(L_AL_B \mid S_CS_D)(1-\delta_{CD})]$	$(S_A \mid \frac{q^S_A}{r_A} \mid S_A) \rightarrow F_2$ $\frac{q^S_Aq^S_B}{R_{AB}} \rightarrow F_0$ $O\,[(S_AS_B \mid S_CS_D)(1-\delta_{AB})(1-\delta_{CD})]$	'Point/(single Gaussian)'– q^S distributions F_2 elements added to F_1 $\sum_B(S_A \mid \frac{q^L_B+q^S_B-Z_B}{r_B} \mid S_C) \approx 0$

* If model 2 is specified without evaluation of the LS- and SS-class of integrals (via INTFLG or INTCNV keywords).

All models can be switched off after convergence to a specified threshold (SV1COFF) to return to the full integral scheme.

Bibliography

[1] V. R. Saunders. An introduction to molecular integral evaluation. In G.H.F. Diercksen, B.T. Sutcliffe, and A. Veillard, editors, *Computational Techniques in Quantum Chemistry and Molecular Physics*, page 347. 1975.

[2] L. E. McMurchie and E. R. Davidson. *J. Comp. Phys.*, 49:3083, 1968.

[3] I. Panas and A. Snis. *Theor. Chem. Acc.*, 97:232, 1997.